

A VISUAL STUDY OF THE DYNAMICS
OF POLYMER EXTRUSION

DISSERTATION

Presented in Partial Fulfillment of the Requirements for
the Degree Doctor of Philosophy in the Graduate
School of The Ohio State University


By

Mazen Yacoub Anastas, B.Sc., M.S.

* * * * *

The Ohio State University
1973

Approved by



Adviser
Department of Chemical Engineering

ACKNOWLEDGMENT

Words are incapable of expressing the author's feelings of gratitude and deep appreciation for his esteemed friend, and super adviser of this work, Professor Robert S. Brodkey. The author will always remember the invaluable guidance and boundless understanding both of which were liberally afforded him by Professor Brodkey during the execution of this work. It was both a pleasure and a privilege to have been associated with him.

The author wishes to register his gratitude to Dr. R. Emerson Lynn, the coadviser of this work. His numerous and inspiring suggestions were of great help in completing the experimental phase of this work. Many heart-felt thanks are due Professor Aldrich Syverson, Chairman of the Department of Chemical Engineering, The Ohio State University. The personal interest which he took in this work and the generous and enthusiastic support which he provided during all its phases will always be remembered.

The author wishes to acknowledge the valuable assistance rendered him, during the experimental phase of this work, by Specialist Michael B. Kukla, and Mechanic Keldon Latham, both of the Department of Chemical Engineering at The Ohio State University. Mr. Kukla cheerfully offered many excellent suggestions on the execution of many parts of the experimental program. The author will always remember the speed

and admirable dexterity with which Mr. Kukla repaired and built many of the pieces of equipment used. Mr. Latham, in addition to his help in laying-out the extrusion equipment, taught the author much about the machine shop. To both Messrs. Kukla and Latham the author wishes to express his most sincere gratitude.

The author wishes to acknowledge the superb craftsmanship displayed in the fabrication of the experimental extrusion equipment used in this work. Most of the fabrication and machining was carried out by members of the staff at the Physical Plant Machine Shop at The Ohio State University. Messrs. Rondol W. Wright and Harold F. McCullough generously and enthusiastically provided excellent suggestions on the fabrication and machining of parts for the equipment. John T. Bennett and Donald E. Williams did the large part of the excellent fabrication and machining. Welding of many of the parts used was meticulously carried out by Hayden E. Coleman.

The author wishes to express his deep appreciation for the assistance rendered him by members of the staff of the Department of Photography and Cinema at The Ohio State University. Much gratitude is due Thomas L. Snider for his help in editing the movies that were obtained during the experimental phase of this study. Clara Murray directed the effort involving the enlargement and printing of single frames taken from the movies for the purpose of constructing the solid bed profiles. The work was carried out by Dale Kistmaker, Dennis McArthur and Paul Wilcox. To all of them are due the many thanks of the author.

All members of the author's family shared in the accomplishment of this work. Both his father, Yacoub J. Anastas, and his brother, Bassam Y. Anastas, gave him a lot of their love and support, both moral and material. The faith and love of his mother, Lamia Anastas, and his brothers, Makram and Raja Anastas, was a constant reminder to work a little harder everyday.

The author wishes to register his gratitude to his very good friend, Miss Mary K. Berlo. She was always affectionately tolerant and generously helpful during the execution of this work. The author will always be indebted to his friend Mrs. Anna Wood. She provided him with a home, away from home, and always thought him better than what he really is. The author also wishes to take this opportunity to acknowledge the positive influence on his life exerted by the many women whom he either had the privilege of knowing personally, or would have liked to know better. They have provided an inspiration beyond description.

Finally, the author wishes to express his gratitude to Messrs J. Walker and J. Daniels whose fine spirits helped over many a hurdle.

VITA

November 23, 1944 . . . Born - Jerusalem, Palestine

June, 1965 B.Sc. Chemistry, University of Baghdad,
Baghdad, Iraq

December, 1969 M.S. Chemical Engineering, The Ohio State
University, Columbus, Ohio

1969-1971 Louis A. and Lucille Roberts Memorial Fellow
in Chemical Engineering, The Ohio State
University, Columbus, Ohio

1971-1972 Teaching Associate, Department of Chemical
Engineering, The Ohio State University,
Columbus, Ohio

1971-1973 Part-time Research Engineer, Battelle's
Columbus Laboratories, Columbus, Ohio

FIELDS OF STUDY

Major Field: Chemical Engineering

Studies in Fluid Mechanics. Professor Robert S. Brodkey

Studies in Polymer Engineering. Dr. R. Emerson Lynn

Studies in Thermodynamics. Professor Webster B. Kay

Minor Field: Mechanics of Materials

Studies in Viscoelasticity. Professor Kamran Majidzadeh

TABLE OF CONTENTS

	Page
ACKNOWLEDGMENTS	ii
VITA	v
FIELDS OF STUDY	v
LIST OF TABLES	viii
LIST OF PLATES	viii
LIST OF FIGURES	ix
LIST OF SYMBOLS	xii
INTRODUCTION	1
 Part	
I LITERATURE SURVEY	3
Solids Conveying Zone	
Melting Zone	
Melt Conveying Zone	
Mixing in Extruders	
Dynamics of Extrusion	
Twin Screw Extruders	
II EXPERIMENTAL	21
Visual Extrusion Equipment	
The Extrudate	
The Transparent Barrel	
Operation of the Extrusion Setup	
Experimental Runs	
III RESULTS AND DISCUSSION	48
Steady State Conditions	
Dynamics of Melting	
Solid Bed Rupture	
Transient Solid Bed Profiles	
Transients in Solid Bed Velocity	

TABLE OF CONTENTS (Continued)

Part	Page
IV SUMMARY AND CONCLUSIONS	88
V RECOMMENDATIONS	91
Solids Conveying	
The Melting Zone	
Melt Conveying Zone	
Twin Screw Extrusion	
APPENDIX	96
REFERENCES	137

LIST OF TABLES

Table	Page
1. Summary of movies taken in Zone 1 and the conditions under which they were taken	44
2. Summary of movies taken in Zone 2 and the conditions under which they were taken	45
3. Summary of movies taken in Zone 3 and the conditions under which they were taken	47
4. Location of transients for movies G7, H7, G3, and H5 . . .	98
5. Measured pitch versus axial distance d for movies G7, H7, and G3	107
6. Cumulative correction to d as a function of axial distance d	112
7. Summary of time and true axial distance calculation from f and d	118
8. Summary of axial distance-time measurements taken from movie G7	119
9. Summary of axial distance-time measurements taken from movie H7	124
10. Summary of axial distance-time measurements taken from movie G3	132
11. Summary of axial distance-time measurements taken from movie H5	135

LIST OF PLATES

Plate	Page
I Development, in time, of solid bed rupture in movie G7 . .	56
II Transient solid bed profiles obtained from movie H5	64

LIST OF FIGURES

Figure	Page
1. Schematic picture of a plasticating extruder	5
2. The shape of a typical metering type screw	5
3. Exploded view of visual extruder	26
4. Detail drawing of metering type screw used	28
5. Detail drawing of feed section	29
6. Detail drawing of barrel	30
7. Detail drawing of the die connector	32
8. Polymer preparation apparatus	34
9. Double Cowles dissolver	36
10. Position of camera relative to screw when taking Zone 2 movies	42
11. Top view of unwrapped screw channel with polymer	50
12. Cross section of the screw channel in the melting zone . .	50
13. Top view of unwrapped screw channel at instant of solid bed rupture	54
14. A schematic representation of the method employed in obtaining elements of the helical flow which were later used in constructing the solid bed profiles . . .	71
15. Axial displacement of solid bed as a function of time obtained from observation of solid particles indicated for movie H7	74
16. Axial displacement of solid bed as a function of time obtained from observation of solid particles indicated for movie G7	75

LIST OF FIGURES (Continued)

Figure	Page
17. Axial displacement of solid bed as a function of time obtained from observation of solid particles indicated for movie G3	76
18. Axial displacement of solid bed as a function of time obtained from observation of solid particles indicated for movie H5	77
19. Transient axial velocity profile at axial distance of 5.5 inches for movie H7	78
20. Transient axial velocity profile at axial distance of 5.0 inches for movie G7	79
21. Transient axial velocity profile at axial distance of 9.0 inches for movie G3	80
22. Transient axial velocity profile at axial distance of 7.0 inches for movie H5	81
23. Schematic showing the buildup of shear stress as a result of a step change in shear rate for a typical polymer melt or concentrated solution	83
24. Three-plate system of barrel, screw channel bottom and solid bed with melt in the gaps between them	83
25. Buildup of shear stresses on both sides of the solid bed	85
26. Transient development of velocity profiles in the solids portion of the flow in the melting zone	87
27. Location of transient for movie G7	100
28. Location of transient for movie H7	101
29. Location of transient for movie G3	102
30. Location of transient for movie H5	103
31. Axial distance measurement of particle of solid polymer	104
32. Plot of screw pitch versus axial distance d on screen for movie G7	109

LIST OF FIGURES (Continued)

Figure	Page
33. Plot of screw pitch versus axial distance d on screen for movie H7	110
34. Plot of screw pitch versus axial distance d on screen for movie G3	111
35. Cumulative correction applied to d , plotted versus axial distance d	113

LIST OF SYMBOLS

d	axial distance from the reference line to the center of that part of the screw channel in which a colored particle of solid resides on top of the solid measured, in inches, from a projected movie frame
d_a	actual axial distance of a solid particle, from the beginning of the helical channel as calculated from \underline{d} , inches
d_{pc}	axial distance measured on the movie frame between solid particle centroid and channel center, inches
f	frame number (0-4000) with respect to zero (reference) as given by frame counter
R	actual axial distance between reference line and beginning of helical screw channel, inches
t	time in seconds
t_o	time at which transient is introduced, seconds
t_∞	time at which a new steady state is achieved after transient, seconds
V	axial velocity of screw at root, inches per second
V_o	axial velocity of screw at root at time of introduction of transient, inches per second
V_∞	axial velocity of screw at root at new steady state after transient, inches per second
V_s	axial velocity of solid bed, inches per second
V_{s_o}	axial velocity of solid bed at time of introduction of transient
V_{s_∞}	axial velocity of solid bed at new steady state after transient, inches per second
Δ	correction applied to \underline{d} to account for wide angle lens distortion, inches

LIST OF SYMBOLS (Continued)

- τ shear stress on barrel and screw sides of solid bed, dynes per cm^2
- τ_0 shear stress on barrel and screw sides of solid bed at time of introduction of transient, dynes per cm^2
- τ_∞ shear stress on barrel and screw sides of solid bed at new steady state after transient, dynes per cm^2

INTRODUCTION

The process of extrusion is widely employed in the conversion of thermoplastic polymeric materials into various products. More than 50 percent of all polymers produced are extruded at least once. The demand for products fabricated from polymeric materials has risen sharply. More rigid constraints are also placed on the quality and uniformity of these products. These and other factors stimulated considerable interest in the basic principles of extrusion.

As will be seen in Part I, there are still many deficiencies in the state of knowledge of the process. These deficiencies have been caused, in part, by the complexity of the process itself. The complex flow/mechanical properties of the extrudate in addition to the geometrical complexity of even the most elementary of screws used in practice, have presented extreme difficulties to investigators in their attempts at complete understanding of the process.

Extrusion parameters, such as melt pressure and temperature profiles and quality of extrudate cannot be predicted to a high degree of accuracy. Despite the availability of some reasonably adequate mathematical models describing steady state flow, relatively little knowledge is available on the dynamic behavior under transient conditions. Ideally a complete model of the dynamics of extrusion would accurately predict the dependency in time of all the significant parameters, when

one or more of them are changed. Obviously, the attainment of such a model would directly lead to automatic control of the process, thus eliminating much of the art work that has been prevalent to date. Such a complete description would be reflected in higher productivity in plastics manufacture and processing, more uniform quality in products, and much shorter startup times.

The complexity of both flow geometry and rheological properties of polymers has rendered the attainment of a complete dynamic model virtually impossible. However, complex flow problems have been studied visually in the past. Such visual studies involved the recording on photographic film of a continuous record of the events taking place in certain locations of the flow field and the progress of such events with time. Examples of such studies can be found in both laminar and turbulent flow where records of complex motions of fluid elements have been obtained and documented. Some of these studies have aided in arriving at quantitative descriptions of the events that they represented. Based on this and the measures of success that some visual studies in extrusion have attained, it was felt that a visual study of the dynamics of extrusion would be useful. New insights gained from such a study could be directly applied toward the ultimate goals previously mentioned. For the results of such a study to be meaningful and applicable to practical situations, the real process will have to be simulated. Real and time varying disturbances will have to be applied to it.

This, then, is the subject matter of this work.

PART I
LITERATURE SURVEY

In a plasticating single screw extruder, solid polymer, in the form of pellets or powder, is introduced at the feed end through a feed hopper. Between this point and the polymer's exit through the die, it is, simultaneously being conveyed forward and melted. In the first several turns of the screw, mostly solid polymer is being conveyed forward. Then, over the larger portion of the screw, the polymer is melted and the solid and liquid coexist. Finally, the completely molten polymer is pumped at high pressure and temperature by the last several turns of the screw. Based on their function there are three main sections along a screw. These are : 1) Solids conveying zone, 2) Melting zone, 3) Melt conveying or pumping zone.

In past theoretical and experimental work in the area of plasticating screw extruders, the tendency was to study the three functions of the screw separately. Recently, Street (57) suggested that, since the three functions of the screw may take place simultaneously and in a continuous manner, a unified approach is more realistic and beneficial. The advantages of such an approach would be reflected in more efficient machine design and computer control. However, for purposes of the study at hand, the traditional approach was taken and, where possible, the three functions of the screw were studied separately.

It may be noted at this point, that from a dynamic viewpoint the functions mentioned earlier cannot be separated since the quantity and quality of the product are largely determined by the interrelationships of these three functions.

Figure 1 is a schematic representation of a single screw extruder. Since most of the experimental and theoretical work done in this field was made on machines with screws that are geometrically similar to that presented in Figure 2, the discussion will be limited to such screws unless otherwise noted. This screw is called a metering screw. It is characterized by a constant pitch and has three geometrical sections. These are, a feed section with a relatively deep channel, a tapered or compression section in which the channel depth is decreasing continuously, and the metering or melt-pumping section which has a relatively low channel depth. The ratio of the channel height in the feed section to that in the metering section is called the compression ratio of the screw. In what follows an attempt will be made to present an overview of the basic knowledge that is available in the field of plasticating extrusion.

Solids Conveying Zone

In the first few turns of the screw, the solid polymer is conveyed forward by the advancing flights. Comparatively little work has been done toward understanding the mechanism of flow in this zone. Early work done by Decker (11), Pawlowski (41), Maillefer (31), and Simonds (52) was directed at obtaining mathematical expressions for material flow rate related to such variables as screw geometry and speed

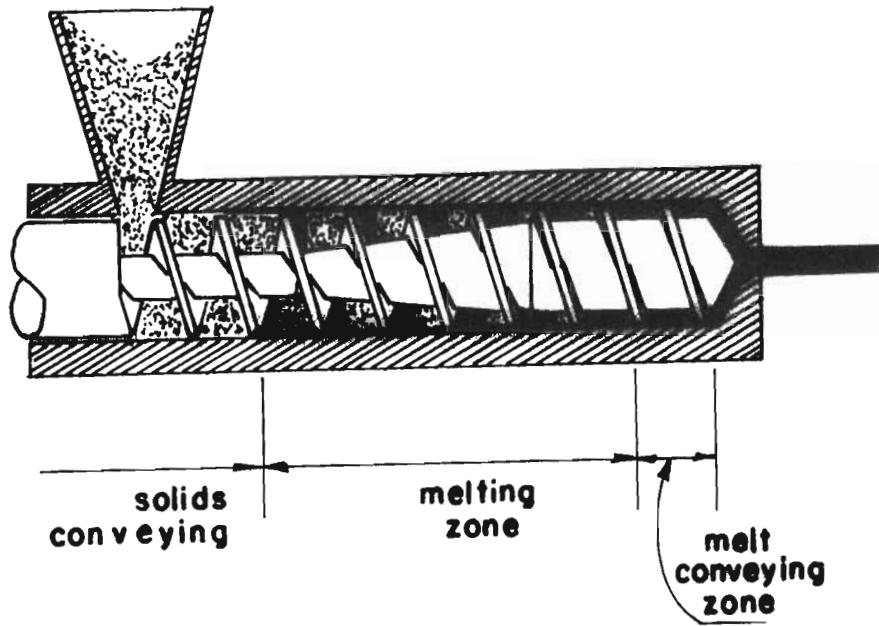


Figure 1. Schematic picture of a plasticating single screw extruder. Source: Reference 60 p. 8 .

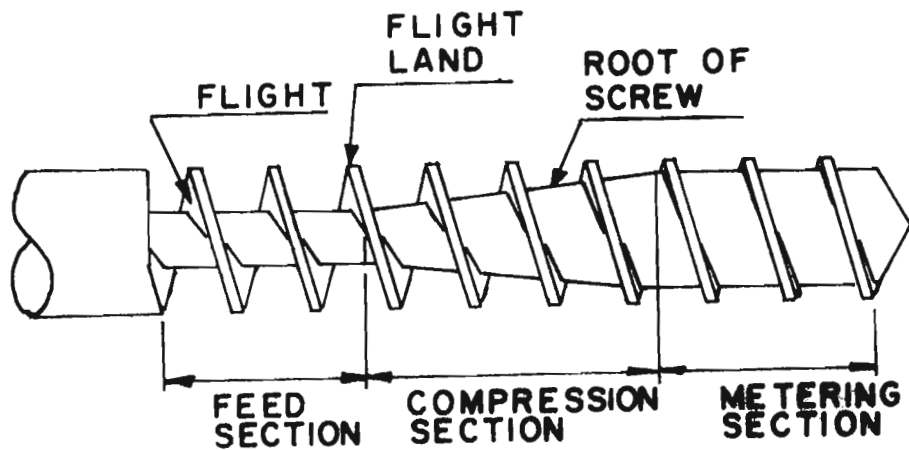


Figure 2. The shape of a typical metering type screw. Source: Reference 60 p. 8 .

of rotation. Later, Darnell and Mol (10) presented a mechanism for the flow of solids with due regard to past experience. They theorized that the solids moved forward as a plug and that polymer to metal friction at the barrel was responsible for the forward motion. Friction between polymer and screw surface was said to inhibit the flow. To verify the notion of plug flow in this region, Darnell and Mol constructed an extruder with a transparent (Plexiglass[®]) barrel. Operation of this extruder revealed no plug flow of the polymer pellets. Instead, the polymer particles were turning, tumbling, stacking and bridging.

The solid - solid friction mechanism, as presented by Darnell and Mol, was recently criticized by Chung (8). He conducted experiments in which a slab of polymer was set in motion over a hot smooth metal surface. The surface was maintained at temperatures below, at, and above the melting point of the polymer. The force required to move the slab at constant speed was measured together with the normal (pressure) force. It was found that the ratio of those two forces was not constant, and furthermore that it increased with temperature up to the point where the metal plate was at the melting point of the polymer. No variation of this ratio with the speed at which the slab moved was observed. At plate temperatures above the melting point of the polymer, the force required to move the slab was found to increase with increasing slab speed. Chung concluded that with barrel (and screw) temperatures above the melting point of the polymer, a film of melt exists between all metal surfaces and adjacent solid polymer. While still retaining the idea of plug flow of solids, Chung implied that the screw motion was

transmitted to the plug through a thin layer of polymer melt. Also, another layer existed between solid and barrel surface.

Griffith (19) studied the effect of polymer pellet size on extruder output and screw torque. He noted that feeds made up of finely divided solid polymer gave lower output rates and required less torque. Also he observed that a considerable internal shearing took place in partly "plastified" or melted plugs. The explanation given was that the "plug ruptured into balls of melt enclosed powder." This mechanism may explain the existence of air bubbles in extrudates originating from powdered solid feeds.

Melting Zone

In this portion of the screw, the solid polymer and its melt coexist in a segregated manner. This zone starts at a point where an appreciable amount of polymer melt flows in the downchannel direction along with the solid. It ends at a point along the screw where solid polymer no longer exists.

The mechanism of the melting process was first studied by Maddock and Street (30,56). They performed experiments in which natural solid polymer was mixed with a small concentration (3-5 percent) of a dyed variety, and fed to a specially designed 2 inch extruder. After steady state conditions were attained, the extruder was stopped and the screw and barrel were cooled. Then the screw was pushed out of the barrel with a hydraulic ram. The solidified helical ribbon of polymer that was formed on the screw was peeled off and sectioned, in a

direction perpendicular to the flights, at various points along its length. These sections showed the positions of the melt and solid in the channel and revealed certain aspects of the flow. It was found that the solid moved as a continuous helical ribbon adjacent to the trailing (or rear) flight of the channel. The cross section of this solid bed was found to continuously decrease in the downchannel direction, becoming negligible at the end of melting. The polymer melt accumulated against the pushing (or advancing) flight. It was also found that secondary cross-channel flows, originating at the top of the solid bed, took place in the melt. In the channel, the solid and liquid are separated by an irregular interface. Maddock's (30) experiments enabled him to postulate a melting mechanism. He stated that in the first few turns of the screw, solid polymer, in contact with the hot barrel surface, melts and is smeared thereon by the advancing flight. This process continues until the film of molten polymer becomes greater in thickness than the clearance between the hot barrel and the screw. Thereafter, the advancing flight scrapes off the excess melt and causes it to accumulate in the rear of the channel. This results in the solid being pushed to the front of the channel. The heat energy required to complete the melting of the solid comes from two sources. The first is the heat conducted through the barrel wall and the second is obtained by viscous dissipation of the screw power by shearing of the melt film between the barrel and the top of the solid bed.

The freezing technique as devised by Maddock and Street was later used by many workers to further study the melting mechanism (7,15,16,21,34,59). Tadmor, Duvdevani, and Klein (59) performed

experiments in which a variety of polymers were extruded under a wide range of operating conditions and using screws of various sizes. Their observations indicated that the above mechanism held regardless of polymer type, operating conditions or screw size. Furthermore, the sections of polymer showed that the solid bed broke up, at one or more points, into lengths of 2 to 4 turns each. This was exhibited by the sudden disappearance of solid from the section and later reappearance in a section further down the channel. Marshall et al. (34) further pursued the observation of this phenomenon by installing thermocouples at various points where only solids would occur in the absence of solid bed break up. The explanation offered by Tadmor and Klein (60c) was as follows: The solid bed, composed of a weak aggregate of pellets of polymer, is dragged forward by the screw against a large positive pressure gradient. This, in addition to the melt being conveyed at a faster rate, would tend to break up the bed. The gap that is created is rapidly filled with melt and the broken segment (2 to 4 turns) continues to move forward and melt according to the mechanism described above. This breaking up may occur more than once. It was experimentally found that break up might occur when the solid bed width became about half that of the channel. Many factors were cited as contributing to the incidence of this phenomenon. Some of these are, polymer type, pellet size, and screw geometry. Early breaking up may be brought about by a large pellet size, while taper in the screw tends to delay it.

Rousselet (48) conducted experiments in which he attempted to elicit information about the nature of the flow in this zone. He used

an extruder with a split barrel the top half of which was hinged to the lower half and could be rotated about the hinge to uncover the screw. Colored PVC was fed continuously after the natural polymer has been fed for some time. After the screw was stopped, the front between colored and natural polymer was examined. The shape of the front indicated that plug flow prevailed in the solid bed while internal shear in the melt gave a "helical" velocity profile.

Another zone which is closely associated with the melting zone is called the delay-in-melting zone. It is characterized by the lack of any substantial melting of the polymer for several turns despite the appearance of a melt film in the back of the channel. The film apparently retains its small thickness and does not show a tendency to grow for several (2-3) turns. This was regarded (60c) as a loss to the melting capability of the extruder and may contribute to the deterioration of product quality. This delay has been ascribed to a relatively large clearance between barrel and screw or to insufficient barrel heating in the region where this phenomenon occurs.

Melt Conveying Zone

The point, in the screw channel, at which melting of solid polymer is completed, marks the beginning of the melt conveying zone. Here the polymer melt is conveyed forward at relatively high temperature and pressure and then enters the die at the end of the helical path. In this region heat input to the polymer melt consists of that which is conducted from the barrel heaters through the barrel wall and

that which is generated by viscous dissipation of screw power. The length of this zone depends, mainly, on operating characteristics and the material being extruded.

This region of the flow received much attention in both experimental and theoretical studies. As an aid in visualizing the flow, early workers "unwrapped" the helical channel of the screw and had the flat barrel moving over the resulting flat channel at an angle equal to the helix angle and at a velocity equal to the peripheral velocity of the screw. This arrangement leads to a downchannel velocity component, responsible for forward motion, and to a cross channel component.

Most commercially extruded polymer melts exhibit complex rheological properties (5,60d). These properties include time-dependent non-Newtonian behavior and viscoelasticity. For polymer melts, the time-dependent non-Newtonian behavior exhibits itself as a decrease in viscosity with increasing level of shear and time of its application. Viscoelasticity is associated with partial recovery of a shearing strain together with the development of normal stresses that are, in principle, separable from those associated with fluid pressure. The combined effect of complex rheology and geometry has detracted from obtaining an accurate description of the flow in this region.

All theoretical expressions obtained thus far have been rather restricted solutions of the equations of change for a fluid flowing in a rectangular channel. Boussinesq (4) solved the Navier-Stokes equations for the case of fluid flowing in a channel with one wall in motion. This approach was later taken by Rowell and Finlayson (49,50)

and Carley et al. (6) who presented a solution for the isothermal flow of a Newtonian fluid. This was thought to be the case for a relatively deep channel and for low screw speeds. McKelvey and Wheeler (29) and later Booy (3) theoretically analyzed the pressure distribution for the Newtonian isothermal case in both the cross and down channel directions. The result of this analysis was that both distributions were linear in their respective directions. This was later born out by experiments in which pressure traces were obtained at various points along the barrel.

More recently, mathematical solutions, reflecting the nonisothermal, rheologically complex nature of the flow have been presented. DeHaven (12) used the Ellis model to derive the velocity profile for flow between infinite parallel plates. Ram and Narkis (46), Kroesser and Middleman (26), and Glyde and Holmes-Walker (20) used the power-law model for the same geometry. Griffith (18) later included the cross channel component of velocity which was neglected by DeHaven (12) and subsequent workers (20,26). He also continued his calculations for the case of nonisothermal flow assuming constant temperature along a streamline. The work of Pearson (42) removed that restriction. Some workers attempted to study the effect of the viscoelastic nature of the melt on the flow. Experimental velocity measurements for the flow of a viscoelastic fluid in a square duct, were performed by Wheeler and Wissler (62). They showed the existence of secondary flows that caused both negative and positive deviations from the velocity profile of a Newtonian fluid flowing in the same geometry. White and Metzner (64)

attempted to derive expressions for the normal stresses in screw extruders using the infinite parallel flat plate geometry. They concluded that the isotropic pressure is a function of channel height as well as being a function of cross and down channel directions. Kaiser (22) showed, by order-of-magnitude calculations, that normal stresses were small in comparison with pressures developed in screw extruders.

In order to gain a more accurate picture of the flow in this region, visual experiments were conducted, in which the flow patterns were directly or indirectly inferred. In the course of consecutively extruding colored rubber compounds in an extrusion plastometer, Marzetti (35) observed a "telescopic motion of concentric, differently colored layers" at the discharge end of the device. Eccher and Valentinotti (17) repeated this experiment by extruding the colored rubber compounds through a rod die using an actual extruder. They found that the resulting rod was covered with the first compound and a section through the rod showed a concentric arrangement of the other colors with the color that was fed last at the center. Their conclusion was that there was little or no slip at the wall and that the flow was laminar. Flow visualization in the screw channel was first attempted by Maillefer (32). He determined the flow lines produced by molten polythylene flowing in a rectangular channel. The flow was induced by moving the upper boundary and after injecting die at various points in the cross section. Later, he froze the melt and obtained sections of the flow in the down channel direction. This, however, could not be related to flow in extruders since it ignores the

existence of a cross channel component of velocity as qualitatively established earlier and as found experimentally by Maddock and Street (30,56) in their cooling experiments as described in the section on the melting zone. In those experiments, a section in the helical ribbon of frozen polymer was found to contain circulatory flows in the cross channel direction.

Eccher and Velentinotti (17) measured the velocity profiles in a short ($L/D = 2.0$) 1.0 inch diameter extruder with a screw channel height of 0.0276 inch. In this extruder, the transparent barrel rotated while the screw was stationary. The barrel rpm was of the order of 0.15. The fluid used was a solution of polyisobutylene in paraffin oil with a viscosity of 1530 poise at 20° C and contained aluminum particles of 0.0011 inch average diameter. The motion of the individual particles was followed by a microscope mounted perpendicular to the axis of the screw. The movement of the microscope was precisely determined with extensometer type dials which registered the coordinates of a particle micrometrically. The direction of motion of a particle was followed by an ocular micrometer and the angle of motion was measured by a goniometer. The velocity profiles constructed from data were in excellent agreement with solutions of the Navier-Stokes equations. Three different types of profiles were obtained depending on whether the extruder was running under conditions of closed, open, or half-closed discharged. Also, the existence of a "back-flow" in the down channel direction was clearly demonstrated by resolution of the velocity vectors into their respective components.

The mid-channel streamlines as constructed by Eccher and Valentinotti from experimental measurements were obtained in a different manner than those established by Mohr et al. (38). Their experimental setup consisted of a 3.5-inch-diameter, extruder with a transparent rotating barrel. They used a 23.4-inch long, square-pitched screw with a channel depth of 0.25 inch. The fluid used was a 43° Bé corn syrup with a viscosity of 1000 poise at 25° C. A probe made of hypodermic tubing with its end plugged, was installed in the middle of the channel and perpendicular to the screw axis. The probe had short tubes installed along its length and in a direction perpendicular to its axis. Black dye was injected into the probe after the barrel was set in motion at frequencies of the order of 0.15 rpm. The angles that the streamlines made with the down channel direction were measured as a function of channel height and found to be in close agreement with those calculated from the isothermal Newtonian model. The same equipment was used to experimentally measure the variation of the down channel velocity component with channel depth (39). Resin particles of 25-30 mils in diameter were used to mark the flow. Two cameras at right angles to each other and to the screw axis were used in conjunction with a stroboscopic light source. Analysis of the photographic records showed that the down-channel velocity profile obtained resembled that obtained from the isothermal Newtonian model. Further experimentation with a non-Newtonian material (28 percent solution of hydroxymethylcellulose in water) having the same basic shear diagram as molten polyethylene, gave the same profiles and streamlines as did the corn syrup. This lead the

authors to the conclusion that non-Newtonian fluids exhibit the same characteristics as Newtonian fluids in extruders. This, however, may be the case only under conditions of very low shear rates where non-Newtonian fluids behave as Newtonians.

Mixing in Extruders

In the mixing of fluids of low viscosity, turbulence is usually associated with good mixing and is usually employed in achieving a uniform product. Danckwerts (9) introduced some useful definitions that helped fix ideas about the notion of good mixing. He stated that the objectives of a process in which two components were being mixed, were the reduction of the intensity and scale of segregation between them. If one of the components is visualized to be dispersed in the other component, then the former is called the segregated phase or minor component and the latter is called the continuous phase or major component. The size of the "particles" of the minor component is a measure of the scale of segregation whereas the distance between those particles is a measure of the intensity of segregation. In turbulent flows, the reduction of those parameters is achieved by a convective transport of "clumps" of material from one location to another in relatively short times. The direct result of this action is to increase the surface area between the two components.

Polymer melts, however, are usually very viscous. Thus, laminar flow of the melt persists even at high screw rpms or, equivalently, high shear rates (37,60e). Mohr et al. (36) applied their

theory of mixing in laminar flow to mixing in extruders. They used ideas put forward by Spencer and Wiley (55), who mathematically proved that shear straining of a material increased the surface area and decreased the striation thickness or intensity of segregation as applied to laminar flow. As mentioned earlier, an element of fluid in the channel of an extruder screw was thought to experience both a cross- and a down-channel movement. In addition to being conveyed forward it alternately faced the barrel and screw sides of the channel. Therefore the total strain that this element has experienced may be obtained from a knowledge of the point values of shear rate over the entire time interval which the element spent in the extruder.

The time spent by a fluid element in the helical channel has been thought to depend, primarily, on its initial position and the screw rpm. Based on the isothermal Newtonian model, expressions for the residence time distribution of elements of fluid in the channel, were derived together with expressions for the average shear strain (28,37,60e). The product of the average shear strain and the residence time was used as an index of good mixing. Therefore, any operating variables which tend to affect either the residence time or the shear strain will affect the degree of mixing. Good mixing was associated with relatively low screw speeds, high back pressures, and shallow screw channels, among others.

Dynamics of Extrusion

Modern extrusion practice calls for machines of large capacity and high product quality. The previous discussion of mixing has shown that product quality and uniformity decreases with increased rate of output. Poor quality has been associated with random or cyclic fluctuations of extrudate temperature, pressure, and flowrate (60f). The measures of product quality that are in use today are related to appearance, dimensional uniformity (such as thickness of sheet), or mechanical strength. Tadmor and Klein (60f) distinguished between two classes of extrudate quality. The first was the steady state quality which was said to depend on the value of the operating variables such as temperature, pressure, and flowrate. The second was the unsteady state quality associated with fluctuations of the operating variables about time average values.

Fluctuations in output, or surging, have been studied and classified by Wheeler (63). He stated that it might be a result of:

- 1) The solids conveying controlling the output, giving rise to high frequency (60 rpm) fluctuations. This phenomenon was said to occur at low back pressures.
- 2) Break up of the solid bed giving rise to fluctuations of intermediate frequency.
- 3) Poor feed section design giving rise to random fluctuations.

Another phenomenon associated with large pressure fluctuations was recently explained by Klein (24). He noted that in compression

sections with large angles of taper, the solid feed may exceed the melting capacity of the extruder causing the channel to be plugged with solid thereby preventing the melt pool from moving in the down channel direction. The ensuing improvement in melting was said to cause the channel to become unplugged again. A cyclic repetition of this sequence of events was said to cause large variations in pressure, flow rate, and quality of extrudate.

Kirby (23) attempted to mathematically define surging using the techniques of process control theory together with simple steady state expressions of the flow rate in the various zones of the screw. He was able to relate surging to such quantities as length of melting, screw rpm, back pressure, and screw helix angle.

Twin Screw Extruders

Some of the problems encountered in polymer processing using single screw extruders have been solved using the so-called twin-screw variety. In these machines two intermeshing screws rotate simultaneously such that material is positively conveyed forward (1). This is achieved by the action of the flight of one screw on the material in the channel of the other. At every point the helix angles of both screws are equal which is, of course, a necessary condition for intermeshing. The net result is that material in one full turn of one screw is sealed off by the flight of the other (44). This situation gives rise to areas of relatively high shear in the clearance between the two screws (14).

Problems in single screw extrusion as lack of good mixing have been solved by twin-screw extrusion. Good product uniformity has been achieved at relatively low shear rates. Here the residence time distribution of material is narrow with a relatively low peak (in comparison to single screw). Also, more efficient feeding of the material was attained, since the ability to convey does not depend on the size and shape characteristics of the solid polymer feed (1).

PART II
EXPERIMENTAL

Given the motivation to study the dynamics of extrusion visually, the development of the facility required taking into consideration many constraints and limitations. Obviously, the flow of polymer in the screw had to be amenable to visual observation. Therefore, this dictated the use of a transparent barrel. However, in practical extrusion equipment the barrels are thick cylinders of steel designed to withstand temperatures of the order of 400° F and pressures of the order of 1000-10,000 psia. The high barrel temperatures are necessary because of the high melting points of polymers and because at least part of the thermal energy required to melt the solid polymer is obtained from conduction of heat through the barrel wall. The balance of the thermal energy requirement is obtained from viscous dissipation of screw horsepower in shearing the melt film between the bed of solid polymer and the inside barrel surface. This dissipation is also obtained from the secondary cross channel flows mentioned in Part II.

When all of the thermal energy requirement is obtained from dissipation of screw horsepower, the extruder is said to be operated autogeneously or adiabatically. Bernhardt and McKelvey (2) were able to operate an extruder adiabatically by setting the barrel heaters at a temperature slightly above that of the melting point of the polymer

being extruded. Although the adiabatic conditions of extrusion can be only approximated, the feasibility of the idea was clearly demonstrated by the experiments mentioned above. This principle of operation was used in this work to extrude a special polymer solution with a melting point that is lower than room temperature. Furthermore, elimination of continuous barrel heating was necessary since the use of such devices would not only block the view of an optical system of visual observation, but would also unduly complicate the system. Probably the best methods of introducing heat continuously through the barrel, if it were necessary, would be by radiant heat transfer, since most transparent materials are poor conductors of heat with thermal conductivities of the order of 10^{-2} to 10^{-5} Btu/hr-ft-°F (25). Extremely high temperature gradients would be required in order to conduct appreciable quantities of heat through the barrel wall.

The relatively high viscosities of polymer melts cause the generation of the high pressures encountered in extrusion. Additionally, the levels of operating pressures are raised in practice in order to achieve higher quality in extrudates by increasing the degree of mixing. The transparent barrel was required to withstand a pressure of 2000 psia. Common to most materials investigated for the barrel construction was a tensile strength of about 8000 psi. Elementary calculations of hoop stress in thick cylinders together with the application of a simple theory of failure indicated a wall thickness of 1 inch at the indicated yield strength. The candidate materials ranged between some specialty glasses like quartz, silica and Cervit[®] and transparent plastics like

Lexan[®], Lucite[®], Plexiglass[®] and Selectron 50111[®]. The specialty glasses proved hard to fabricate in thick sections, costly, and their performance was not guaranteed. These would, however, have offered dimensional stability and integrity under conditions of large temperature gradients and in chemical environments that are usually detrimental to the transparent polymers. When the use of the specialty glasses was eliminated, more attention was paid to the temperature at which the extrusion was to be carried out.

At the time this study was initiated, another was in progress as part of a comprehensive program aimed at gaining a better understanding of the principles involved in polymer processing. In that study, a 2-1/2 inch NRM extruder was instrumented to gather data on transients in pressure, melt temperature and melt-flowrate in a sheet extrusion train. The extrudate was a high-impact polystyrene. It was thought that useful information from the present visual study might be applied to the interpretation of the data obtained from the 2-1/2 inch system. However, polystyrene has a melting point of 400° F. Therefore, using this polymer as extrudate in the visual extruder with a plastic barrel was, of course, not feasible. Brodkey (5) has gathered and correlated a large amount of rheological data on polymer solutions. He has stated that concentrated solutions of polymers, at correspondingly lower temperatures, exhibited the same general rheological behavior as polymer melts. The requirements for the extrudate were that it should have a die viscosity in the neighborhood of 10^5 poise and should be a solution of polystyrene with a melting point much lower than 400° F.

Such viscosities were obtained by Spencer and Dillon (53,54) for molten polystyrenes of various molecular weight. Inspection of the literature on the physical properties of solutions of polystyrene (33,61) indicated the possibility of phase separation of the solid polymer from solution at about 25° C. To eliminate this it was finally determined that plasticizers rather than solvents should be used to lower the glass temperature (or melting point) of polystyrene (45). A further inspection of the literature revealed the existence of rheological data on concentrated solutions of polystyrene in diethylphthalate plasticizer. Shishido and Ito (51) obtained basic shear diagrams of the system for solutions up to 53 percent polystyrene and at about 25° C. Crude viscosity measurements on a 40 percent by weight (270,000 average molecular weight) mixture of polystyrene in diethylphthalate, indicated a zero-shear value of about 10^5 poise at 25° C. An approximate differential thermal analysis of a sample of the material gave a melting point of about 0° F and a glass temperature lower than -50° F. As expected, no separation of solid polystyrene was observed upon reheating the frozen mixture.

Having decided that the 40 percent solution was a suitable extrudate, the only requirement that the barrel had to satisfy was that it retain its integrity in an environment containing diethylphthalate. This condition was satisfied only by solid sections cast from Selectron 50111[®]. This material is a thermosetting polyester resin that gels to a hard, tough solid by the action of small amounts of methyl ethyl ketone peroxide at room temperature.

In what follows, a description of the equipment used and the experimental runs that were made will be given.

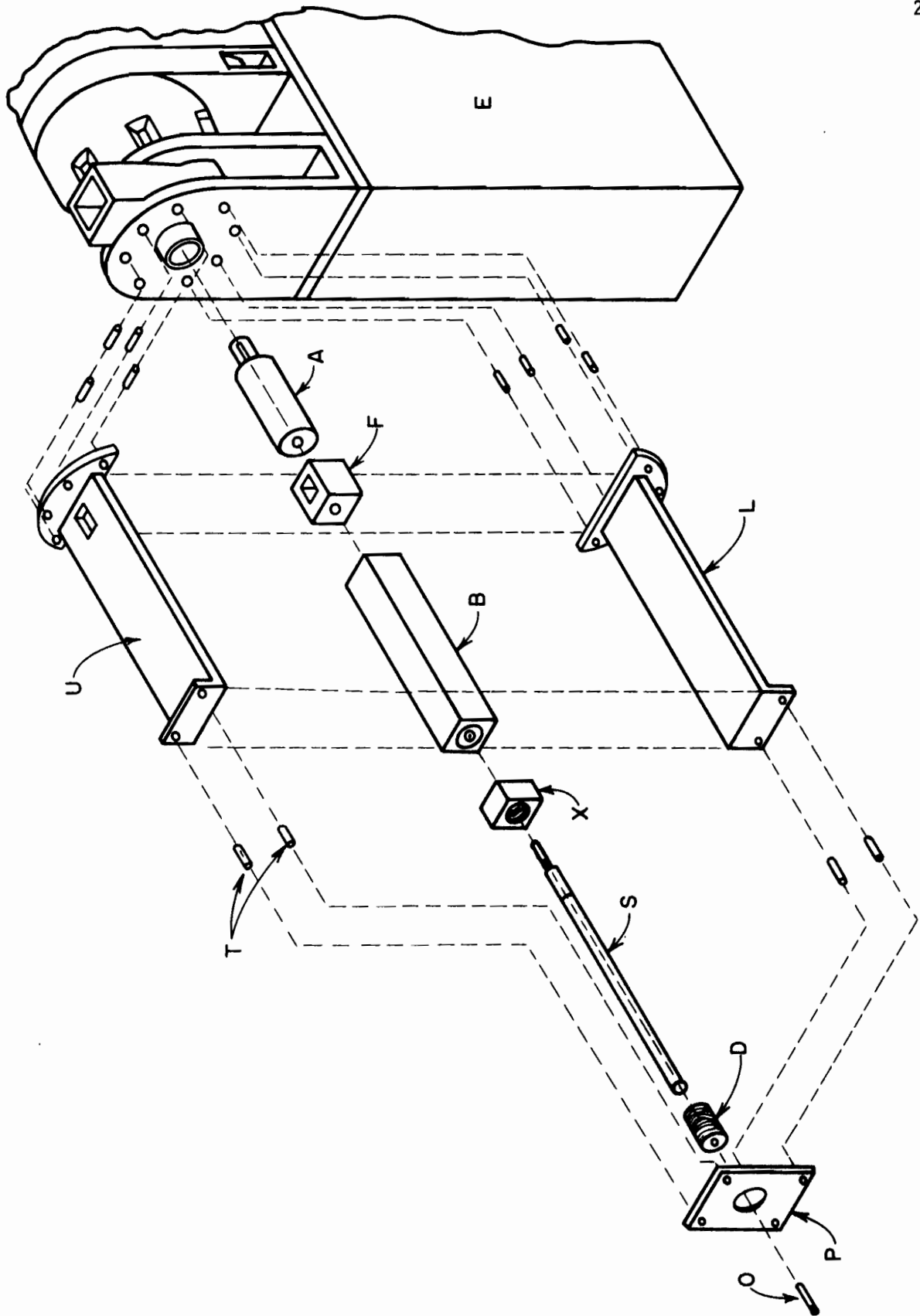
Visual Extrusion Equipment

The extrusion setup used in the visual observations was obtained by modifying a 2-1/2 inch Egan extruder built by the Frank W. Egan and Company of Somerville, New Jersey. The modifications consisted of replacing the existing 2-1/2 inch screw, barrel and die assembly with a metering type 1-inch screw and a transparent barrel. An exploded view of the extrusion setup is shown in Figure 3. Assembly of the system was achieved as described below.

First, the adapter (A), the key-end of which had the same dimensions as the original 2-1/2 screw, was inserted into the thrust-bearing assembly of the extruder (E). Then the lower plate (L) was bolted to the body of the extruder with 3/4-10 NC 2-1/2 inch long studs (T). A 1/16-inch thick 20 x 2-1/2 inch square neoprene sheet was laid along the length of the lower plate (L) to cushion the stresses that might develop as a result of barrel (B) rotation during operation. The metering screw (S) (detail in Figure 4) was then wetted with liquid polymer (to be described later) and gradually inserted into the feed section (F) (detail in Figure 5) and transparent barrel (B) (detail in Figure 6) until its tip appeared at the groove end of the barrel. Wetting of the barrel was necessary in order to avoid scratching the smooth inside barrel surface. The resulting screw-barrel-feed section assembly was then carefully pushed along the lower plate until the

Figure 3. Exploded view of experimental extruder.

- A- Adapter
- B- Transparent Barrel
- D- Die Connector
- E- Egan Extruder
- F- Transparent Feed Section
- L- Lower Plate
- O- Rod Die
- P- Flange
- S- Screw
- T- Studs
- U- Upper Plate
- X- Barrel and Die Connector Support



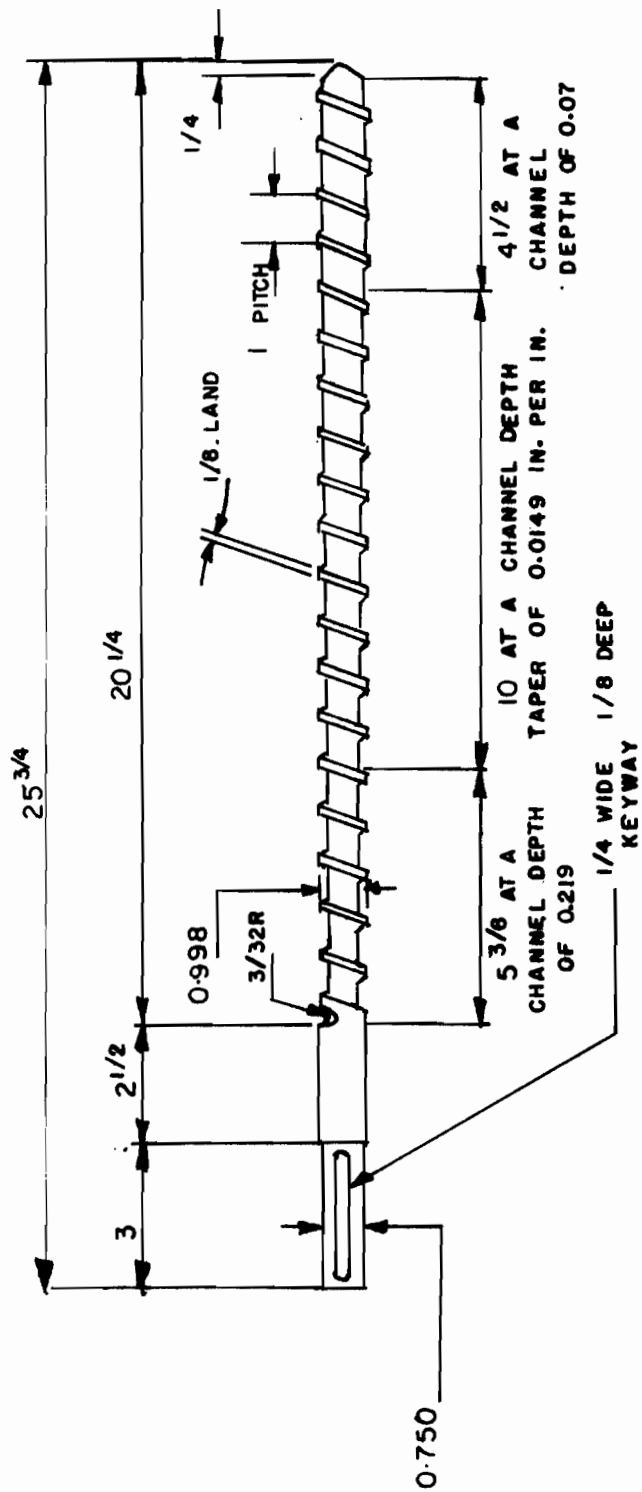


Figure 4. Detail drawing of metering type screw used. Note: All dimensions are in inches.

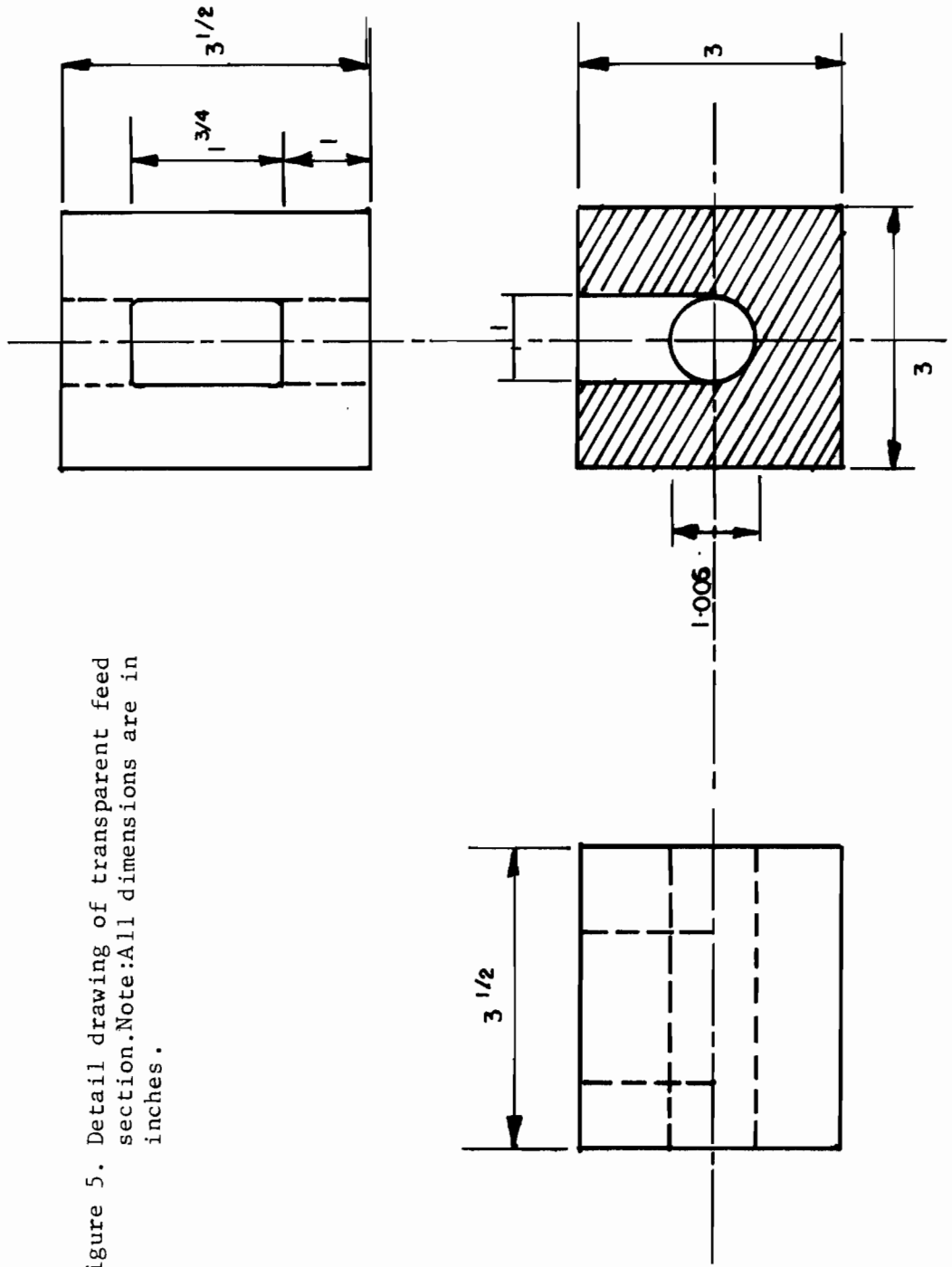


Figure 5. Detail drawing of transparent feed section. Note: All dimensions are in inches.

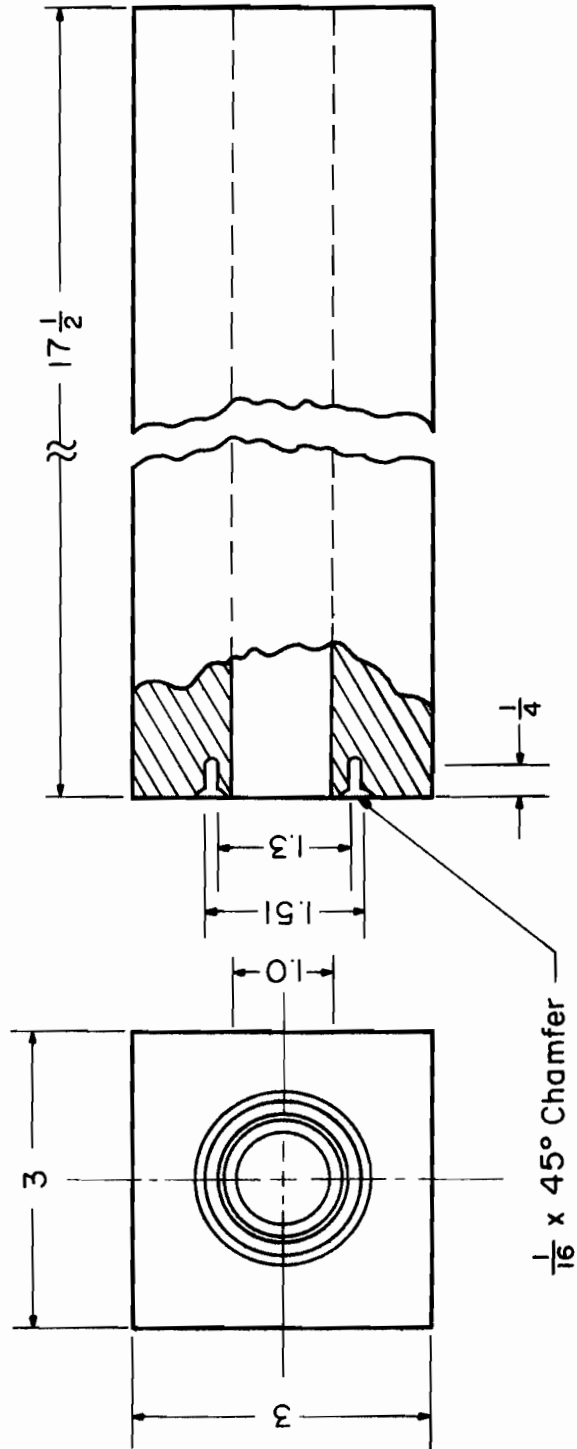


Figure 6. Detail drawing of transparent barrel. Note: All dimensions are in inches.

key-end of the screw barely engaged the adapter (A). Thereafter, the upper plate (U) was laid on top of the barrel and both were pushed into place against the body of the extruder. Subsequently, the barrel-and-die-connector-support (X) was placed between the upper and lower plates and against the grooved end of the barrel.

The die connector (D) (detail in Figure 7) was screwed into (X) until the lip at one of its ends touched the neoprene O-ring, placed in the grooved end of (B), and caused a separation of about 1/4 inch between the adjacent faces of (X) and (B). The flange (P) was then set against (X) and connected to (L) and (U) with 4 studs (T) held in tension with 3/4-NC 10 nuts screwed at both ends. The tension in the studs caused a compressive action against (X), (B), and (F) causing their faces to seal. Several 3 x 3 inch square neoprene gaskets were placed between faces in compression in order to seal the assembly and to absorb any point stresses resulting from misalignment of the parts or overdue tension in the studs (T). The appropriate tension/compression could only be realized through experience. Too large a tension caused the barrel to crack at the groove end; when it was too small polymer leaked between faces. Finally, a 2-1/2 inch long 1/4-inch I.D., "rod die" was screwed into (D). Wooden wedges were hammered in between barrel (B) and upper plate (U) in order to prevent the barrel from rotating. This rotation may have caused failure in some earlier runs because of the generation of point stresses at the edges.

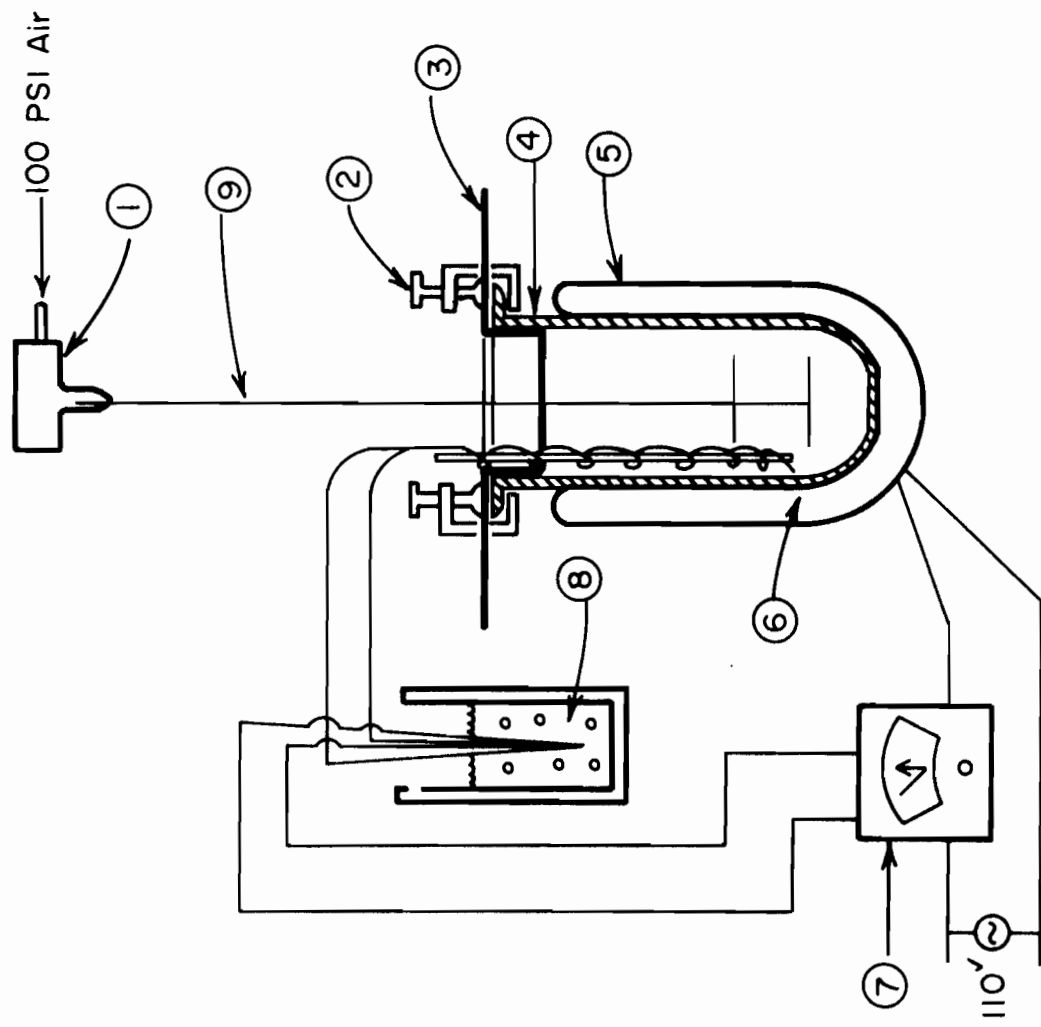
The Extrudate

Feed material to the experimental visual extruder described earlier consisted of frozen particles of 40 percent (by weight) Dylene-2 in Kodaflex plasticizer. Dylene-2 is a natural general-purpose polystyrene of average molecular weight of 270,000 manufactured by Sinclair-Koppers, Pittsburgh, Pennsylvania. Kodaflex is a plasticizer manufactured by Eastman Kodak, Rochester, New York, and is a commercial name for diethyl o-phthalate. The mixture is a viscous liquid at room temperature with a viscosity of about 10^5 poise at 25° C.

The mixture was prepared in 7-pound batches using the apparatus shown schematically in Figure 8. Rodriguez (47) mentioned that plasticization was most rapid and efficient at temperatures in the range 350°-400° F. The upper limit of the range, namely 400° F, was chosen as the plasticization temperature. A copper-constantan thermocouple was used to measure the temperature of the mixture which was controlled by interposing a millivolt indicator-controller (7) in the power supply circuit to the electric heating mantle (5). The steps involved in the preparation of the materials were as follows. First, approximately 1200 grams of Dylene-2 and 1600 ml of Kodaflex were introduced into the 4000 ml resin kettle (4). The double Cowles dissolver (9), a drawing of which is shown in Figure 9, was set in motion. The dissolver was powered by a 100 psig air motor (1) manufactured by the Chemical Rubber Company, Cleveland, Ohio. Nylen and Sunderland (40) recommended the use of a single dissolver to expedite the dissolution of a polymer in a solvent. A double dissolver was used in

Figure 8. Polymer preparation apparatus.

- 1- Air Motor
- 2- Clamp
- 3- Splash Guard
- 4- 4000 ml. Resin Kettle
- 5- Heating Mantle
- 6- Copper-Constantan Thermocouple
Hot Junction
- 7- Millivolt Indicator-Controller
- 8- Thermocouple Cold Junction
(Water-Ice mixture)
- 9- Double Cowles Dissolver



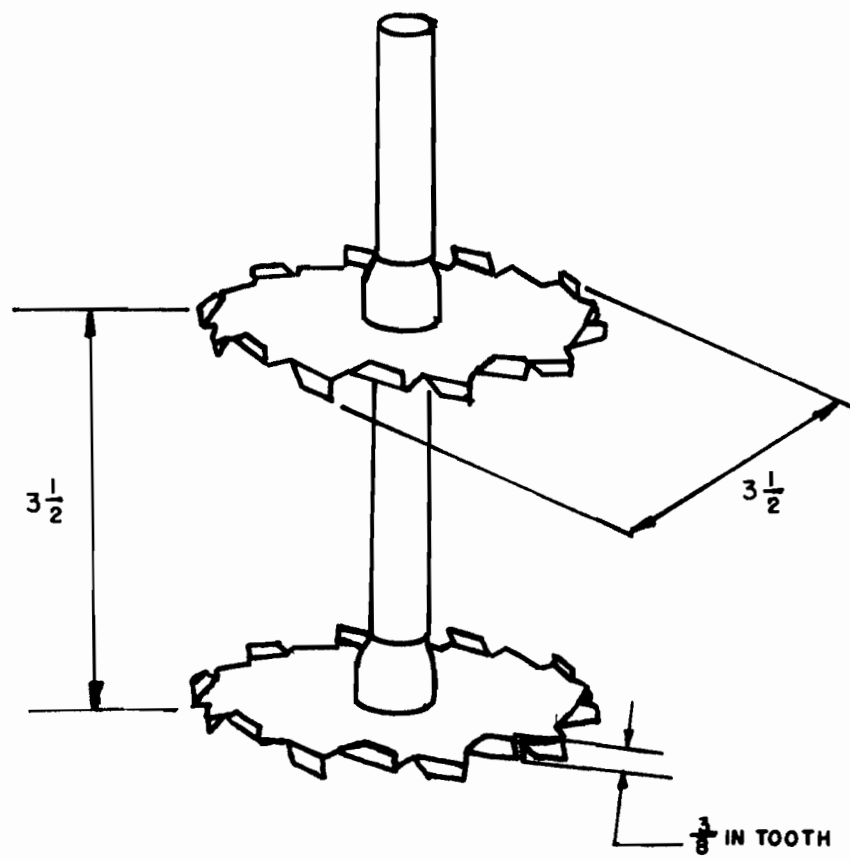


Figure 9. Double Cowles Dissolver.

this instance because of the length of the column of the material to be mixed (about 9 inches). Then the power supply to the heating mantle was turned on until a clear homogeneous product was obtained. The time taken was approximately 1/2 hour. The hot mixture was then poured over the weir-shaped splash guard 3 into a 5-gal steel drum and allowed to cool.

Freezing the mixture into a solid feed material in pellet form was achieved by extruding the liquid at room temperature through a perforated plate (1/32-inch diameter perforations) under air pressure. The pressure vessels used for this purpose consisted of 18-inch lengths of 3-inch cast iron pipe. These vessels were capped at the top and the perforated plates described earlier were screwed into the bottom end. Air under pressure was admitted through a manifold welded into the side of the vessel and toward its top. After the cylinder was charged with polymer mixture and capped, air was admitted and strands of the liquid issued through the perforations. These strands fell directly into 1-gal Dewar beakers filled with liquid nitrogen. Freezing took place rapidly and some strands disintegrated in an explosive manner under the thermal strain. The diameter of the strands was controlled by controlling the air pressure. The resulting frozen "spaghetti" was subsequently emptied into a 1-gal stainless steel Waring Blender and pulverized to an average particle size of about 1/32 inch.

Some of the natural (white) material was dyed in order to facilitate visual observation of material flow in the transparent extruder. A red-colored dye, SUDAN III, and a blue-colored dye,

GENTIAN VIOLET, were used to color small batches of polymer. A 1-gal, sigma-blade mixer was used to dissolve the dye in the polymer mixture. Less than 0.1 gms of each dye was sufficient to impart the respective color to about 1 gallon of the polymer. Frozen pellets of the red and blue material were mixed with the natural pellets in the ratios of 40:1 and 120:1 respectively. These concentrations were experimentally obtained. Higher values caused the dyed material to "dominate" the flow field.

The Transparent Barrel

The transparent barrel was machined from blanks cast in a mold with a 1.006 O.D. polished stainless steel tube fixed along its axis. The internal dimensions of the mold were 3 x 3 x 24 inches. Two sides of the mold were made of plate glass in order to obtain a smooth, highly finished, transparent surface through which observation of the flow could be made. The polished stainless steel tube used in the center also gave a transparent inside barrel surface.

As mentioned earlier, the material from which the barrel was molded was Selectron[®] using ethyl methyl ketone peroxide as "initiator" or hardener. After the mold was assembled and made leak-proof, 3500 ml of Selectron, with 6 ml of hardener mixed in, were introduced in 1750-ml batches. The material was then allowed to gel completely for 2 days at room temperature. The mold was then disassembled and the steel rod was gradually pushed out of the section

using a 60-ton press. The resulting 3 x 3 x 24 inches blank was then ready for machining into the barrel and feed section.

Operation of the Extrusion Setup

Operation of the system was started by first removing polymer from the first two turns of the screw. This liquid polymer was initially present since the screw was dipped in it at the time of assembly. Removal was effected by passing a jet of cold nitrogen gas over the slowly rotating screw and peeling off the resultant solid with the tip of a screwdriver. Then, the rpm was increased to 60 and batches of the frozen pellets were poured continuously into the feed throat. Simultaneously, a 1/2-inch spatula was used to press the column of pellets against the upturning flight. This was continued until the various zones of the flow were clearly developed.

It should be mentioned at this point that extreme difficulty was encountered in gravity-feeding the pellets of polymer through a specially designed hopper. The 1 x 1-3/4 inch feed throat, through which the frozen pellets were introduced to the screw, was adequate insofar as standard designs were concerned. The first 1-1/2 turns of the screw were exposed to the stream of falling pellets. However, the flow characteristics of the pellets were such that their free fall from the hopper was insufficient to satisfy the requirements of the extruder. They behaved as "wet" solids which tended to compact and cling to each other and the walls of the hopper. The hopper used was double-walled such that cooling of the inside wall was achieved by introducing liquid

nitrogen in the space between the inner and outer walls. Because of the problems mentioned above, the use of the hopper was discontinued. Instead, the feed requirements of the screw were satisfied by pressing the 1-3/4 inch column of pellets against the underlying screw turns with a 1/2 inch spatula. The column was continuously replenished by manual means. This mode of feeding proved adequate and was employed in all experimental runs. By this means the inlet flight was always kept full and the control on the feed rate of solids was dictated by the needs of the extruder.

Experimental Runs

The experimental runs consisted of taking 100-foot rolls of color 16 mm film type Ektachrome 7242. This was done for the various zones of the screw at steady and unsteady operating conditions. The camera used in this study was a modified 16 mm Eastman High Speed movie camera Type III manufactured by Eastman Kodak, Rochester, New York. The modifications involved fitting it with a wide-angle lens and replacing its variable speed drive. The wide-angle lens was a f:1.5 13 mm focal length, with Fastax adaptor manufactured by Elgeet Lens Co. (now defunct). The newly installed power drive consisted of a DC motor and a speed controller. The motor was 1/15 HP, 115 volt, Type NSH-34, manufactured by Bodine Electric Company, Chicago, Illinois. The speed control used was manufactured by the Minarik Electric Company, Los Angeles, California. The results of the modifications of the camera were such that

motion pictures of objects 1-2 ft away from film could be taken at framing speeds of 10 to 300 frames per second.

With the movie camera mounted on a movable platform and the axis of its lens perpendicular to the axis of the screw, trial movies of the flow were initially taken in order to determine the amount of detail given by the optical system. The visible length of the screw was 19-1/2 inches. First, movies in which the whole screw was in the field of view of the camera were taken. Then, movies in which only part of the screw was in the view of the camera were taken. Inspection of these movies indicated that insufficient detail was obtained from movies of the whole flow whereas movies of only small portions of it did not allow following the material flow for appreciable lengths of time along the screw. An optimum in detail and ability to follow sections of the flow in the axial direction was obtained by dividing the 19-1/2 inch length into three 6-1/2 inch lengths. The resultant lengths of screw that were visible were termed, starting from the feed end, Zones 1, 2, and 3, respectively. Figure 10 is a schematic of the layout of camera and screw with the above-mentioned zones marked thereon.

A series of steady and unsteady runs were made in which several movies of each zone were obtained in the course of one run. The E-series runs consisted of five 100-ft films of Zone 2 with a camera speed of 90 frames per second and a steady screw speed of 65 rpm. The F-series consisted of ten movies with a camera speed of 90 fps and a steady screw speed of 65 rpm. Unsteady state operation of the screw was induced by introducing either a step increase or step decrease in

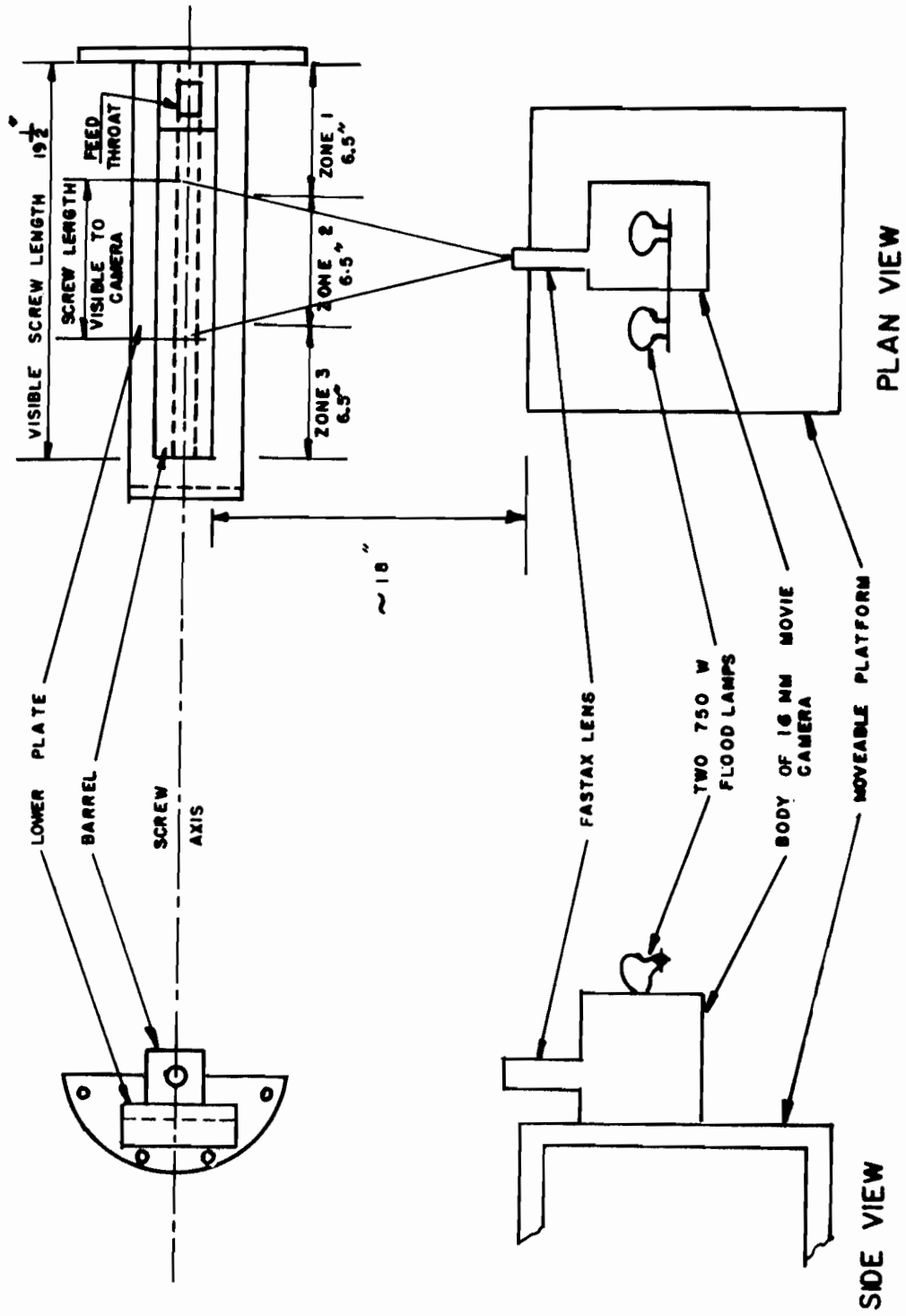


Figure 10. Position of camera relative to screw when taking Zone 2 movies.

the rpm. The G-series consisted of 11 films with a camera speed of 90 fps and screw speeds ranging between 60 and 75 rpm. The H-series movies represented 8 films taken with a camera speed of 10 or 15 fps and screw speeds in the range of 60 to 75 rpm.

The framing speed of the camera was measured by photographing a stop watch that gave time to within 1/10 of a second. Also, color Polaroid pictures of samples of the extruder output were taken using an MP3 Polaroid Land Camera and Type 48 Polaroid film. These pictures were taken to examine the output for degree of mixing and to detect any variability in the conditions of mixing upon changing the screw rpm. Tables 1 through 3 are a summary of the runs taken in each zone together with a listing of the extruder operating conditions under which they were taken.

Table 1. Summary of movies taken in Zone 1 and the conditions under which they were taken.

Movie Designation	Nominal Camera Speed (fps)	Screw Speed (rpm)	Frame Range	Polaroid* Picture of Output
F1	90	65	0-4000	Y
F4	90	65	0-4000	Y
F7	90	65	0-4000	Y
F10	90	65	0-4000	Y
G7	90	60	0-860	Y
	90	75	860-4000	
G8	90	75	0-900	Y
	90	60	0-4000	
G9	90	60	0-817	Y
	90	75	817-4000	
H3	15	60	0-630	Y
	15	75	630-2345	
	15	60	2345-3135	
H6	15	60	0-615	N
	15	75	620-3000	
H7	15	60	0-250	N
	15	75	240-1350	
	90	75	1350-4000	

*Y indicates that a picture of a sample of the output was taken.
N indicates that no picture was taken.

Table 2. Summary of movies taken in Zone 2 and the conditions under which they were taken.

Movie Designation	Nominal Camera Speed, (fps)	Screw Speed, (rpm)	Frame Range	Polaroid* Picture of Output
E1	90	65	0-4000	N
E2	90	65	0-4000	N
E3	90	65	0-4000	N
E4	90	65	0-4000	N
E5	90	65	0-4000	N
F2	90	65	0-4000	Y
F5	90	65	0-4000	Y
F8	90	65	0-4000	Y
G1	90	65	0-540	N
	90	75	540-4000	
G2	90	75	0-630	Y
	90	65	630-4000	
G3	90	65	0-880	Y
	90	75	880-4000	
G10	90	75	0-900	Y
	90	60	900-400	

Table 2. Continued

Movie Designation	Nominal Camera Speed, (fps)	Screw Speed, (rpm)	Frame Range	Polaroid* Picture of Output
G11	90	60	0-900	Y
	90	75	900-4000	
H2	10	60	0-200	Y
	10	75	200-2400	
	15	75	2400-2500	
	15	60	2500-3100	
	15	75	3100-4000	
H5	15	60	0-450	Y
	15	75	450-4000	
H8	15	60	0-450	Y
	15	75	450-1800	
	15	60	1800-2700	

*Y indicates that a picture of a sample of the output was taken.
N indicates that no picture was taken.

Table 3. Summary of movies taken in Zone 3 and the conditions under which they were taken.

Movie Designation	Nominal Camera Speed, (fps)	Screw Speed (rpm)	Frame Range	Polaroid* Picture of Output
F1	90	65	0-4000	Y
F6	90	65	0-4000	Y
F9	90	65	0-4000	Y
G4	90	75	0-900	Y
	90	60	900-4000	
G5	90	60	0-900	Y
	90	75	900-4000	
G6	90	75	0-900	Y
	90	60	900-4000	
H4	15	60	0-300	Y
	15	75	300-1500	
	15	60	1500-2390	
	15	75	2390-2700	
	15	60	2700-4000	

*Y indicates that a picture of a sample of the output was taken.
N indicates that no picture was taken.

PART III

RESULTS AND DISCUSSION

The movies of the 3 zones, taken as described earlier, were used to identify significant events in the extruder under steady and unsteady conditions. The analysis of the movies involved projecting them on an 8 x 11 inch screen. The projector used was a motion analyzer of Kodak Analyst design and modified by LV Photo Products Company. It had the capability of projecting at 1 to 24 frames per second (fps) as well as a manual single frame advancement. This was helpful in the observation of events with a relatively short duration and in the breaking down of events with long duration.

Although the analysis of the movies was primarily directed at achieving a better understanding of extrusion under unsteady state conditions, it was necessary to initially establish the steady state characteristics of the flow. This provided the base conditions and allowed the observation of significant departures due to the transient flow. The steady state picture of the flow will be given first. Thereafter, a discussion of the observed transient characteristics will be presented.

Steady State Conditions

From a preliminary observation of all the movies taken, the characteristics of the steady flow were obtained. Movies taken in

Zone 1 showed the 2 to 3 screw turns of the delay-in-melting zone and the early part of the melting zone. A pure solids conveying section was not amenable to observation in the first few turns of the screw. This region of the flow, which would have probably extended to about an axial length of 2-1/2 inches of the helical channel, was obscured by the "crazing" of the feed section and the formation of a translucent layer of frozen moisture on its outer surface. Zone 2 movies showed the major part of the melting zone which was about 8 screw turns. In Zone 3 movies the last 2-3 turns of the melting zone were observed, and in the rest of the screw length only melt conveying could be seen.

The development of the melting zone conformed to the mechanism proposed by Maddock (30) and later confirmed by Tadmor et al. (59). In the first few turns after solids conveying, a melt film was clearly visible. This film enveloped all the visible sides of the solid bed. These sides were the top of the bed adjacent to the barrel surface, and the two that were adjacent to the advancing and the trailing flights. The melt film adjacent to the advancing flight retained its thickness for 2 to 3 turns in the down channel direction. Then the thickness of this film increased and continued to gradually increase through Zone 2 until melt occupied the entire channel width in the first part of Zone 3. Of course the solid bed width decreased from almost that of the channel to zero at the end of melting. This is schematically represented in Figures 11 and 12. Figure 11 shows a top view of the "unwrapped" helical channel with the three zones of the flow indicated. In Figure 12 the relative positions of solid polymer and melt are indicated. The movement of the

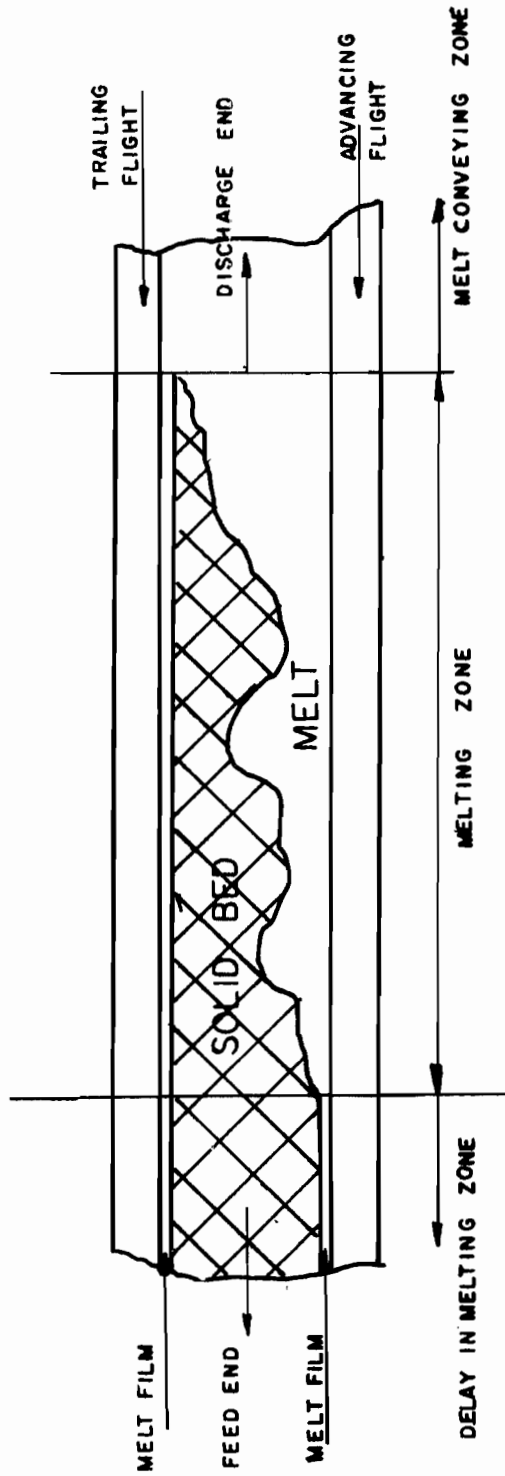


Figure 11. Top view of unwrapped screw channel with polymer.

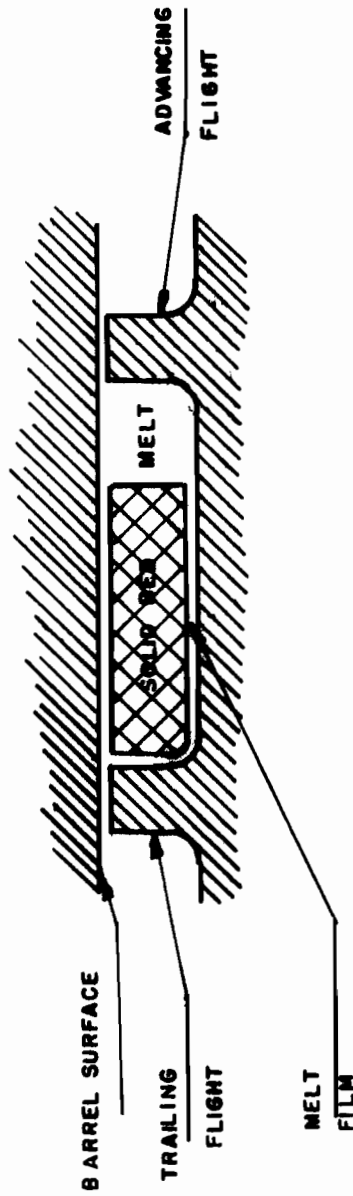


Figure 12. Cross section of the screw channel in the melting zone.

solid bed was followed by observing the progress of the colored solid particles that were visible at its top.

The progress of the colored particles in the down channel direction could be easily followed since they retained both their shape and position for a considerable length of time (over 8 to 9 turns of material). Observation of a single particle or a group of particles was effected by first identifying the shape of the particle or particles and then advancing the film until it or they completed one revolution. This technique was later used to study the dynamics of the process semiquantitatively.

A further confirmation of the melting mechanism was obtained by following the change in particle shape that took place as a result of melting. In addition to the observed "swelling" of the particles, streaks originating from their centroids and directed toward the solid bed melt interface were seen. This is believed to confirm earlier reports of flow lines originating from the top of the solid bed and extending into the melt pool, as found by Maddock and confirmed by Tadmor and Klein (30,59).

Breakup of the solid bed was seen to occur, rather occasionally, in some Zone 2 movies. This phenomenon was exhibited by the separation of 2 to 3 turn sections of the solid bed at a point that was about two-thirds down the channel from the beginning of the melting zone.

All the observations of the melting zone at steady state amplify the findings of past workers. Furthermore, no evidence was found to contradict the overall melting mechanism explained earlier. The melt

portion of the flow was not amenable to observation. The flow patterns that may have been described by the melt were too fine for the optical system to record. However, after melting of the solid bed was completed, small dark elements of material were seen to cross the "bright spots" in the screw channel. These "spots" represented diffuse bands of reflected light along the axis of the screw. The Polaroid pictures taken of samples of the output indicated that mixing was incomplete in the range of screw speeds employed. This was taken to explain the flow of the small dark elements of material previously mentioned.

Dynamics of Melting

As explained in the preceding section, only the melting zone and the solids movement associated with melting were amenable to visual observation. Therefore, the analysis of the visual dynamics was restricted to that of the process of melting. In particular, the analysis covered the effect of step changes in screw speed on the solid bed movement in the down-channel direction. Briefly, the analysis involved observation of the solid bed profile and determination of the velocity of solid movement in the axial direction, under transient conditions.

Solid Bed Rupture

It was found that a severe rupture of the solid bed often took place after the introduction of a step-up in screw speed. This was accompanied by a disruption of the steady state flow régime downstream

from the point where rupture occurred. Instead of a solid bed moving adjacent to the trailing flight with melt adjacent to the advancing flight, islands of solid were seen to be moving with the flow in the down channel direction. This occurred in Zone 1 movies G7, G9 and H6 and in Zone 2 movies G3, H2 and H5. Movies in which a step-down in screw speed was introduced did not show solid bed rupture. These movies were G8 of Zone 1 and G1 and G10 of Zone 2. Also, movies H3 and H7 of Zone 1 in which a step-up in screw speed was introduced did not show the solid bed rupture.

This rupture was different from the separation that was observed at steady state where a ribbon of solid 2 to 3 screw turns long, separated and was conveyed forward by the same steady melting mechanism described earlier. The unsteady state rupture exhibited itself as a cavity formed at an axial distance approximately one-third the length of the screw from its feed end. At that point, the solids appeared to tumble, turn, and fall. Also a portion of the screw surface was obvious. The solids were pushed forward by the advancing flight. An inspection of Zone 1 and Zone 2 movies involving a step-up in screw speed revealed that this phenomenon occurred at an axial position of about 6.5 inches (1/3 of screw length) and at a time between 2 to 3.5 seconds after the introduction of the step change. This phenomenon is schematically shown in Figure 13 where the location of the solid bed rupture is indicated.

The development, in time, and actual location of rupture were observed from an analysis of movie G7. Magnified (5 x 7) photographic prints of a number of frames, located before and after the change in

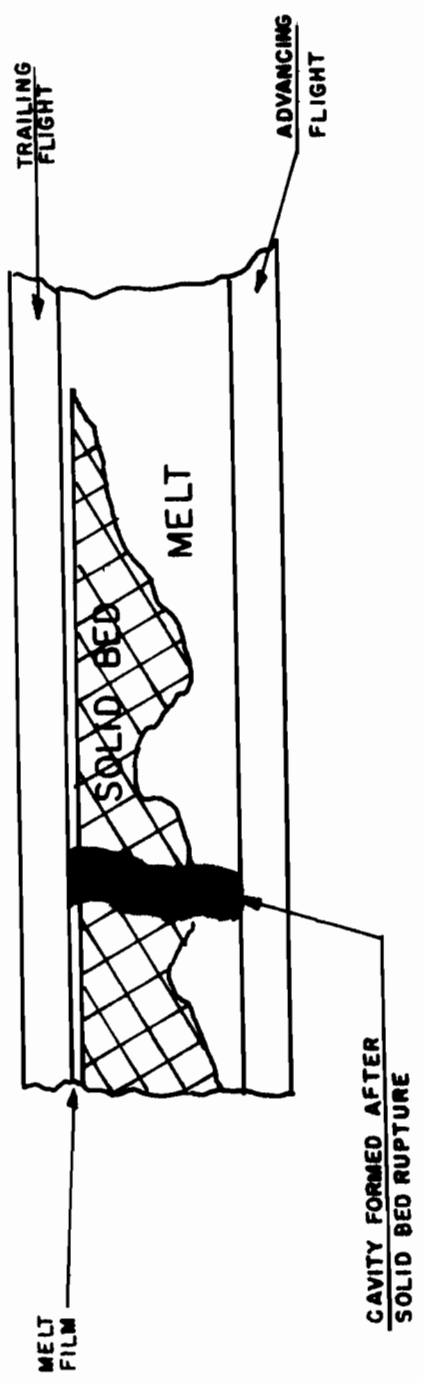
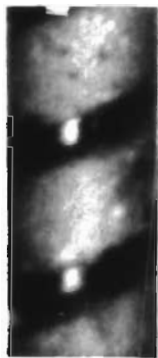


Figure 13. Top view of unwrapped screw channel at instant of solid bed rupture.

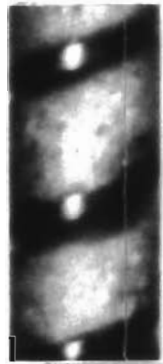
screw speed, were obtained. Segments of these frames, showing the screw between axial lengths of 5.8 and 8.4 inches, are presented in Plate I. The times which these segments represented were calculated by noting, for each, its displacement (as the number of frames) from the frame at which the screw speed was changed (frame 860 for this case as shown in Figure 27). The displacement was considered negative if the frame was located before the transient and positive otherwise. Reduction of the displacement to time involved division by the measured framing speed of 89 frames per second. An inspection of Plate I shows that solid bed rupture was first sighted at 2.52 seconds after the transient. From that time onward the steady flow régime (represented by the time sequence between -1.35 to the time of rupture) progressively deteriorated as seen in the time sequence from 2.52 to 31.42 seconds. In these latter frames, the channel is seen to be partially filled with solids. It should be noted that a layer of melt adjacent to the pushing flight (that which is to the right) persists in the screw turn immediately to the right of that in which rupture occurred. This clearly indicates that the steady state melting process is undisturbed at locations upstream of the point of rupture. This also leads one to believe that inadequate feeding of solids to the upstream flow is precluded as being directly responsible for solid bed rupture.

A possible explanation for the rupture may be as follows: The solid bed is a compact mass of solid polymer particles surrounded by polymer melt. The melt may in part also fill the voids of the solid. Since past evidence (48) indicated no internal shearing of the bed, it seems fair to assume that the bed velocity is the same as that of the

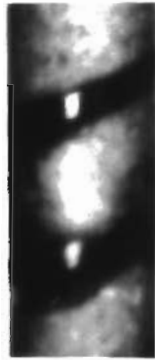
DIRECTION OF INCREASING AXIAL DISTANCE



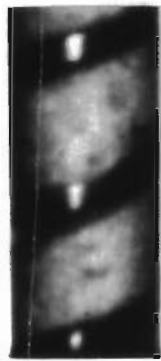
-1.35



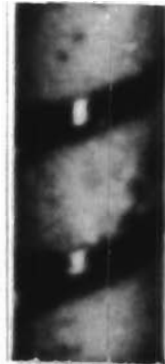
0.00



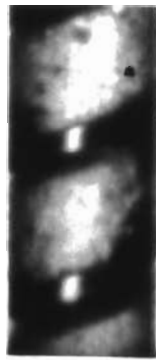
0.94



-0.90



0.31



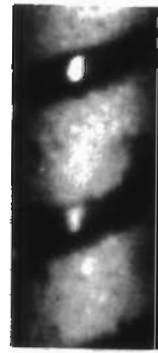
1.26



-0.45



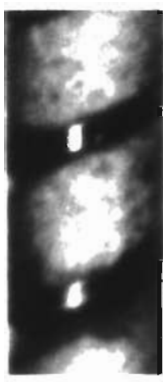
0.63



1.57

PLATE I. A SEQUENCE OF SCREW PICTURES TAKEN FROM MOVIE G7 AND SHOWING THE DEVELOPMENT, IN TIME, OF THE PHENOMENON OF SOLID BED RUPTURE BETWEEN AXIAL LOCATIONS OF 5.8 AND 8.4. THE TIMES REPORTED BELOW EACH PICTURE ARE REFERRED TO THE TIME AT WHICH THE SCREW SPEED WAS CHANGED FROM 60 TO 75 RPM.

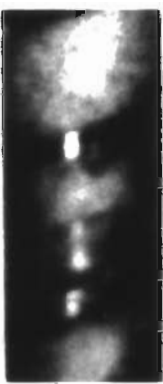
DIRECTION OF INCREASING AXIAL DISTANCE



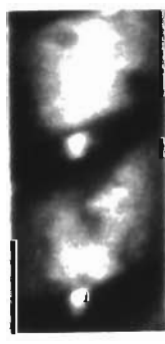
1.89



2.83



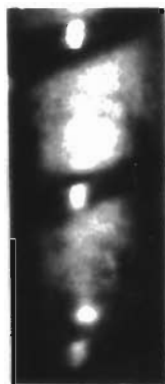
7.19



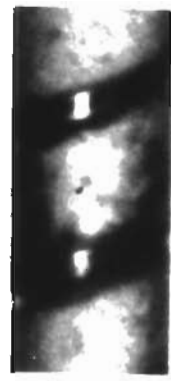
2.20



3.03



7.50



2.52



3.35



7.82

DIRECTION OF INCREASING AXIAL DISTANCE



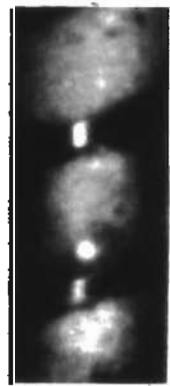
10.56



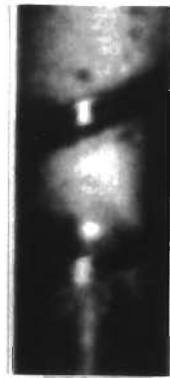
12.81



17.30



10.88



13.12



17.62



11.19



13.44

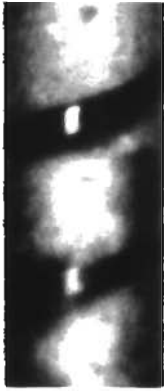


17.93

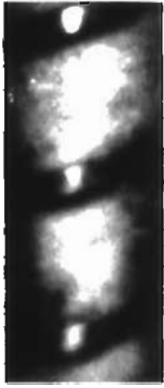
DIRECTION OF INCREASING AXIAL DISTANCE



24.04



27.42



30.79



24.36



27.73



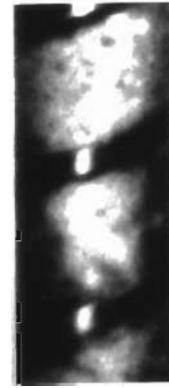
31.10



24.67



28.04



31.42

layer of melt in contact with its bottom side and facing the screw surface. This layer may be seen in Figure 12. A transient in the screw speed would, therefore, be transmitted to the solid bed through that layer of melt. The rise of the velocity of the solid bed in the down channel direction, to the new higher level would be expected to reflect the transient response of the layer of melt when a sudden shearing motion is applied to it. The transient response of viscoelastic liquids to suddenly impressed shearing forces has been studied and documented. For example, Lee and Brodkey (27) obtained data for a material similar in rheological properties to the one under consideration, namely, concentrated solutions of polymethylmethacrylate in diethylphthalate plasticizer. The transient response of such materials also depends on temperature. As the temperature is increased the time necessary for equilibrium conditions to be established, decreases. This was verified by studying the transient response of the liquid extrudate in a cone-and-plate viscometer. There, it was noted that decreasing the temperature from 65° F to 0° F (close to the melting point of the polymer), the time taken to reach equilibrium after a step change in shear rate was introduced, increased from about 1 to 100 seconds. Therefore, it was concluded that axial temperature gradients in both the barrel and screw could be responsible for the solid bed rupture. Such temperature gradients could induce a more sluggish response in the melt film at the colder feed end of the screw. As a result, a momentary imbalance in the shear forces, responsible for the forward motion of the solid bed, may be set up. The net effect of this imbalance may be an increase in

material flow, in regions that are closer to the die end of the screw, that is not compensated for by a corresponding increase in material flow in regions that are closer to the feed end. Consequently, a net tensile force that is greater than the tensile strength of the solid bed may be created. This will cause the solid bed to rupture at a point where the axial temperature gradient is relatively steep. The material downstream from such a point is, therefore, conveyed faster than material upstream.

In contrast to the solid bed rupture as explained above, the separation of segments of the solid bed (2 to 4 screw turns long) under steady state conditions is different in two respects. First, with respect to location, the separation was found to occur at axial distances of $1/2$ to $2/3$ the length of the screw; the taper in the compression section of the screw has been found to delay its occurrence (60c). Secondly, no tumbling of the particles of solid was seen to occur. The void created by the steady state separation was quickly filled with melt. It seems that sufficient melt was available to fill the gap created by the separation in contrast to the rupture.

Recovery of the flow regime to that of the steady state has been estimated to occur during a time period of 5 to 10 minutes after the transient. The recovery process was not recorded because of the relatively short length (100 ft) of the films employed. At camera framing speeds between 15 and 90 frames per second, the time of observation was in the approximate range of 1 to 4 minutes. The estimate of the time for recovery was made by noting that each run (or movie) was started with a

steady state. From a knowledge of the sequence in which the movies were taken and the time span of each movie (number of frames divided by the framing speed) an approximate calculation of the time of recovery could be made. The estimate given above was made from observation of movies H2 and H3.

In providing a rational explanation for the incidence of solid bed rupture, the basic assumptions used were that screw motion was transmitted to the bed through a layer of melt and that the transient response of the bed closely followed that of the melt film. This was substantiated by the analysis of indirect measurements of solid bed velocity under transient conditions, to be presented shortly.

Transient Solid Bed Profiles

The incidence of solid bed rupture observed in Zone 1 had a marked effect on the melting flow régime downstream from the point where it originated. This effect was noted by constructing solid bed profiles before and after the transient. These profiles revealed many aspects of the departure of the flow from steady state.

The profiles were constructed from visual information recorded on Zone 2 movie H5. This movie contained a record of a transient involving a step-up in screw speed. Preliminary observation of this movie showed a "mild" disruption of the flow for about the first 50 seconds after the transient and a severe disruption thereafter. In the first 500 seconds the disruption was restricted to a separation of short ($1/2$ to $1-1/2$ screw turns long) segments of the solid bed and considerable

meandering in the melt-solid interface. As expected, this was accompanied by an increase in the length of melting. This length is the helical (or axial) length of the screw channel in which solid and liquid are seen to coexist. The latter part of movie H5 showed a severe rupture in the solid bed at an axial distance that is 1 or 2 screw turns away from the start of the visible field of Zone 2. Upstream from the void caused by this rupture, melting was seen to occur in the "normal" steady state manner. At that point, particles of solid were seen to fall rapidly into the void which was noticeably lacking in melt. Further down from this void, streaks of solid were seen to permeate the entire melt-filled channel. Some of the solid appeared to be "floating around". This state of affairs persisted throughout the latter part of the movie.

A more detailed summary of the events taking place in this movie can be seen in a series of solid bed profiles presented in Plate II. These were obtained by a method (given below) which implied "unwrapping" of the helical screw channel as schematically shown in Figure 12. The solid bed obtained from the steady state melting process is given by the first profile at 0.73 seconds after the transient. There it is seen that the solid bed progressively decreases in thickness and is reduced to thin streaks of unmelted solid in the latter third of the "unwrapped" helical length. The next two profiles at 1.73 and 3.00 seconds show an increase in the length of melting together with increased meandering of the thin streaks of solid (appearing as dark clouds in the field) in the latter third of the profile. The seven profiles between 4.2 and 57.13 seconds show the separation of short

TIME AFTER
TRANSIENT
(SECONDS)

0.73



1.73



3.00

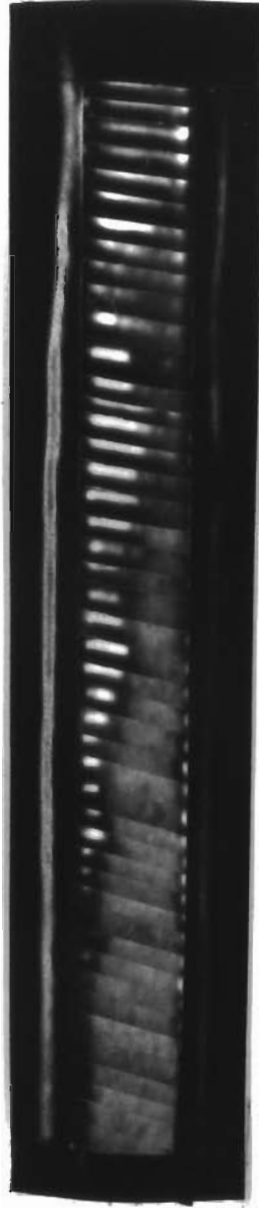
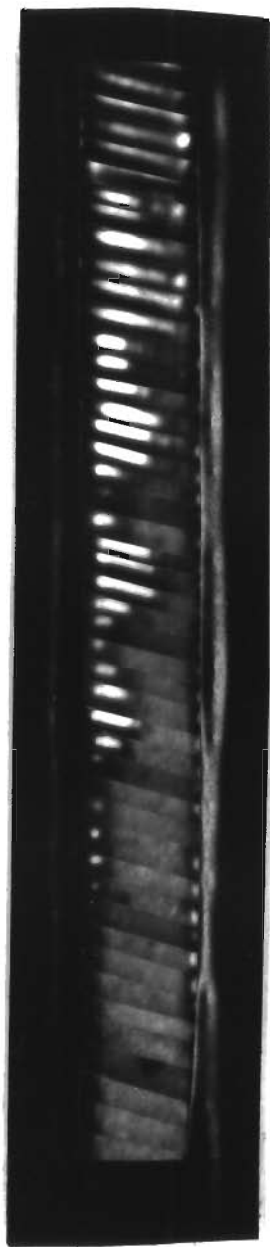


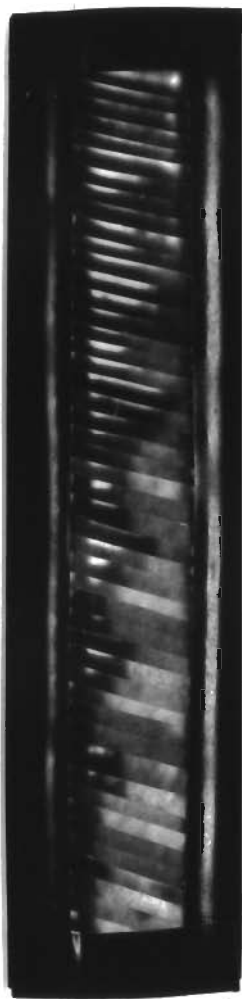
PLATE II. TRANSIENT SOLID BED PROFILES OBTAINED FROM MOVIE H5
AT DESIGNATED TIMES AFTER CHANGE IN SCREW SPEED

TIME AFTER
TRANSIENT
(SECONDS)

4.20



4.80



17.20

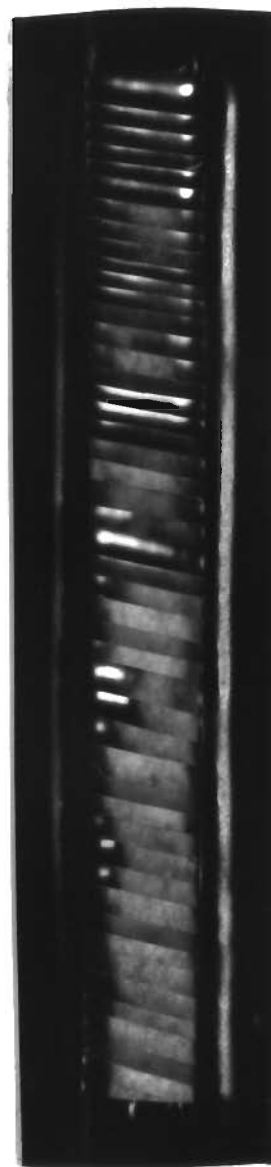
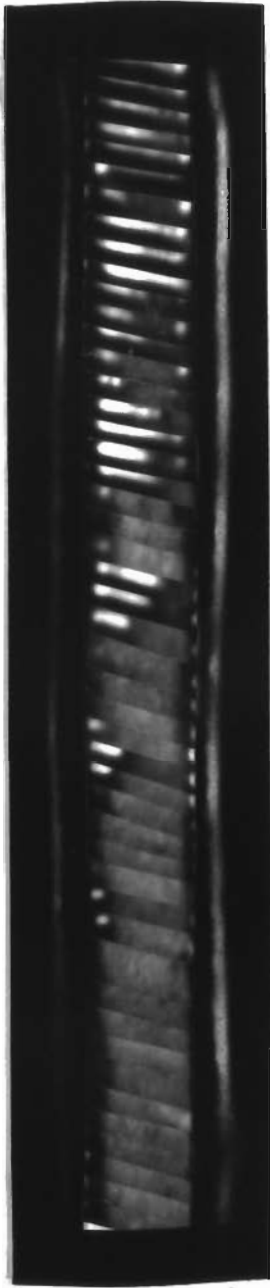


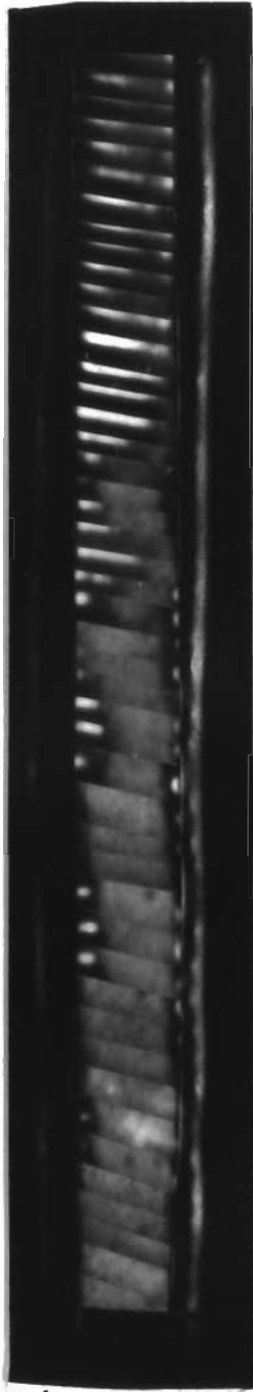
PLATE II. CONTINUED

TIME AFTER
TRANSIENT
(SECONDS)

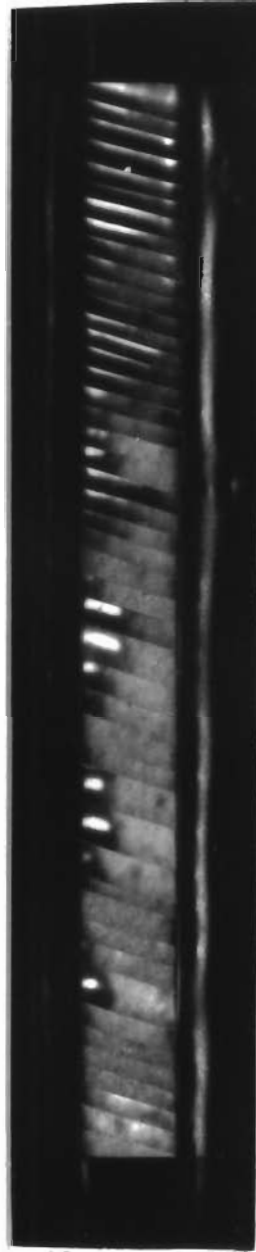
53.53



54.73



55.93



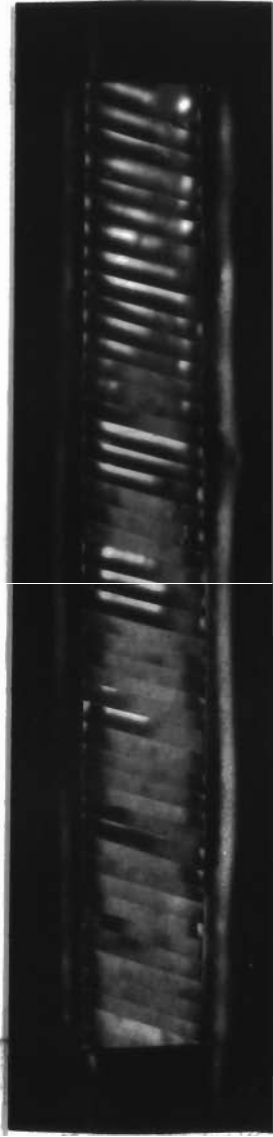
66

PLATE II • CONTINUED

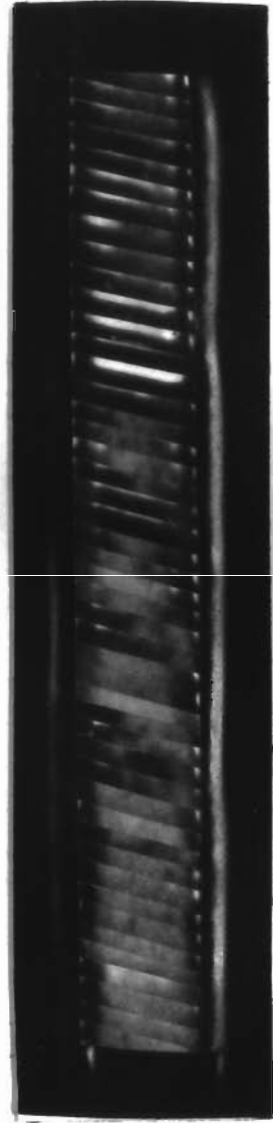
TIME AFTER
TRANSIENT
(SECONDS)



57.13



60.73



64.33

PLATE II. CONTINUED

TIME AFTER
TRANSIENT
(SECONDS)

93.87



133.86



180.53

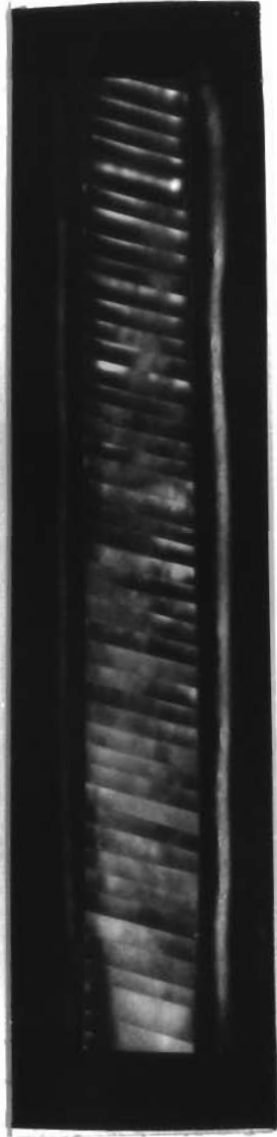


PLATE II. CONTINUED

(approximately 1 screw turn) segments of the solid bed. These segments appear as maxima interposed between consecutive minima in solid bed thickness. The formation of these segments can be explained on the basis of the mechanism for rupture of the solid bed as previously explained. In this case a void in the screw channel will not form since enough melt is available to quickly fill it. In the last five profiles (between 60.73 and 180.53 seconds) the severe rupture of the solid bed, mentioned earlier, apparently caused the solid to disperse in the liquid phase thereby spreading it over the entire channel. The "suspended" solid would be dragged forward by the melt. The net result is a loss of melting capacity since viscous dissipation in the melt film between the top of the solid and the barrel is lost as a source of heat necessary for melting. This will undoubtedly lead also to a deterioration in the quality of the product.

The construction of the solid bed profiles presented in Plate II was achieved in the following manner: The parts of the movie which were of most interest were first noted. Then the time taken by a point (colored particle) on top of the solid bed to make one complete revolution was obtained as the total number of frames for each particle revolution. The details of how this was done are presented in the Appendix. The results for movie H5 showed that about 22 frames were required for each revolution of a particle (and hence for the entire solid bed) as seen from an inspection of Table 11 for frame numbers above 500. It was determined that only six frames (out of a possible 21) were necessary to give a reasonable representation of the solid bed

profile. Three-sixteenths-inch wide elements of the total helical flow were obtained from magnified (5 x 7) prints of each frame in the manner shown in Figure 14. Only elements representing one channel width along the axis of the screw were taken. Each frame gave 8 such elements. A total of 48 elements were then used to construct the profiles presented in Plate II. The grouping of the elements was done by laying each set of elements, side by side, trailing edge to the bottom. There were 8 sets of 6 elements each. For the first set the first element from the first frame was laid down first. Then the first element from the second frame followed by the first element from the third frame and so on through the first element of the sixth frame. This gave an "unwrapped" version of the first turn of material. Considerable attention was given to "matching" the elements at points of contact as they were laid down in order to eliminate artificial discontinuities that may result from an insufficient number of elements describing the "unwrapped" picture of one turn of the screw. This "matching" process resulted in a reduction of the total helical length obtained, since only part of the 3/16 inch width of each element was utilized.

The profiles obtained in this manner are considered to be "compressed" versions of the true profiles. The length of the helical channel in Zone 2 is about 27 inches. The profiles gave an actual length of about 10 inches. This is about 1/3 the actual length. Using, for example, elements 1/16 inch in width would require about 54 frames (as compared to the 6 used here) for "unwrapping" of each revolution of the helix. This is obviously too laborious and is beyond the resolution

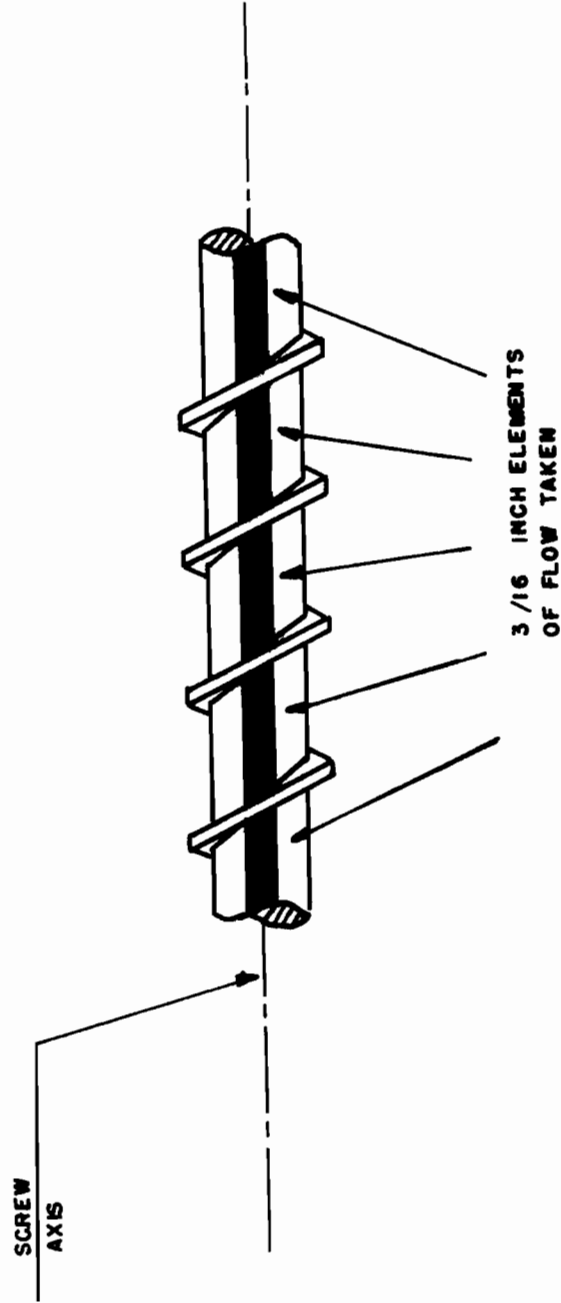


Figure 14. A schematic representation of the method employed in obtaining elements of the helical flow which were later used in constructing the solid bed profiles.

obtained from movie H5 (which had only 22 frames per revolution). Profiles obtained in the manner described would be accurate under steady state conditions; however, this limitation is not critical since drastic changes in the profiles took place over a period of time that is much longer than that over which the 6 frames were obtained (about one second). This is apparent from inspection of the profiles between 4.2 and 55.93 seconds after the transient. These six profiles indicate the same general pattern of behavior. The same may be said of the three profiles between 93.87 and 180.53 seconds after the transient. The differences in length between the profiles are a result of the "matching" process in which only part of the 3/16 inch width of each element was actually utilized.

Transients in Solid Bed Velocity

In order to substantiate some of the assumptions regarding the mechanism of solid bed rupture, measurements of its axial velocity were made from movies in which this phenomenon either did or did not take place. In Zone 1 colored particles in the solid bed could be followed between axial distances in the range of 3 to 6.5 inches. Particles in Zone 2 could be followed between axial distances of 5.0 to 11.0 inches. Zone 1 movie G7 was a record of a step-up in screw speed and showed severe rupture in the solid bed at an axial distance of about 6.0 inches. Zone 2 movies G3 and H5 represented step-ups in screw speed and showed the consequences of solid bed rupture at axial distances downstream from about 6.0 inches. Movie H7 showed a case where no rupture in the solid

bed occurred upon a step-up in screw speed. It also was taken in such a way as to cover some of Zone 2 in addition to covering Zone 1. This helped to follow particles between axial distances of about 3.5 to 10.0 inches.

Where possible, the axial displacements of the colored particles marking the top of the solid bed were measured as a function of time from the movies just described. Measurements for individual particles were taken between the time they were sighted and the time they either melted or disappeared from the field covered by the optical system. The details of time-axial distance measurements for movies G7, H7, G3 and H5 are presented in the Appendix. Plots of the data taken appear in Figures 15 through 18 for movies H7, G7, H5 and G3, respectively. The time at which the step-ups in screw speed were introduced were marked for each case. At the right of each figure are sketched the geometries of the section under study. Calculation of the axial velocity of the solid bed at any point in the zone under consideration was achieved by drawing best curves through the data and taking the slope of the curve at that point. Figures 19 through 22 give the calculated axial velocity with time for movies H7, G7, G3 and H5, at specific axial locations. An inspection of the plots, with "best" curves drawn through the points, favors the explanation, offered in the last section, for the incidence of solid bed rupture. Where no rupture occurred, the transient profile for the axial velocity has the shape given in Figure 19. This shows a gradual increase of the velocity to the new steady state value. The transient velocity profile at a point upstream from a bed rupture shows

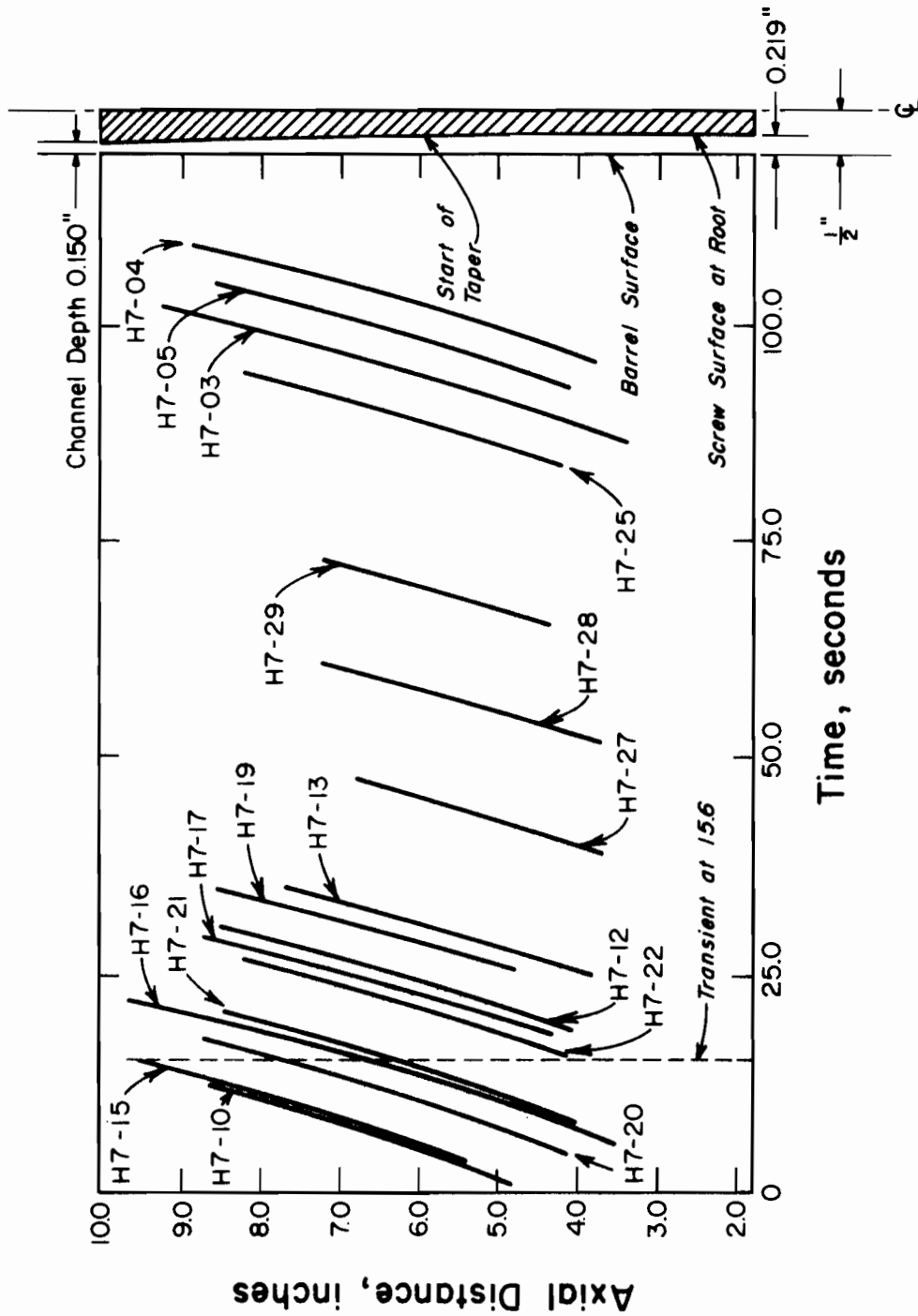


Figure 15. Axial displacement of solid bed as a function of time obtained from observation of solid particles indicated for movie H7. The variation of channel height with axial distance is shown schematically to the right of the figure.

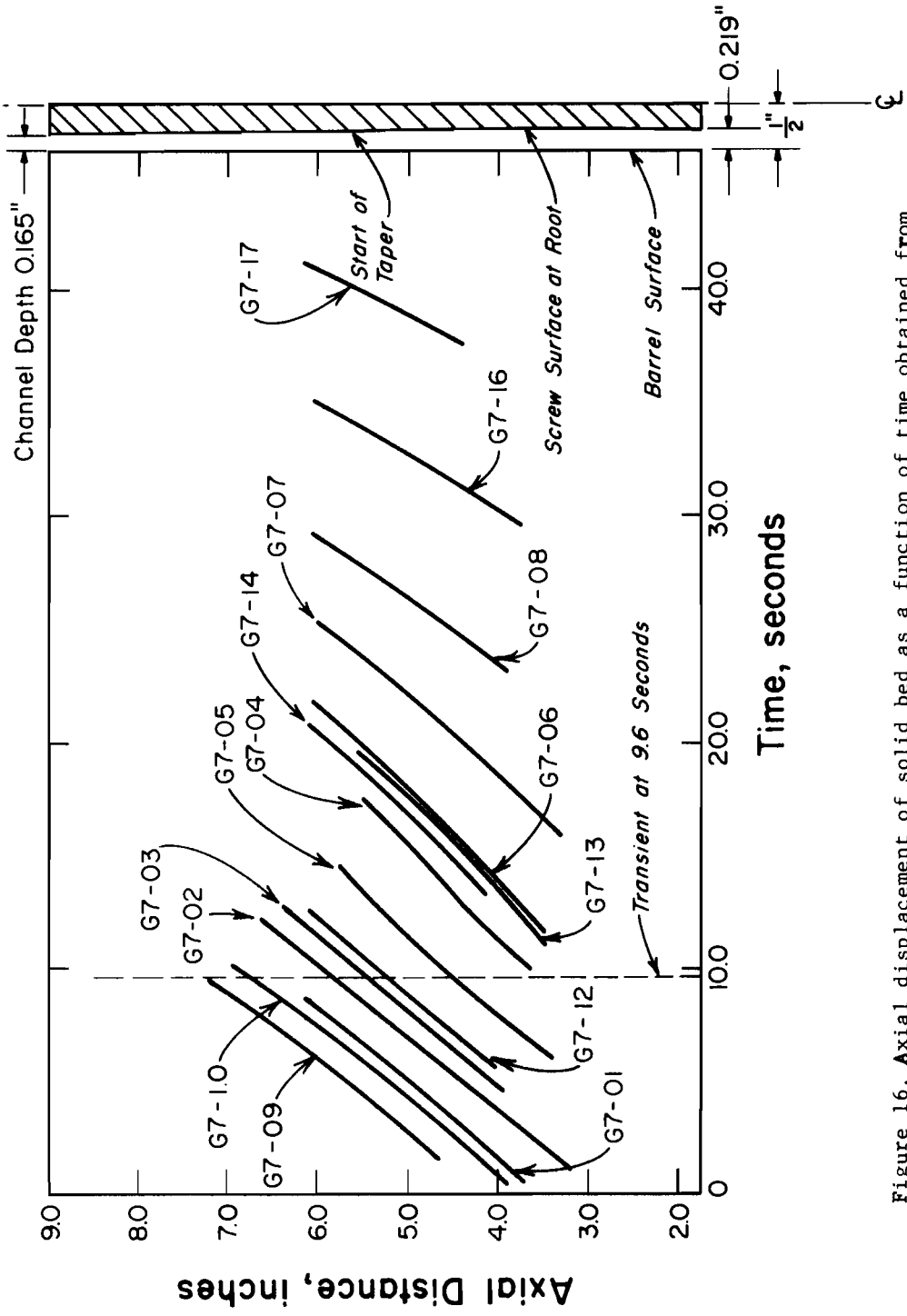


Figure 16. Axial displacement of solid bed as a function of time obtained from observation of solid particles indicated for movie G7. The variation of channel height with axial distance is shown schematically to the right of the figure.

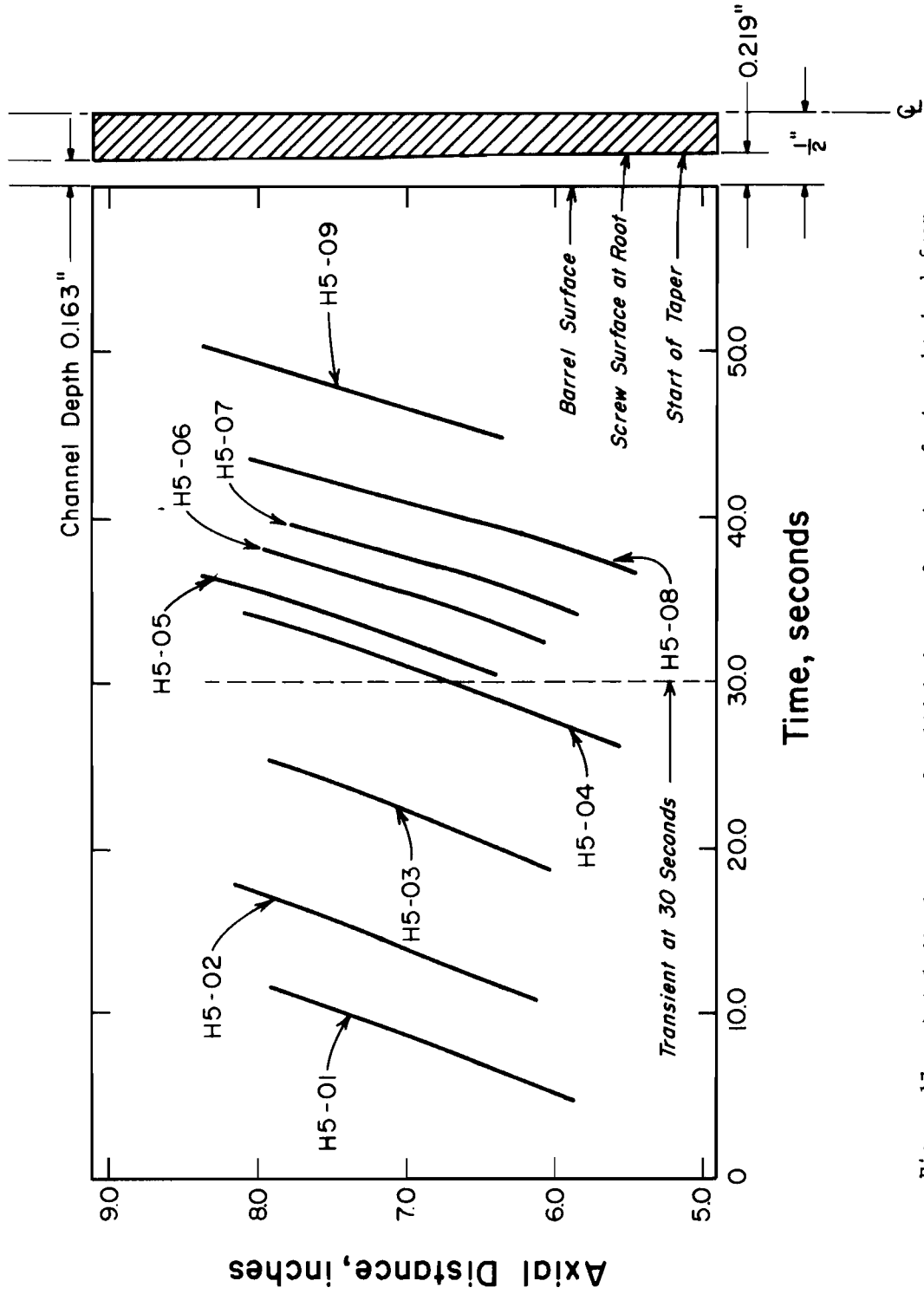


Figure 17 . Axial displacement of solid bed as a function of time obtained from observation of solid particles indicated for movie H5. The variation of channel height with axial distance is shown schematically to the right of the figure .

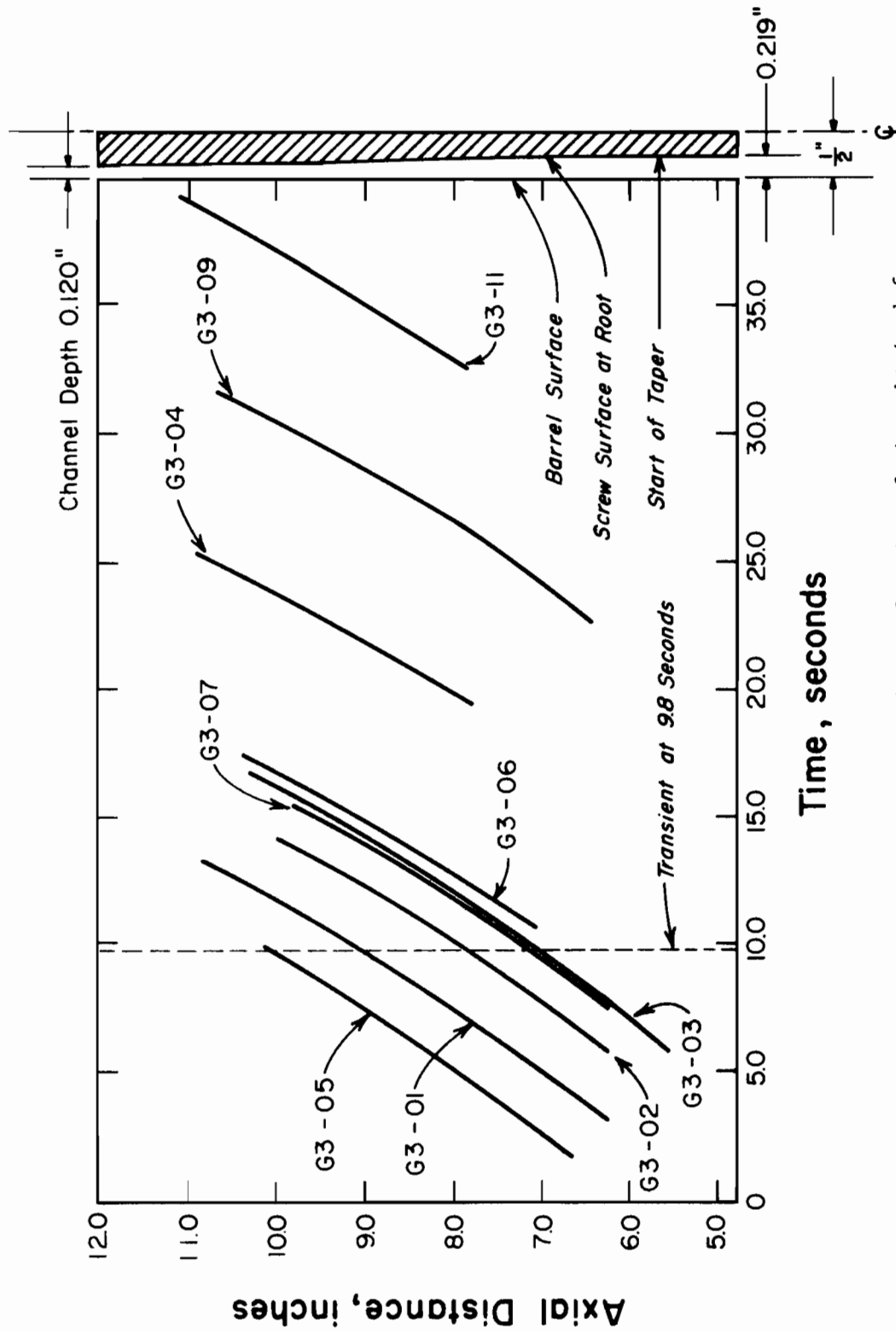


Figure 18. Axial displacement of solid bed as a function of time obtained from observation of solid particles indicated for movie G3. The variation of channel height with axial distance is shown schematically to the right of the figure.

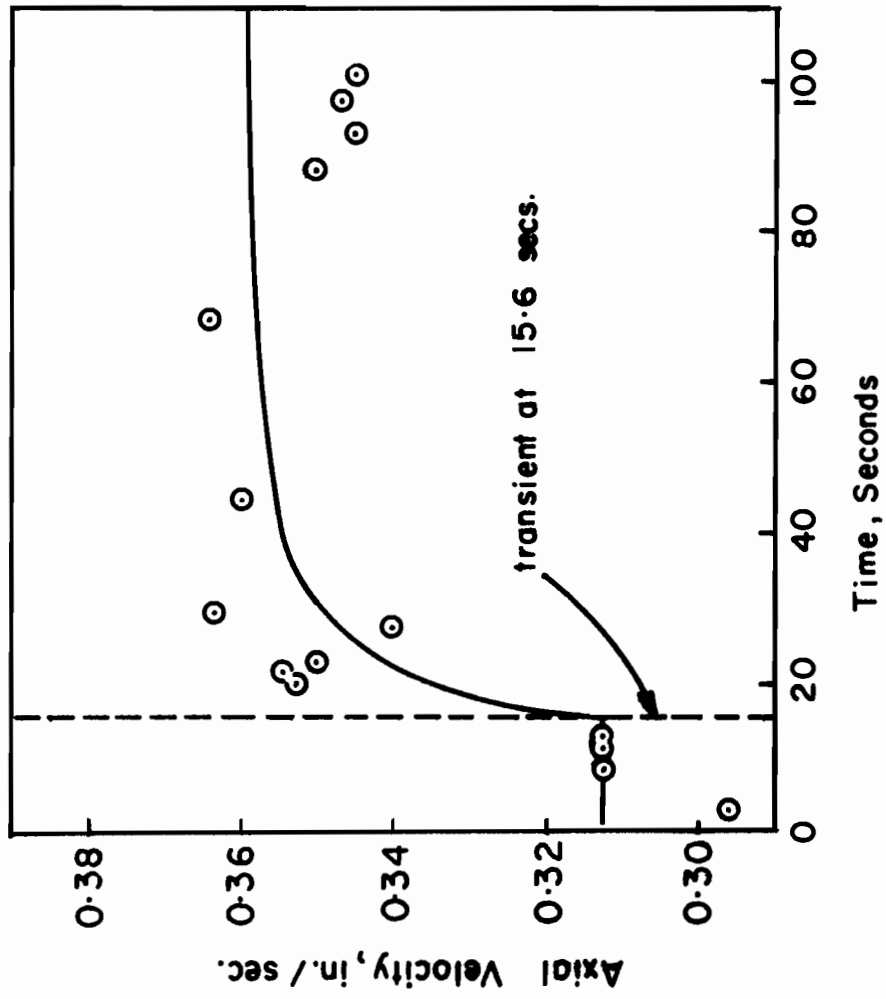


Figure 19. Transient axial velocity profile at axial distance of 5.5 inches for movie H7.

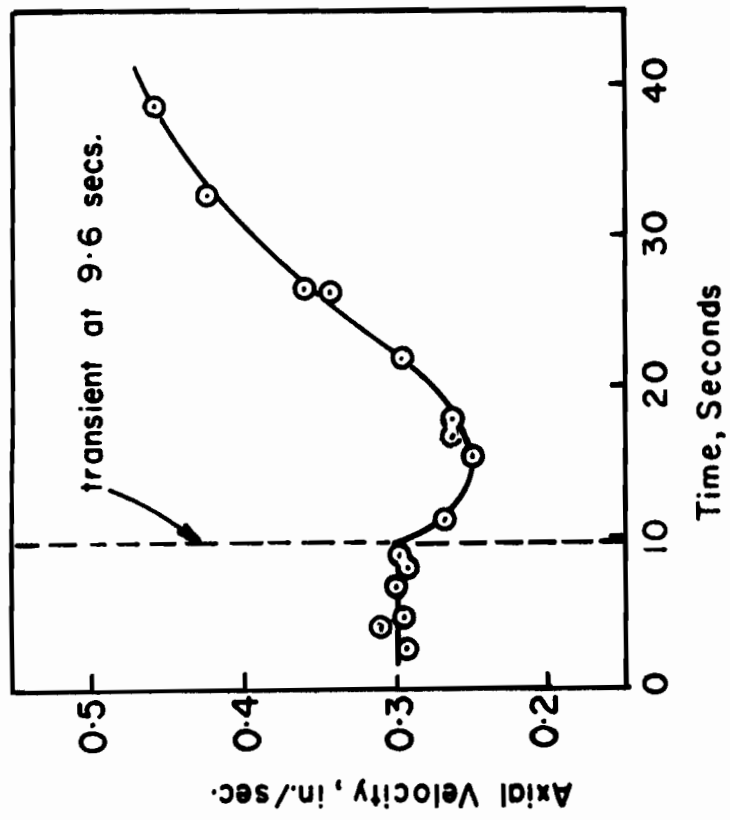


Figure 20. Transient axial velocity profile at axial distance of 5.0 inches for movie G7.

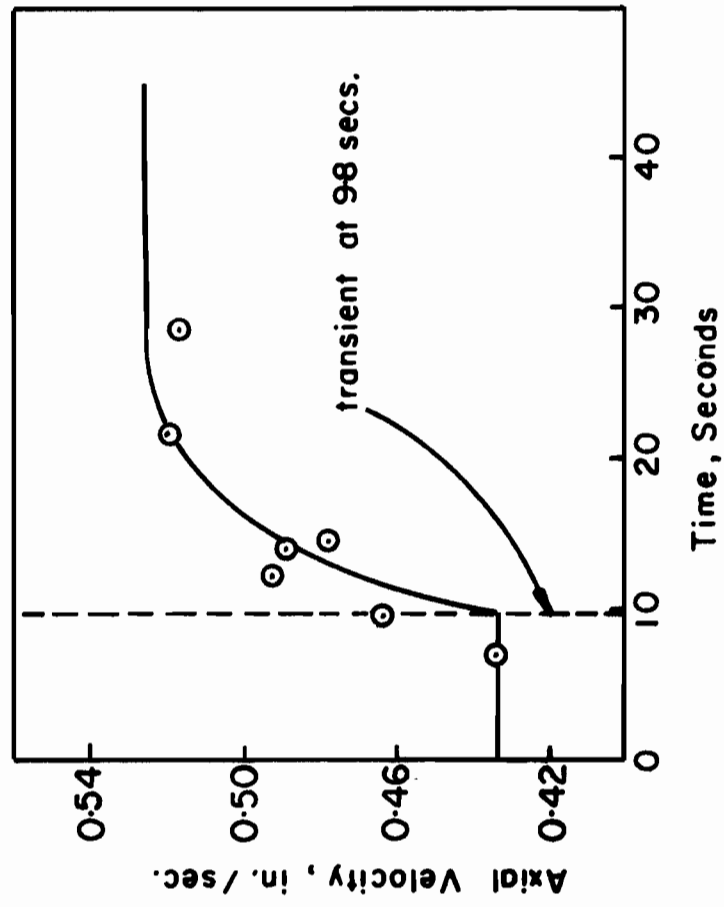


Figure 21. Transient axial velocity profile at axial distance of 9.0 inches for movie G3.

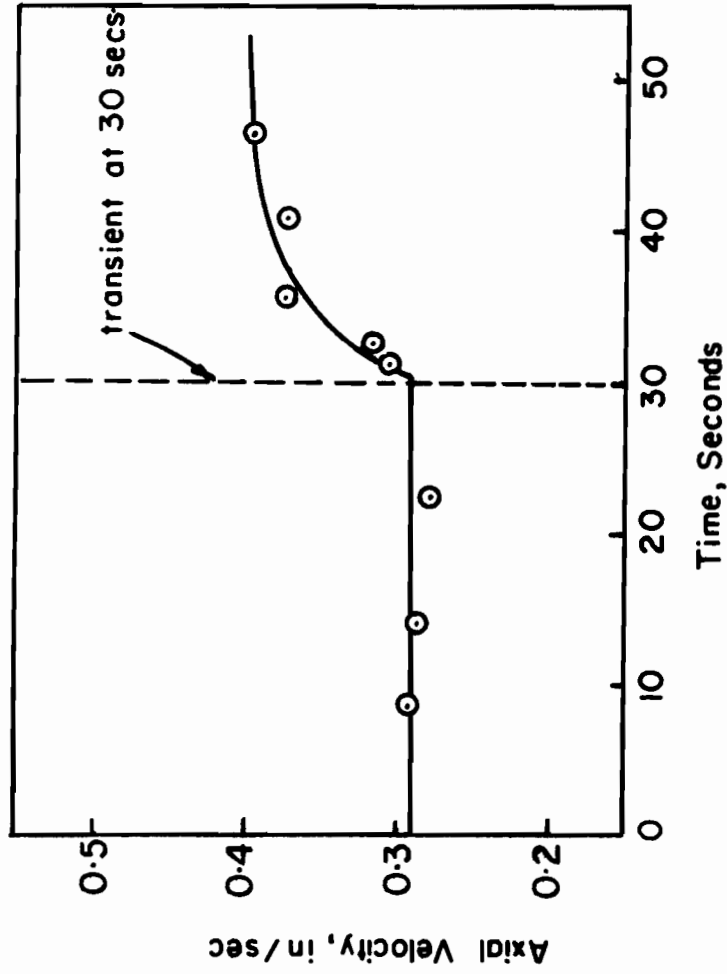


Figure 22. Transient axial velocity profile at axial distance of 7.0 inches for movie H5.

a decline as shown in Figure 20. This decline is attributed to a progressively decreasing solids conveyance as a result of a lack of contact between the melt film coating the surfaces of the screw channel and the solid bed at the point of bed rupture. This contact is necessary for solids conveyance in the melting zone since the screw movement is transmitted to the solid bed through the aforementioned melt film. Downstream from the point of rupture the transient in axial velocity describes a pattern similar to that given by the case of no solid bed rupture. This would be the case especially at times immediately after the transient. Evidence of this is given in Figures 21 and 22. Therefore, the overall effect of solid bed rupture is a decrease in the rate of material conveyance upstream, and an increase in that rate downstream, of the point where it occurs.

The shape of the transient axial velocity profile for the case of no solid bed rupture strongly indicates a relationship to transients in shear stress obtained from the viscometric flows of polymer melts and concentrated solutions of polymers. Examples of such measurements may be found in the literature on rheology. As mentioned earlier, Lee and Brodkey (27) obtained such transient-data for concentration solutions of polymethylmethacrylate in diethylphthalate. For these materials it was found that transient shear stresses, induced by a suddenly impressed shear rate, built up to new steady values as shown in Figure 23. Denny (13) developed for the plate-and-cone configuration a parallel to Szymanski's (58) solution of the Navier-Stokes equations for transient flow in a pipe. From these Lee and Brodkey (27) established that for

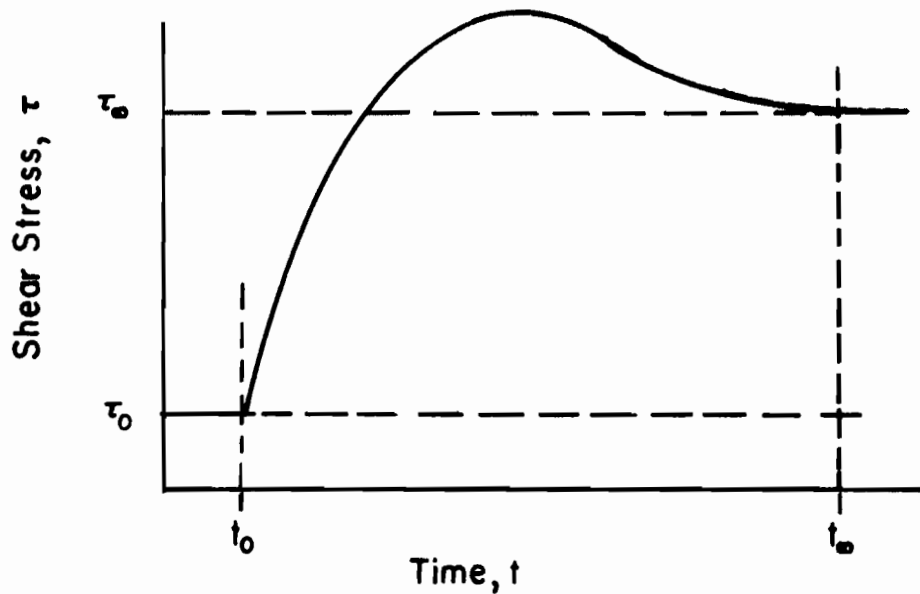


Figure 23. Schematic showing the build-up of shear stress as a result of a step change in shear rate for a typical polymer melt or concentrated solution.

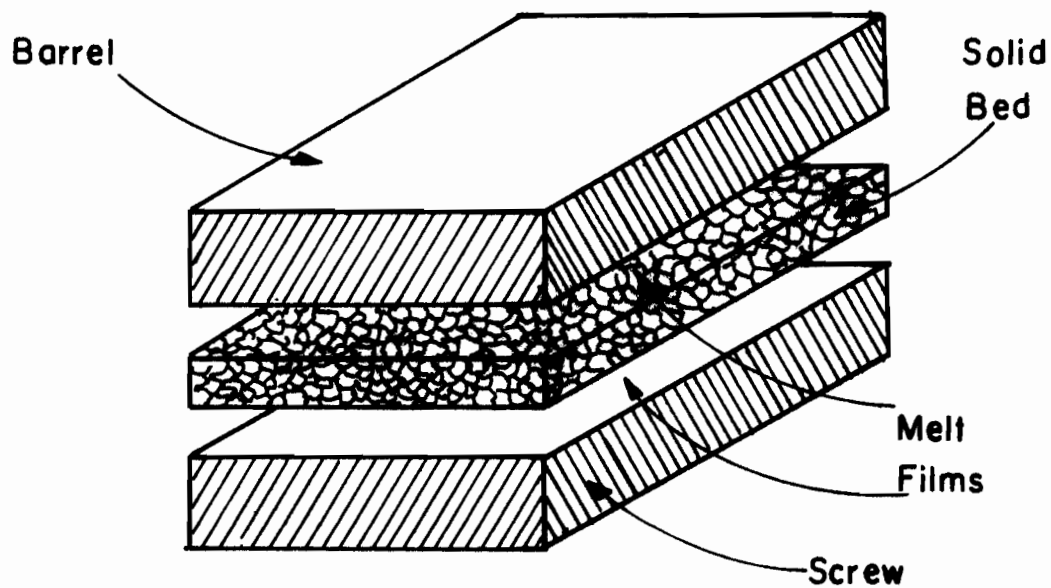


Figure 24. Three-plate system of barrel, screw channel bottom and solid bed with melt in the gaps between them.

very viscous materials the velocity profile is developed instantaneously upon the application of a sudden shearing action. With the aid of Figure 12 it is possible to approximate the flow in the melting zone to a three-plate system with the viscoelastic melt filling the gaps between the plates. This is shown schematically in Figure 24. The effects of the flights have been neglected since shear stresses generated by those boundaries are 4-5 times lower than those generated between the barrel and the bottom of the screw channel. A sudden step-up in screw speed would imply an incremental sudden increase in velocity of the lower plate represented by the screw in Figure 24. The velocity profile in the space between the solid bed and screw is formed instantaneously. However, because of its inertia, the solid bed does not instantaneously assume the higher speed. It can only be accelerated by the build-up of a net force. This net force results from the action of shear stresses on both sides of the solid bed. The build-up, in time, of these two stresses is schematically shown in Figure 25. The screw-side shear stress develops as shown in Figure 23 since the velocity profile in that space develops instantaneously. The development of the velocity profile in the gap between the barrel and solid bed depends on the movement of the latter. Because of the relatively low initial velocity of the solid, the build-up of the shear stress at the barrel side is delayed. This is schematically shown in Figure 25. The difference between the two stresses is proportional to the force necessary for bringing the solid bed up to the new steady state velocity. This difference is reduced to zero at the new equilibrium state. The

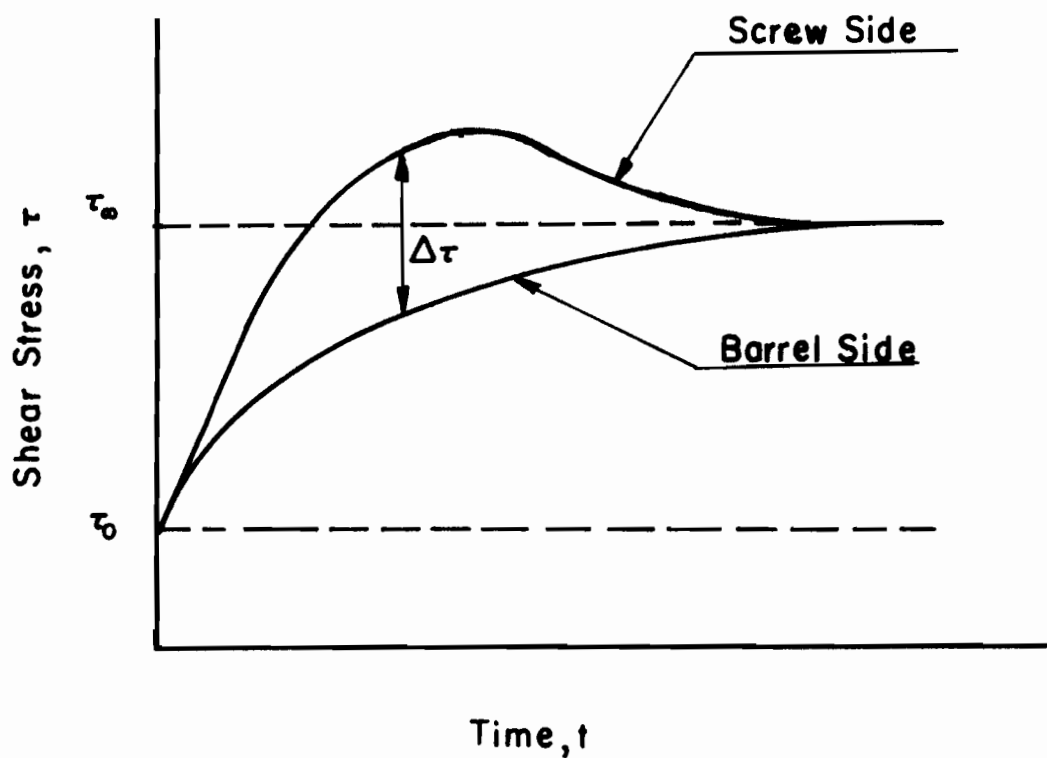


Figure 25. Build-up of shear stresses on both sides of the solid bed.

velocity profiles in the three-plate system under consideration are sketched in Figure 26 for times between $t = 0$ and $t = \infty$. The qualitative manner in which the profiles were obtained and their development between the times mentioned above, adds to the credibility of those obtained (Figures 19 through 22) from the axial distance-time measurements.

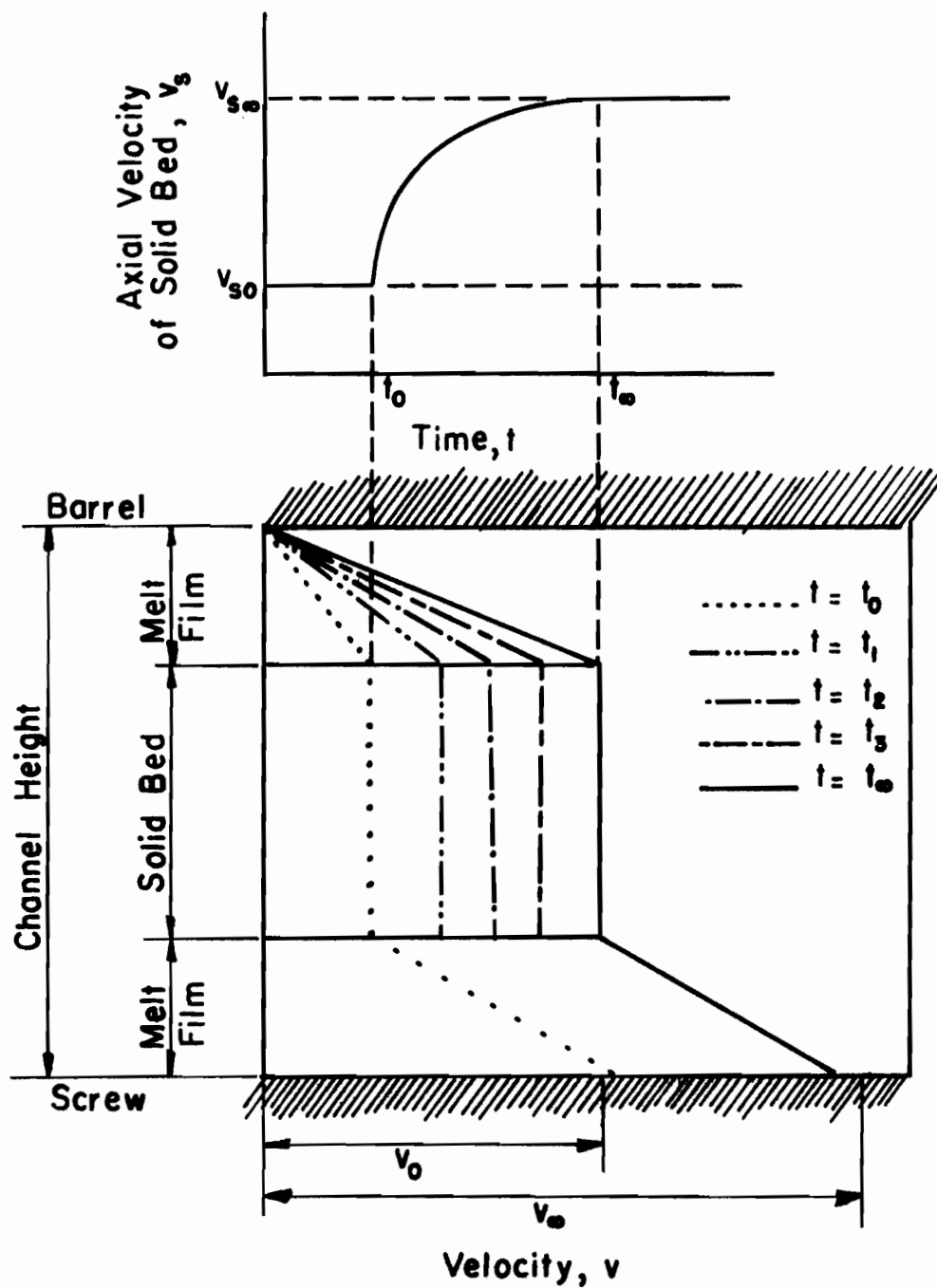


Figure 26. Transient development of velocity profiles in the solids portion of the flow in the melting zone.

PART IV

SUMMARY AND CONCLUSIONS

A great deal of effort has been directed at obtaining a basic understanding of the flow of polymeric materials in the helical channel of single screw plasticating extruders. In a typical extruder, solid polymer in the form of powder or pellets is fed continuously to the screw channel in which it is transformed into a liquid and pumped at relatively high temperature and pressure. In addition to the complexity of the geometry of the screw channel, the extruded materials usually exhibit complex rheological characteristics. This "double-pronged" complexity has retarded the achievement of a detailed understanding of the flow. Many uncertainties exist about our knowledge of the steady flow conditions. The deficiency in the state of knowledge is most noticeable in the dynamic or unsteady state aspects of the flow.

Our study was initiated in order to reveal some of the dynamic aspects of the flow in plasticating single screw extruders. The inherent complexities in the system suggested that a visual analysis of the flow may be helpful in achieving the objectives of this study. On that basis a 1 inch diameter ($L/D = 20$) extruder with a transparent barrel was constructed. Feed material to the system consisted of frozen pellets of a solution of polystyrene in diethylphthalate plasticizer. Some of the material was colored and added to the feed in order to mark its flow.

The visual extrusion system was operated in a nearly adiabatic manner such that there was no energy input through the barrel wall, although heat was conducted in through the screw. Unsteady state conditions in the flow were induced by introducing step changes in the screw speed.

Analysis of the movies revealed some of the flow characteristics in the melting zone where solid and liquid polymer coexist. In this zone it was found that the steady state flow picture was in general agreement with that suggested by past workers. Under transient conditions, however, the flow departed markedly from that observed under steady state conditions. The departures from the steady state were: 1) a rupture in the solid bed early in the melting zone, and 2) an increase in the length of melting together with an eventual lack of segregation between the liquid and solid phases. Measurements of the solid bed velocity under transient conditions suggested a possible connection between the observations and the viscoelastic nature of the liquid polymer under the nearly adiabatic conditions of the extruder operation. It was hypothesized that nearly adiabatic operation of the extruder caused an axial temperature gradient to be set up in both the barrel and screw. This gradient would cause large differences in the response times of the viscoelastic melt films through which the motion of the screw is transmitted to the solid bed. The disruption of the flow in the melting zone was attributed to those differences in response time.

In conclusion it may be stated that:

- a) The steady state melting mechanism as conceived by past workers is reasonably valid.

- b) Adiabatic operation of the extruder can lead to a disruption of the flow regime in the melting zone under transient conditions.
- c) The viscoelastic rheological properties of the extrudate may play an important role in the behavior of the flow system under transient conditions.
- d) The disruption of the flow regime in the melting zone leads to a deterioration in product quality.
- e) Visual studies in extrusion can be employed to study the unsteady state as well as the steady state aspects of the flow.

PART V
RECOMMENDATIONS

Having established that visual studies in extrusion are valuable in revealing the details of the flow, either under steady or unsteady conditions, it is recommended that such studies should be continued in the future. In making specific recommendations, past experience (including that acquired from this study) will be appropriately taken into consideration. Where possible, the schemes suggested will be directed at studying the three zones of the flow as a whole. These three zones, namely solids conveying, melting and melt conveying have been found difficult to study simultaneously, this study notwithstanding. Examples of such difficulties are many. The freezing methods of Maddock and Street (30,56), for instance, gave information about the mechanism of melting and cross channel circulatory flows both in the melting and melt conveying zones under steady state conditions only. This technique, however, failed to provide any insights into the process of solids conveying. The techniques used in this study yielded information only on some of the dynamic aspects of melting. The solids and melt conveying zones were not amenable to visual observation.

In the paragraphs to follow, suggestions will be made for conducting visual studies of the three zones of a single plasticating screw extruder. It will also be recommended that visual studies be

conducted in the more complex flow system of the twin-screw extruder. Many of the problems associated with single screw extrusion have been effectively solved using twin screw extruders.

Solids Conveying

Observation of the flow of solids in the solids conveying section or the screw channel was found difficult. In this study, that part of the channel was obscured by frozen moisture from the atmosphere and "crazing" of the barrel wall because of exposure to liquid nitrogen temperatures. The experiments of Darnell and Mol (10) which involved room temperature extrusion of pellets of polymethylmethacrylate under conditions of open discharge, did not closely resemble the conditions prevailing in actual extruders. It seems that solids conveying should be studied separately in a room temperature extruder with a transparent and scratch-resistant barrel. Also the extrusion of the solid particles should be carried out against a positive gradient in pressure in order to assure simulation to real conditions. A flexible "pressure gland" could be attached to the discharge end to prevent the free flow of solids. The variables to be studied should be those associated with pellet size, mode of operation, and state of the flow. Some colored pellets of the natural polymer should be added in order to mark the flow and follow its progress. This would also indicate whether mixing takes place.

The Melting Zone

In the melting zone, liquid and solid flow side by side. The conditions under which the zone was observed in this study were such that motions in the liquid were not recorded. This could be corrected by adding a colored (or otherwise visible) solid which does not melt under the extruder operating conditions. Following Eccher and Valentinotti (17), small aluminum particles (0.001 inch in diameter or less) could be employed to mark the liquid part of the flow. It is recommended that a high temperature extruder be employed here in order to eliminate axial temperature gradients in the barrel and screw. Heat input through the barrel wall could be achieved by radiation. The barrel, in this case should be fabricated from a heat-resisting specialty glass as Pyrex[®]. This will probably eliminate effects of adiabatic operation on the flow. High temperature operation will have the added advantage of using pure natural polymer as feed material instead of using that prepared by freezing a mixture of the solid polymer and plasticizer at cryogenic temperatures. The use of natural polymer will greatly simplify the problems associated with varying the pellet size with regard to investigating its effect on the properties of the solid part of the flow.

An alternate method of marking the flow and observing some of its characteristics may be achieved by feeding the extruder with consecutive charges of differently colored natural polymer. This would be an extension of Rousselet's (48) investigation of the melting zone. The technique is expected to yield valuable information on: 1) internal

shearing (or lack of it) in the solid bed, 2) mixing patterns in the liquid polymer and 3) the external shape of the velocity profile in the liquid part of the flow. The above may be achieved by following the changes occurring in the front between differently colored layers of polymer.

Melt Conveying Zone

The flow patterns in the melt conveying zone were not observed in this study. However, the techniques used in studying the flow in the melting zone could be effectively used here. In particular the use of small colored particles that do not melt under the operating conditions, could be used to mark the flow. Since the quality of the product is highly dependent on the magnitude of the total strain experienced by the liquid, an indirect method of measuring this total strain may be employed. This method would involve resolidification of the extrudate into geometries of simple cross section. Analysis of thin sections of the product could be performed according to existing (or otherwise formulated) standards of quality. These analyses could in turn be related to the operating conditions of the extruder (steady and unsteady state).

Twin Screw Extrusion

As mentioned earlier some of the problems associated with single screw extrusion have been solved by utilizing twin-screw extruders. The main advantages for use of the latter were found to be 1) more efficient feeding of the solids due to the action of positive displacement,

2) better quality of product due to extensive shearing and "milling" of the material in the gap between the two screws and 3) achieving (1) and (2) at lower pressures than would be necessary in single screw extruders with the same capacity. However, the flow in the twin-screw machine is expected to be more complex than that in a single screw extruder.

Problems may be encountered in building the twin screw extruder with a transparent barrel. This, however, may be done by fabricating it from two symmetrical halves. Since the pressures will not be excessive the sealing problems should not be too difficult to solve. The same techniques applied to studying the three zones of the single screw could be effectively employed in studying the same zones in twin-screw extruders.

APPENDIX

MEASUREMENTS OF AXIAL DISTANCE WITH TIME

Measurements of the instantaneous axial velocities of particles of solid polymer were made as part of studying the transient effects in the visual extruder. The measurements involved projecting the 16 mm movies on an 8-inch x 11-inch screen and measuring the axial progress of the particles, with time, in the helical channel of the screw. As mentioned earlier, the projector used in analyzing the movies was fitted with a frame counter. The frame count (0 to 4000 for each movie) gave a measurement of real time by an appropriate reduction. The movies which were extensively studied in this manner were H7 and G7 of Zone 1 and G3 and H5 of Zone 2. All involved the recording of a step change in screw rpm between 60 and 75 at about 10 seconds after the camera was started.

Location of Transients

The accurate location of the transients or step changes in rpm was deemed important for two reasons. In the first place, this helped in the axial distance measurements by indicating which frames on the film were of most interest. Secondly, this helped in interpreting phenomena that were closely associated with the transient.

The determination of location of the transient was carried out by observing the number of frames taken for the screw to complete 2 turns, or an axial distance that is twice the pitch, for movies taken at 15 fps (G3 and G7), and the number of frames taken for the screw to complete 1/2 turn, or an axial distance that is 1/2 the pitch, for movies taken at 90 fps. Also, the frame ranges, with respect to frame zero as reference, over which the screw rotations took place, were noted. The data obtained are presented in Table 4 and plotted in Figures 27 through 30. The plots of frames to complete the 1/2 or 2 revolutions against the frame range over which these were completed, gave frame locations of the transients as 860, 254, 880, and 500 for G7, H7, G3, and H5, respectively.

Measurements of Axial Distance

As mentioned earlier, the progress of colored individual particles in the solid bed was followed over the visible length of the screw in the zone under consideration. This consisted of measuring the axial distance \underline{d} , in inches, from a predetermined reference line to the screw channel center in the vicinity of which the particle resided. Figure 31 is a schematic representation of the procedure followed in measuring \underline{d} . When the particle appeared and its centroid coincided with the screw axis, the projector was stopped and the channel center was determined with a pair of dividers. Then the distance \underline{d} was measured with a 12-inch scale, divided in one-fiftieths of an inch. The reference lines used were the visible line of separation of feed section (F) and barrel (B) for Zone 1 movies (H7 and G7) and the right edge of the frame for

Table 4. Location of transients for movies G7, H7, G3 and H5.

Movie G7		Movie H7	
Frame Number, f	Frames to Complete 1/2 Screw Revolution	Frame Number, f	Frames to Complete 2 Screw Revolutions
567		134	
	46		30
613		164	
	41		29
654		193	
	43		32
697		225	
	42		30
739		255	
	43		26
782		281	
	41		26
823		307	
	41		25
864		332	
	34		25
898		357	
	34		25
932		382	
	34		
966			
	33		
999			

Table 4. Continued.

Movie G3		Movie H5	
Frame Number, f	Frames to Complete 1/2 Screw Revolution	Frame Number, f	Frames to Complete 2 Screw Revolutions
609	38	340	34
647	41	374	35
688	39	409	34
727	38	443	34
765	37	477	30
802	43	507	28
845	37	535	28
882	33	563	28
915	33	591	
948	33		
981	34		
1015	34		
1049	33		
1082			

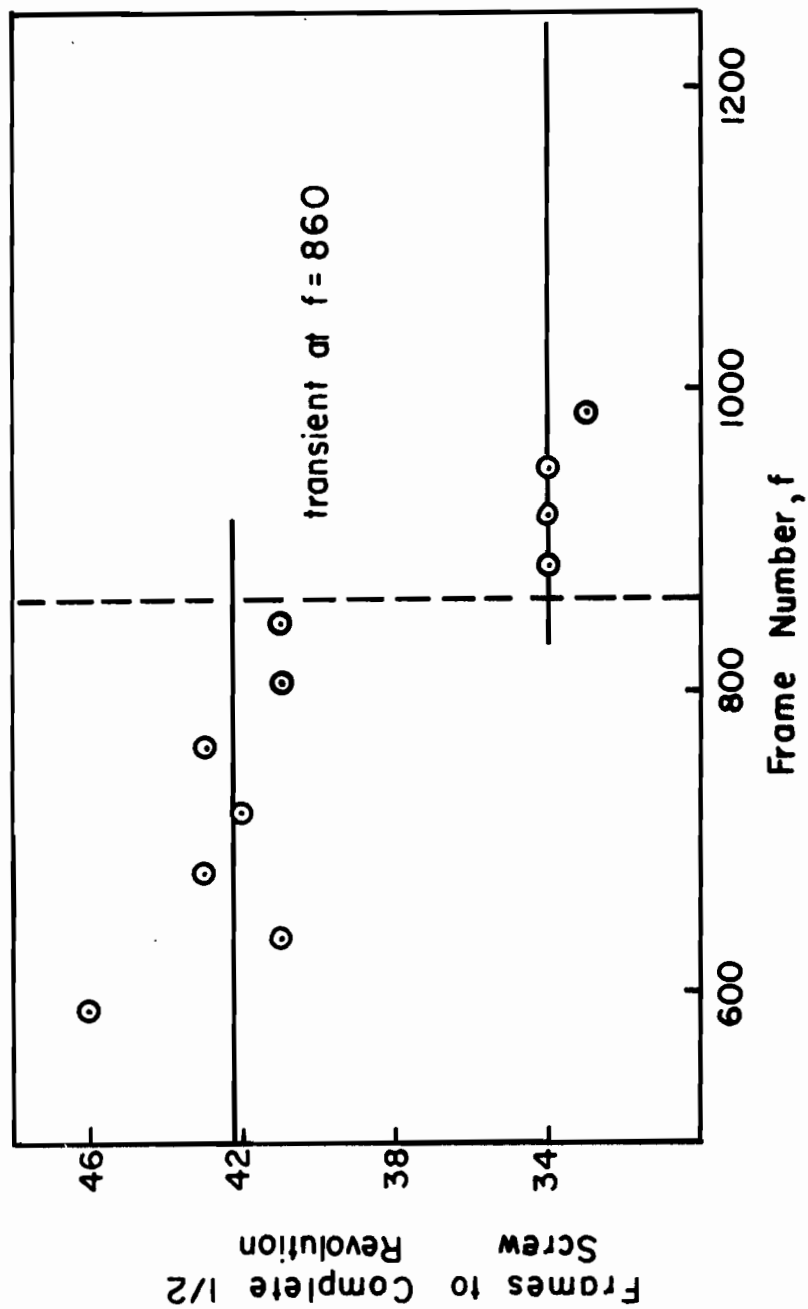


Figure 27. Location of transient for movie G7.

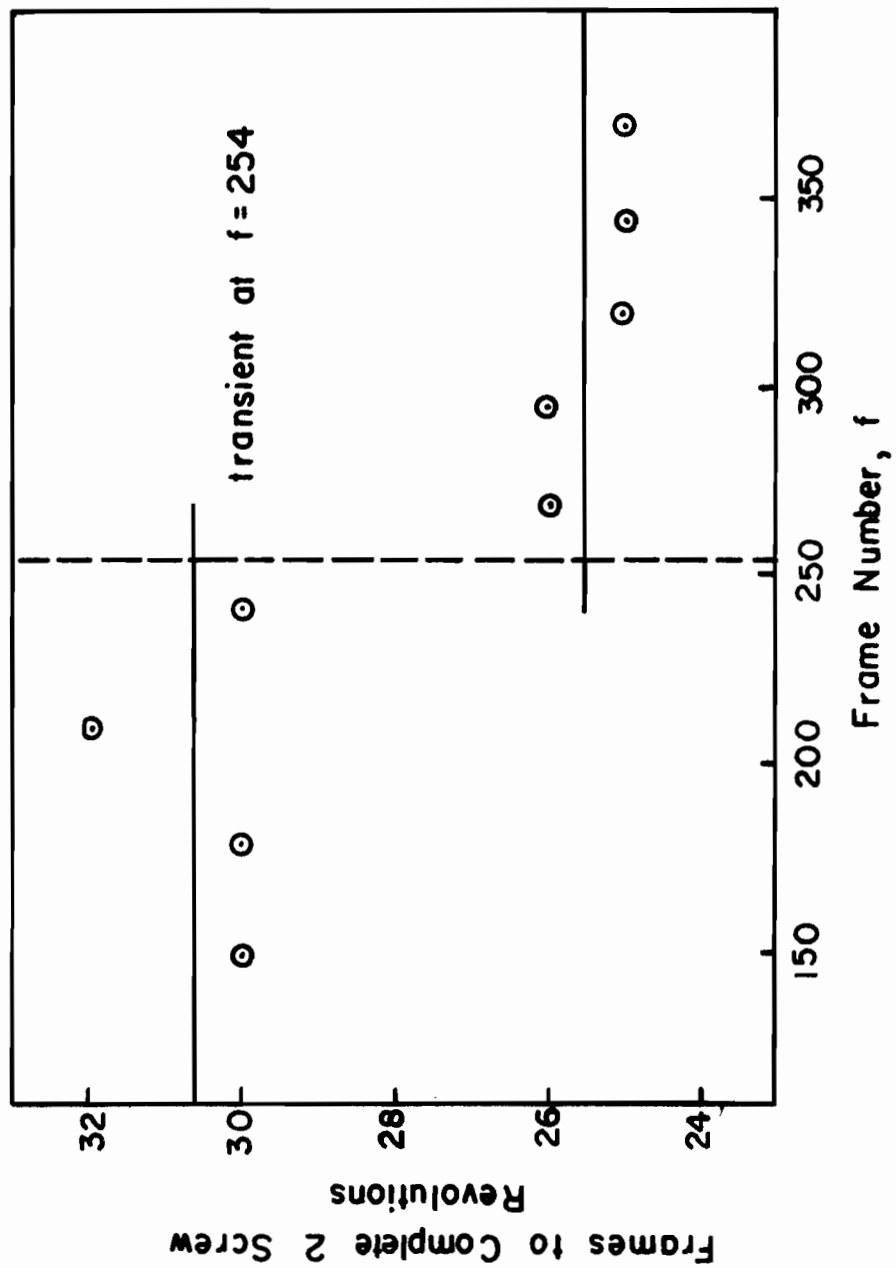


Figure 28. Location of transient for movie H7.

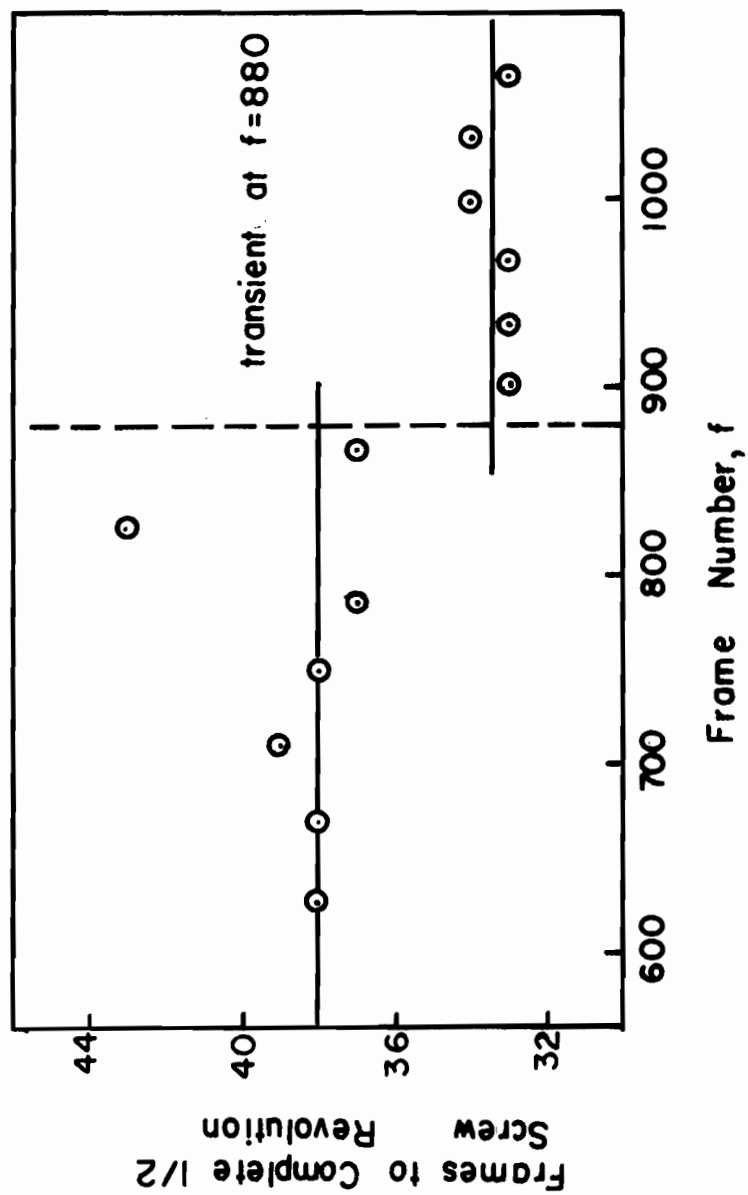


Figure 29. Location of transient for movie G3.

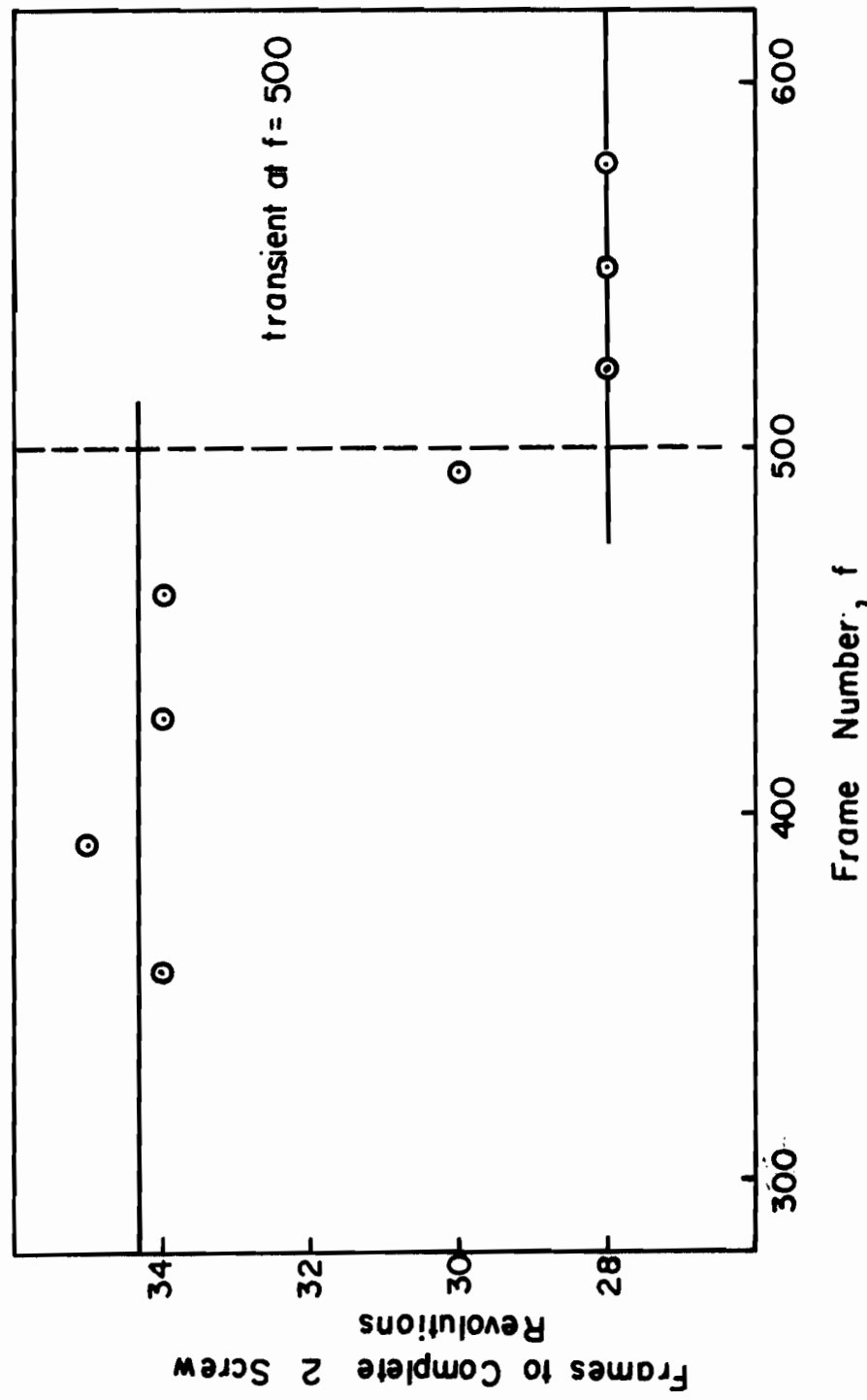


Figure 30. Location of transient for movie H5.

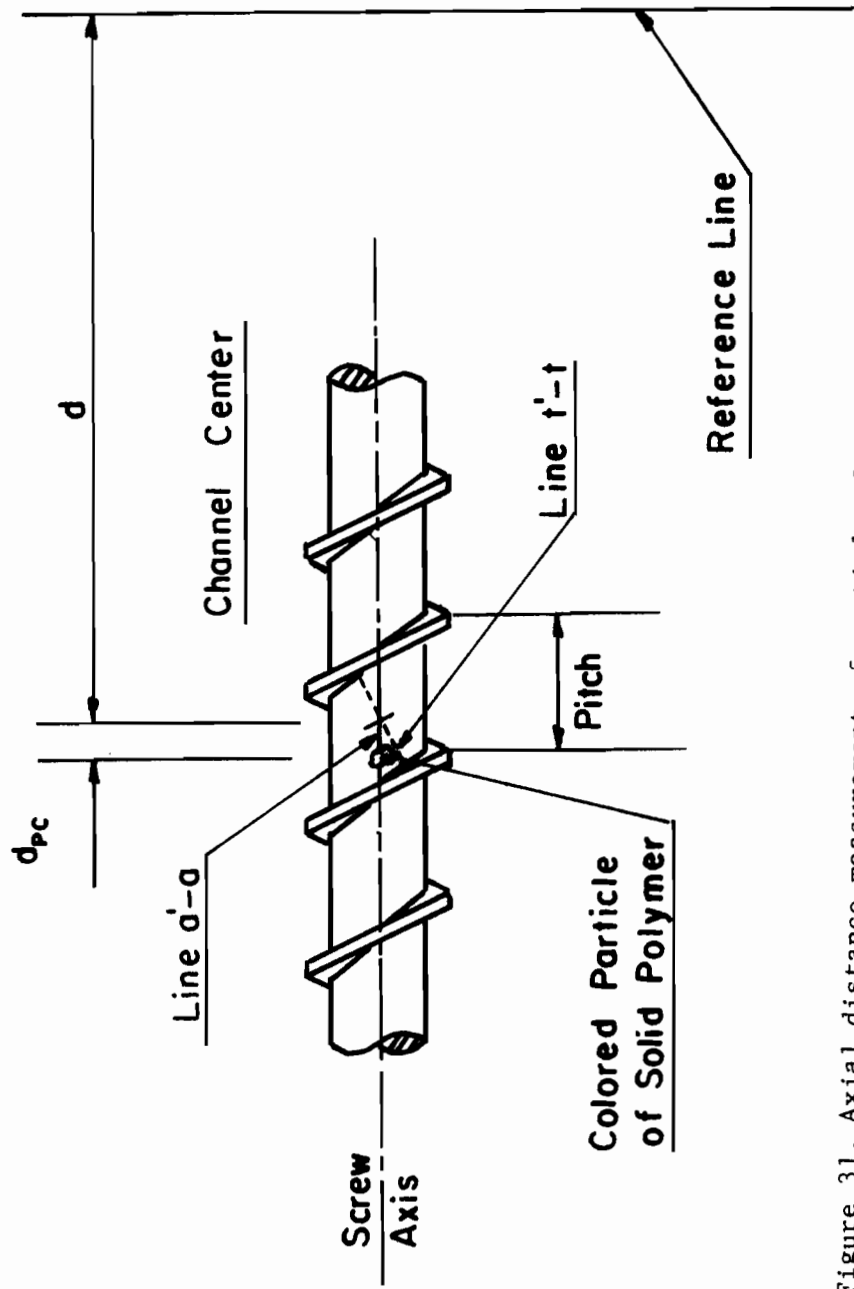


Figure 31. Axial distance measurement of particle of solid polymer.

Zone 2 movies (G3 and H5). The frame number, \underline{f} , was also read from the frame counter. The film was advanced further until the same particle completed one revolution and was visible again. This gave another set of \underline{f} and \underline{d} values for the particle. The process was repeated until the particle advanced beyond the visible range of the screw in the zone under observation or was disfigured beyond recognition because of melting. The \underline{f} and \underline{d} data taken are presented in the first two columns of Tables 8 through 11.

Earlier in the course of measuring axial distances, two effects were observed to take place. The first effect exhibited itself as a change in pitch of the screw with axial distance as the frame was traversed from right to left. The second effect was associated with drift of the centroid of the solid particle with respect to the channel center after the completion of one revolution. In other words, a particle whose centroid was initially to the right of center might have shifted to the left of center after several turns. The change in pitch resulted from the distortion caused by using the wide angle lens at relatively close distances. Since each point in the visible length of the screw was at a different distance from the film, such displacements could have resulted from different magnifications of the various elements of the zone. The shift of the particle with respect to the center was most noticeable at axial positions where the melt portion of the flow was well developed. This was expected since the melt-solid interface in the melting zone continuously shifts position from near the advancing flight toward the trailing flight.

From the point of view of polymer conveyance in the down channel or axial direction, the two effects mentioned above represented inherent errors in the measurements of \underline{f} and \underline{d} . Corrections for these errors were sought and applied, where appropriate, as explained below.

Corrections for Measured f and d

Variations in pitch were measured for each of movies G7, H7, and G3. H5 was considered to be similar to G3 and no such measurements were made for it. The pitch, as indicated in Figure 31, was measured and estimated to the nearest one-hundredth of an inch at different axial locations. The film was then advanced to a frame that was half a screw revolution further. Another set of pitch versus axial distance data was thus obtained. This was repeated for other frames farther down the film. The data taken are presented in Table 5 and plotted in Figures 32 to 34 for G7, H7, and G3, respectively. The plots show a maximum pitch at about the center of the frame. The deviations of the pitch from the maximum were determined and cumulatively added over the entire range of the axial distance \underline{d} . These cumulative corrections, in inches, are presented in Table 6 and plotted in Figure 35 for movies G7, H7, and G3, respectively. The corrections were later applied to the axial distance \underline{d} .

The other inherent error in the measurements of \underline{f} and \underline{d} was associated with the position of a particle of polymer relative to the channel center. In the early part of the measurements, d_{pc} , the axial distance, in inches, between the centroid of the particle and the

Table 5. Measured pitch versus axial distance d for movies G7, H7 and G3.

Movie G7		Movie H7		Movie G3	
Axial Distance, d, in.	Pitch, in.	Axial Distance, d, in.	Pitch, in.	Axial Distance, d, in.	Pitch, in.
1.58	1.30	1.13	1.27	1.60	1.24
2.90	1.30	2.45	1.28	2.79	1.25
4.17	1.27	3.79	1.31	4.05	1.27
5.44	1.24	5.09	1.33	5.34	1.28
		6.36	1.27	6.65	1.27
0.82	7.58	1.26	7.94	1.27	
		8.86	1.24	9.21	1.27
2.20	1.31				
3.46	1.265				
4.80	1.26	1.44	1.27	0.96	1.20
6.09	1.25	2.70	1.30	2.20	1.24
		4.03	1.30	3.44	1.26
0.92	1.31	5.31	1.31	4.58	1.275
2.21	1.31				

Table 5. Continued.

Movie G7		Movie H7		Movie G3	
Axial Distance, d, in.	Pitch, in.	Axial Distance, d, in.	Pitch, in.	Axial Distance, d, in.	Pitch, in.
3.48	1.28	6.35	1.27	5.97	1.29
4.80	1.255	7.87	1.24	7.30	1.29
6.03	1.250	9.11	1.24	8.56	1.27
		1.04	1.28	9.78	1.23
1.3	1.31	2.35	1.29		
2.6	1.295	2.69	1.29		
3.9	1.27	4.90	1.31		
5.2	1.27	6.22	1.29		
		7.53	1.25		
		8.76	1.23		

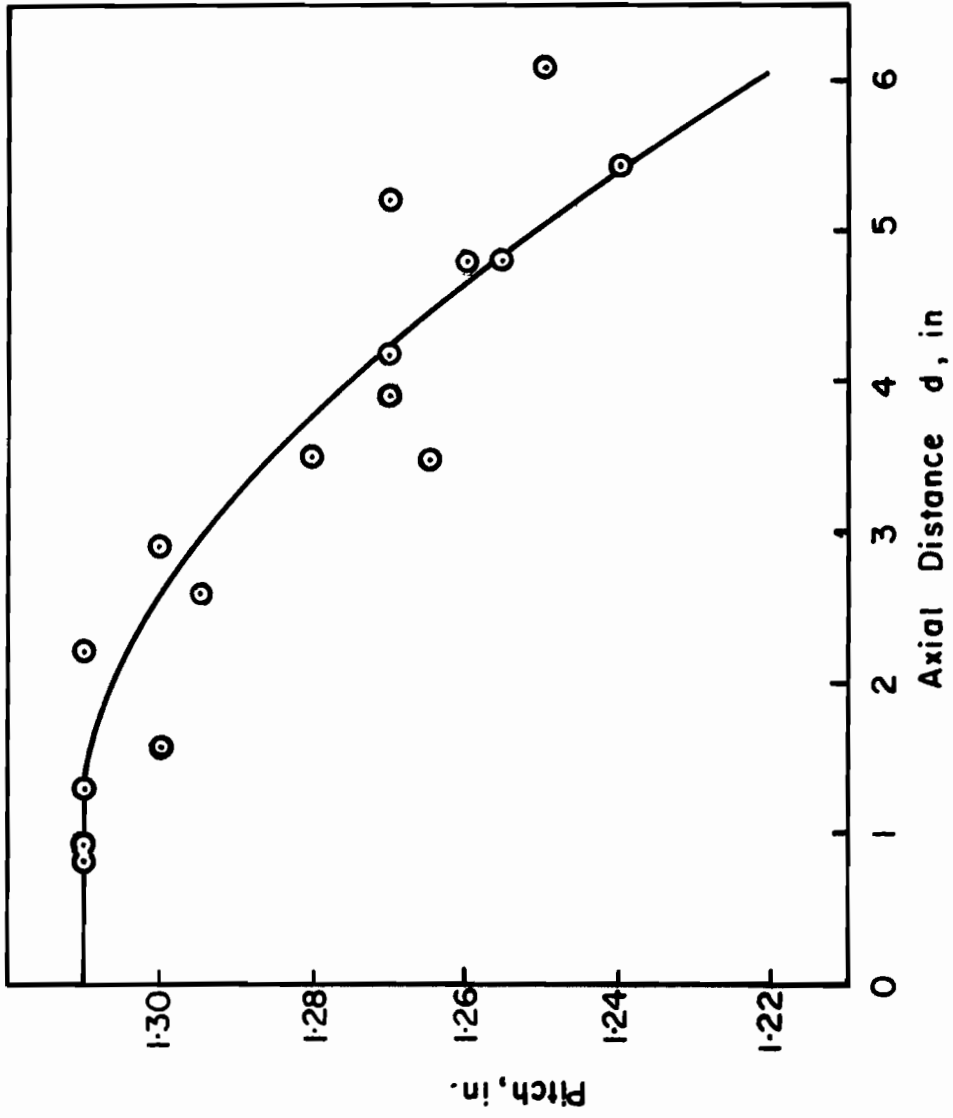


Figure 32. Plot of screw pitch versus axial distance d on screen for movie G7.

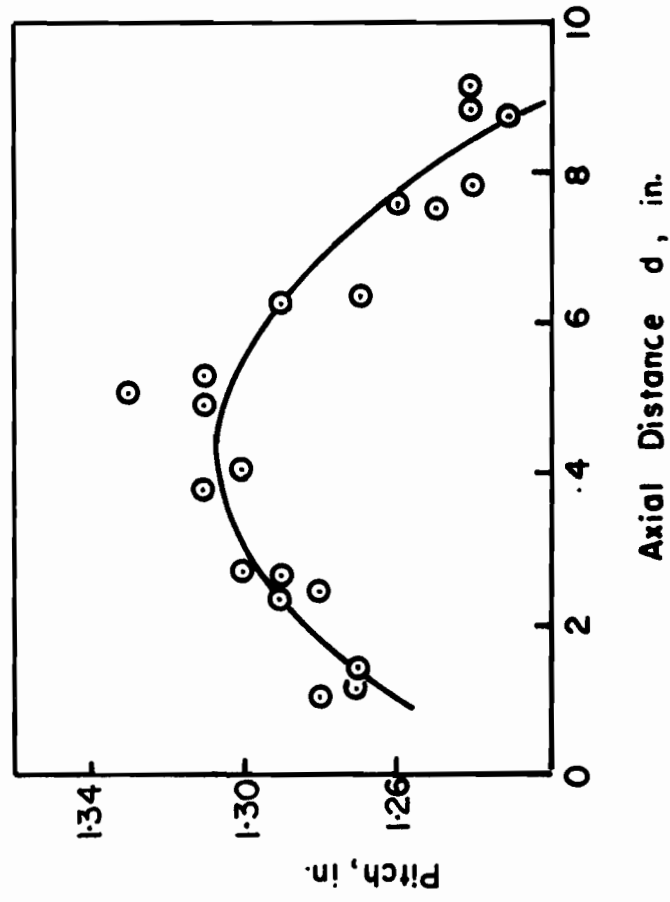


Figure 33. Plot of screw pitch versus axial distance d on screen for movie H7.

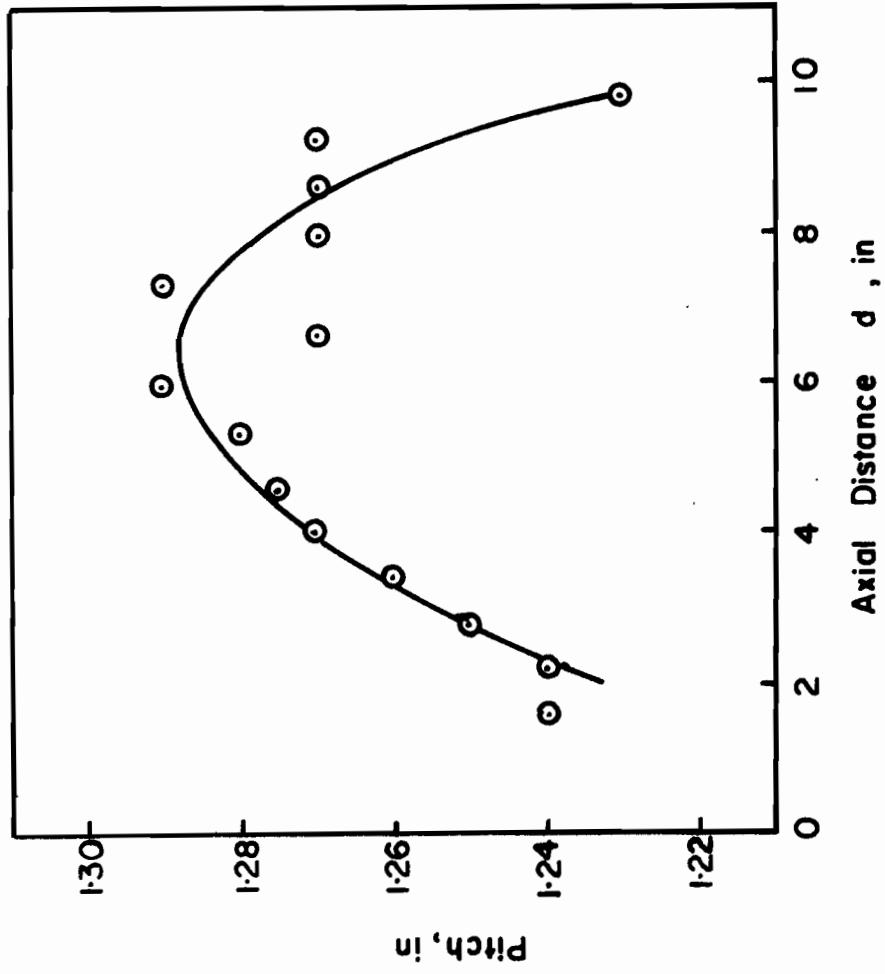


Figure 34. Plot of screw pitch versus axial distance d on screen for movie G3.

Table 6. Cumulative correction to \underline{d} , Δ , as a function of axial distance \underline{d} .

Axial Distance \underline{d} , inches	Δ , inches		
	Movie G7	Movie H7	Movie G3
0	0.000	0.000	0.000
1	0.000	0.053	0.072
2	0.004	0.080	0.126
3	0.020	0.089	0.164
4	0.055	0.089	0.187
5	0.113	0.092	0.196
6	0.201	0.108	0.196
7	--	0.144	0.199
8	--	0.205	0.214
9	--	0.295	0.251
10	--	--	0.315

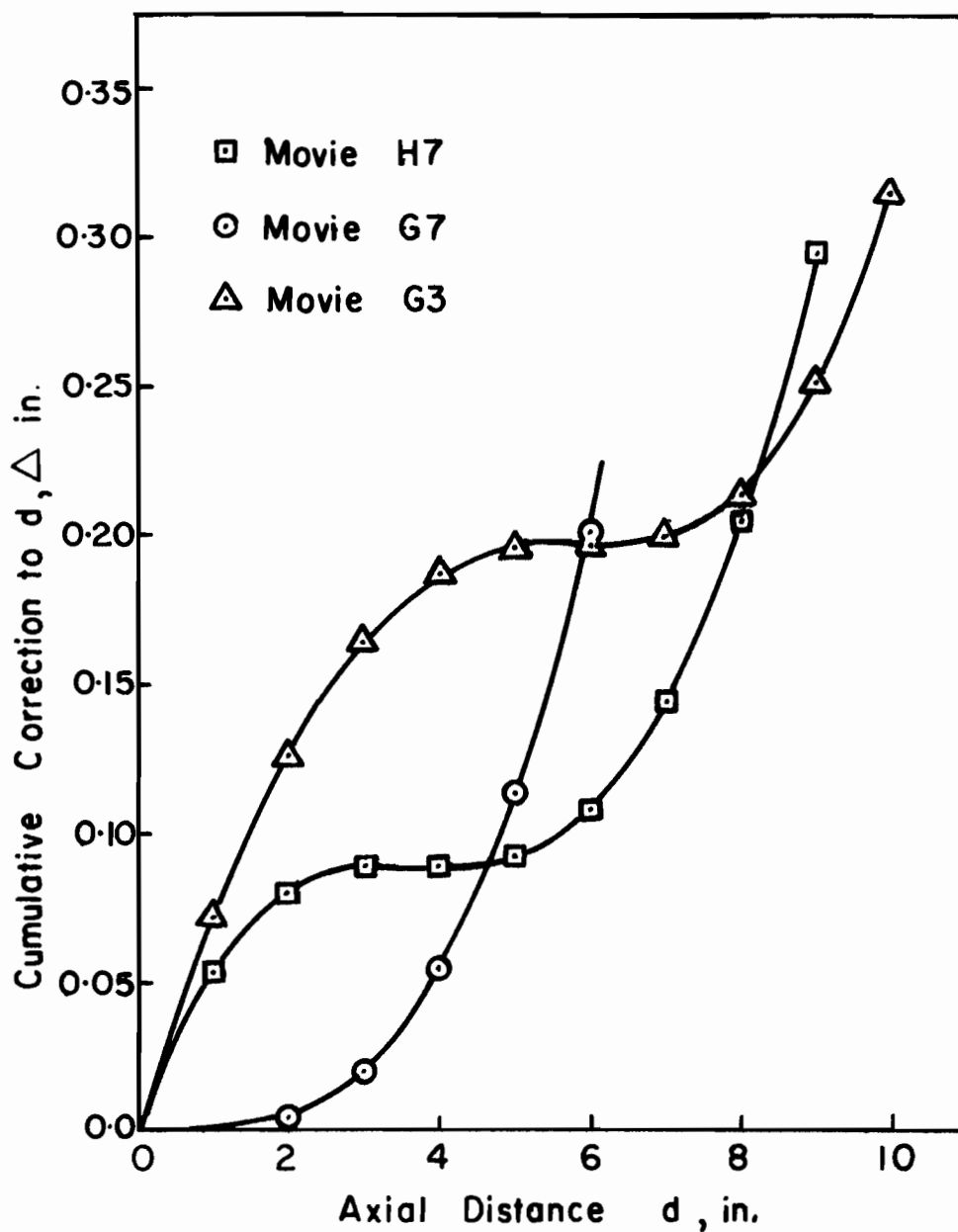


Figure 35. Cumulative correction applied to d plotted against axial distance d .

channel center was reported. This distance was considered negative if the particle was to the right of center and positive if the particle was to the left of it. Where such measurements have been made, they are reported in Tables 8 and 9 (for movies G7 and H7, respectively). Originally, these data were taken in order to, first, account for differences in the dynamic behavior between particles in the vicinity of channel center and those away from it, and, second, to investigate the effects of particle "drift", in the cross channel direction, on the respective values of \underline{f} and \underline{d} . Ideally, the axial distance measurements should have been made in a manner that recognizes the position of the particle centroid with respect to the channel center. The channel center with respect to an eccentric particle could have been obtained by allowing a line $t-t'$, shown in Figure 31, that passes through the centroid of the particle, to bisect the axial line $a-a'$. Line $t-t'$ is drawn perpendicular to the flights. The point of intersection of $t-t'$ and $a-a'$ would then be the true channel center with respect to the particle. In comparison to the channel center measurements that were actually made, the procedure just described would cause the \underline{d} values to shift slightly toward or away from the reference line. The shift would be toward the reference line if the particle were to the left of center, and away from the reference line if the particle were to the right of channel center. In the first case this would lead to a lower value of \underline{d} than was reported and in the second case would lead to a higher value. However, simultaneous shifts in \underline{f} would accompany the measurements such that a plot of \underline{d} versus \underline{f} would be essentially the same for data

actually taken and data obtained by the proposed more accurate method. Furthermore, obtaining the \underline{f} and \underline{d} data using the more accurate method would have entailed locating the line t-t' by a laborious trial-and-error procedure. The benefits accruing from following such a procedure, however, would have been cancelled by the effects of barrel curvature and the slow filming speeds employed for a large number of the particles observed. Because of channel curvature, only an apparent channel center with respect to an eccentric particle can be obtained, since the frame showed only a projection of the line segment between the centroid of the particle and the screw axis in the direction of the helix angle. Also, at low camera speeds (15 fps) the errors in measurement of \underline{d} (and hence of \underline{f}) were of the order of 2.5 percent per particle revolution.

The above justifies the course followed in measurements of \underline{f} and \underline{d} only for particles that do not show a tendency to "drift" in the cross-channel direction away from the liquid portion of the flow. This phenomenon was observed and recorded. It was reflected in a continuous variation of the value of d_{pc} . Analysis of the d_{pc} data was carried out by plotting it against the axial distance \underline{d} . For most cases, a best-straight line could be drawn through the points. Inspection of such plots showed that a correction of about 0.01 inch should be added to \underline{d} after each particle rotation. Since this increment was found to be of the order of the accuracy obtained from the scale measurements, it was neglected.

Reduction of f and d

The measurements of \underline{f} and \underline{d} were later reduced to the corresponding values of real time \underline{t} and true axial distance d_a . The time \underline{t} was calculated by dividing the frame number \underline{f} by the framing speed fps. For G7 the stopwatch technique gave an fps value of 89.0. That for H7 was 16.0 for frame numbers \underline{f} lower than 1345 and 90.0 for \underline{f} greater than 1345. Similarly, the fps values for G3 and H5 were 90.0 for each.

The calculation of the true axial distance d_a involved adding to \underline{d} its correction Δ and dividing by the value of the maximum pitch. The result was then added to \underline{R} , the actual axial distance between the reference line and the start of the helical channel. For Zone 1 movies G7 and H7 the value of R was 2-1/2 inches. This is the actual distance between the beginning of the helical channel and the end of the feed section (F).

Since the line of reference for Zone 2 movies G3 and H5 was taken as the right edge of the frame, the distance \underline{R} was not readily obtainable. A geometrical argument utilizing the visibility of the 1-inch scale, that was fixed to the edge of the lower plate (L), was employed. This scale was fixed at a distance of 2-3/4 inches from the inside surface of the barrel. Because of this distance, the magnifications of the 1-inch barrel diameter and 1-inch lengths on the scale were markedly different, being 1.26 for the former and 1.6 for the latter. The value of \underline{R} was calculated as described below.

Scale numbers visible at

$$\text{Right Edge} = 7 - (1.0/1.6)(1.0) = 6.375 \text{ in.}$$

$$\text{Left Edge} = 12 + (1.2/1.6)(1.0) = 12.75 \text{ in.}$$

Length of scale that is visible

$$12.75 - 6.375 = 6.375 \text{ in.}$$

Screw length visible from edge to edge

$$\text{including correction} = 8.73 \text{ in.}$$

Length to be subtracted from right

scale number

$$(8.73/1.26 - 6.375)/2 = 1.177 \text{ in.}$$

Axial distance of reference line, R

$$6.375 - 1.177 = 5.2 \text{ in.}$$

A summary of the procedure employed in reducing the f and d data for G7, H7, G3, and H5 is presented in Table 7. In Tables 8 through 11 a summary of the data taken for the many particles traced in each movie is presented. Each particle followed was given a four-character designation. The first two characters indicate the movie under observation and the last two denote the number of the particle.

Table 7. Summary of time and true axial distance calculation from \underline{f} and \underline{d} .

Movie Designation	Time, t, sec	True axial distance, d_a , inches
G7	$f/89.0$	$(d + \Delta)/1.31 + 2.5$
H7*	$f/16.0$	Same as G7
G3	$f/90.0$	$(d + \Delta)/1.29 + 5.2$
H5	Same as G3	Same as G3

* For f greater than 1345, t was calculated by using the expression $(f - 1345)/90.0 + 1345/16.0$.

Table 8. Summary of axial distance-time measurements taken from movie G7.

f	d	d _{pc}	Δ	t	d _a
<u>G7-01</u>					
36.0	1.64	0.06	0.001	0.40	3.75
154.0	2.10	0.08	0.004	1.73	4.11
275.0	2.66	0.07	0.012	3.09	4.54
394.0	3.17	0.05	0.024	4.43	4.94
510.0	3.60	0.10	0.038	5.73	5.28
629.0	4.13	0.14	0.058	7.07	5.70
752.0	4.66	0.15	0.083	8.45	6.12
<u>G7-02</u>					
79.0	0.90	-0.40	0.0	0.89	3.19
204.0	1.53	-0.40	0.001	2.29	3.67
326.0	2.01	-0.44	0.004	3.66	4.04
447.0	2.63	---	0.012	5.02	4.52
565.0	3.13	-0.40	0.023	6.35	4.91
683.0	3.59	-0.42	0.037	7.67	5.27
801.0	4.12	-0.37	0.057	9.00	5.69
904.0	4.59	-0.35	0.079	10.16	6.06
990.0	4.92	-0.32	0.098	11.12	6.33
1079.0	5.31	-0.38	0.127	12.12	6.65
<u>G7-03</u>					
399.0	1.96	0.12	0.004	4.48	4.00
519.0	2.46	0.15	0.009	5.83	4.38
637.0	2.96	0.19	0.019	7.16	4.77
755.0	3.45	0.20	0.033	8.48	5.16
869.0	3.95	0.23	0.050	9.76	5.55
955.0	4.32	0.22	0.065	10.73	5.85
1040.0	4.66	0.20	0.083	11.68	6.12
1127.0	5.01	0.19	0.104	12.66	6.40

Table 8. Continued.

f	d	d _{pc}	Δ	t	d _a
<u>G7-04</u>					
877.0	1.49	0.06	0.001	9.85	3.64
964.0	1.89	0.05	0.003	10.83	3.94
1047.0	2.18	0.08	0.006	11.76	4.17
1128.0	2.50	0.08	0.010	12.67	4.42
1210.0	2.70	---	0.013	13.59	4.57
1290.0	2.98	0.08	0.020	14.49	4.79
1372.0	3.24	0.10	0.026	15.42	4.99
1455.0	3.54	0.12	0.035	16.35	5.23
1539.0	3.86	0.15	0.047	17.29	5.48
<u>G7-05</u>					
526.0	1.19	0.07	0.000	5.91	3.41
648.0	1.77	0.06	0.002	7.28	3.85
771.0	2.34	0.08	0.007	8.66	4.29
880.0	2.86	0.09	0.016	9.89	4.69
964.0	3.16	0.09	0.024	10.83	4.93
1047.0	3.45	0.10	0.032	11.76	5.16
1129.0	3.74	0.13	0.042	12.68	5.39
1211.0	3.99	0.13	0.052	13.61	5.58
1293.0	4.27	0.15	0.064	14.53	5.81
<u>G7-06</u>					
1084.0	1.55	-0.25	0.001	12.18	3.68
1166.0	1.85	-0.25	0.003	13.10	3.91
1246.0	2.07	-0.22	0.004	14.00	4.08
1327.0	2.34	-0.27	0.007	14.91	4.29
1412.0	2.65	-0.22	0.012	15.86	4.53
1495.0	2.94	-0.20	0.018	16.80	4.76
1580.0	3.27	-0.15	0.027	17.75	5.02
1663.0	3.60	-0.14	0.037	18.68	5.28
1747.0	3.90	-0.14	0.049	19.63	5.51
1831.0	4.21	-0.08	0.061	20.57	5.76
1918.0	4.58	-0.08	0.079	21.55	6.06

Table 8. Continued.

f	d	d _{pc}	Δ	t	d _a
<u>G7-07</u>					
1399.0	1.11	0.0	0.0	15.72	3.35
1483.0	1.42	0.0	0.0	16.66	3.58
1568.0	1.75	0.0	0.002	17.62	3.84
1653.0	2.07	0.02	0.005	18.57	4.08
1736.0	2.39	0.05	0.008	19.51	4.33
1822.0	2.74	0.03	0.014	20.47	4.60
1906.0	3.12	0.06	0.022	21.42	4.90
1991.0	3.43	0.11	0.032	22.37	5.14
2077.0	3.78	0.10	0.044	23.34	5.42
2166.0	4.21	0.09	0.061	24.34	5.76
2255.0	4.59	0.10	0.080	25.34	6.06
<u>G7-08</u>					
2045.0	1.87	0.27	0.003	22.98	3.93
2134.0	2.28	0.27	0.006	23.98	4.24
2222.0	2.70	0.28	0.013	24.97	4.57
2311.0	3.12	0.30	0.023	25.97	4.90
2400.0	3.53	0.33	0.035	26.97	5.22
2495.0	4.07	0.30	0.055	28.03	5.65
2591.0	4.61	0.33	0.080	29.11	6.08
<u>G7-09</u>					
119.0	2.80	-0.27	0.015	1.34	4.65
237.0	3.31	-0.25	0.028	2.66	5.05
357.0	3.84	-0.25	0.046	4.01	5.47
475.0	4.32	-0.25	0.067	5.34	5.85
597.0	4.84	-0.22	0.094	6.71	6.27
725.0	5.49	----	0.145	8.15	6.80
853.0	6.10	-0.08	0.210	9.58	7.32
<u>G7-10</u>					
58.0	1.90	----	0.003	0.65	3.95
182.0	2.50	-0.15	0.010	2.04	4.42
299.0	2.99	-0.08	0.020	3.36	4.80
417.0	3.48	-0.10	0.031	4.68	5.18
533.0	3.96	-0.10	0.051	5.99	5.56
654.0	4.49	-0.10	0.075	7.35	5.98
780.0	5.05	0.05	0.108	8.76	6.44
897.0	5.71	0.03	0.166	10.08	6.98

Table 8. Continued.

f	d	d _{pc}	Δ	t	d _a
<u>G7-11</u>					
268.0	2.53	0.00	0.010	3.01	4.44
386.0	3.04	0.04	0.020	4.34	4.84
503.0	3.48	0.03	0.035	5.65	5.18
621.0	3.96	0.07	0.051	6.98	5.57
745.0	4.57	0.02	0.078	8.37	6.05
865.0	5.10	0.07	0.110	9.72	6.48
<u>G7-12</u>					
495.0	2.05	0.29	0.004	5.56	4.07
614.0	2.59	0.27	0.011	6.90	4.49
733.0	3.11	0.27	0.022	8.24	4.89
850.0	3.59	0.28	0.038	9.55	5.27
938.0	3.99	0.30	0.053	10.54	5.59
1023.0	4.34	0.28	0.066	11.49	5.86
1106.0	4.62	0.30	0.080	12.43	6.09
<u>G7-13</u>					
1005.0	1.37	0.0	0	11.29	3.55
1087.0	1.66	0.0	0.001	12.21	3.77
1169.0	1.90	0.0	0.003	13.13	3.96
1250.0	2.19	0.0	0.006	14.04	4.18
1332.0	2.43	0.0	0.008	14.97	4.36
1416.0	2.74	0.0	0.014	15.91	4.60
1498.0	3.05	0.0	0.021	16.83	4.84
1583.0	3.37	0.04	0.030	17.79	5.10
1665.0	3.66	0.08	0.040	18.71	5.33
1749.0	4.01	0.08	0.053	19.65	5.60
<u>G7-14</u>					
1183.0	2.21	-0.18	0.006	13.29	4.19
1263.0	2.48	-0.20	0.010	14.19	4.40
1345.0	2.73	-0.16	0.013	15.11	4.59
1429.0	3.07	-0.17	0.022	16.06	4.86
1511.0	3.33	-0.15	0.029	16.98	5.06
1595.0	3.64	-0.10	0.039	17.92	5.31
1679.0	4.00	-0.08	0.053	18.86	5.59
1764.0	4.34	-0.10	0.067	19.82	5.86
1850.0	4.68	-0.08	0.085	20.79	6.14

Table 8. Continued

f	d	d _{pc}	Δ	t	d _a
<u>G7-15</u>					
2113.0	2.05	-	0.004	23.74	4.06
2202.0	2.48	-	0.01	24.74	4.40
2291.0	2.92	-	0.019	25.74	4.74
2380.0	3.32	-	0.029	26.74	5.05
2473.0	3.86	-	0.047	27.78	5.48
2569.0	4.39	-	0.070	28.86	5.90
<u>G7-16</u>					
2629.0	1.69	-	0.002	29.53	3.79
2726.0	2.27	-	0.007	30.62	4.23
2821.0	2.78	-	0.015	31.69	4.63
2916.0	3.37	-	0.030	32.76	5.09
3015.0	3.95	-	0.050	33.87	5.55
3117.0	4.59	-	0.080	35.02	6.06
<u>G7-17</u>					
3349.0	2.62	-	0.012	37.62	4.50
3451.0	3.30	-	0.028	38.77	5.04
3555.0	3.99	-	0.051	39.94	5.58
3662.0	4.73	-	0.086	41.14	6.17

Table 9. Summary of axial distance-time measurements taken from movie H7

f	d	d _{pc}	Δ	t	d _a
<u>H7-03</u>					
1589.0	1.14	0.09	0.052	86.77	3.38
1693.0	1.69	0.09	0.063	87.93	3.79
1794.0	2.15	0.14	0.069	89.05	4.14
1895.0	2.66	0.13	0.0725	90.17	4.51
1996.0	3.13	0.17	0.073	91.30	4.86
2101.0	3.66	0.19	0.073	92.46	5.25
2204.0	4.19	0.24	0.073	93.61	5.64
2309.0	4.74	0.24	0.075	94.77	6.05
2416.0	5.31	0.27	0.079	95.96	6.47
2523.0	5.91	0.29	0.088	97.15	6.92
2634.0	6.58	0.33	0.108	98.38	7.43
2748.0	7.28	0.34	0.138	99.65	7.97
2863.0	7.98	0.34	0.184	100.93	8.52
2982.0	8.74	0.44	0.252	102.25	9.13
<u>H7-04</u>					
2440.0	1.74	----	0.064	96.23	3.83
2543.0	2.3	----	0.070	97.37	4.25
2647.0	2.83	----	0.073	98.53	4.64
2750.0	3.34	----	0.073	99.67	5.02
2852.0	3.88	----	0.073	100.81	5.41
2955.0	4.41	----	0.073	101.95	5.81
3059.0	4.91	----	0.075	103.11	6.18
3166.0	5.50	----	0.081	104.30	6.61
3273.0	6.13	----	0.094	105.48	7.09
3387.0	6.83	----	0.116	106.75	7.62
3500.0	7.55	----	0.152	108.01	8.18
3622.0	8.35	----	0.213	109.36	8.81
<u>H7-05</u>					
2160.0	2.15	----	0.069	93.12	4.14
2262.0	2.65	----	0.072	94.25	4.51
2363.0	3.11	----	0.073	95.37	4.85
2462.0	3.57	----	0.073	96.47	5.19
2567.0	4.24	----	0.073	97.64	5.68
2675.0	4.73	----	0.074	98.84	6.04
2782.0	5.32	----	0.080	100.03	6.48
2888.0	5.95	----	0.089	101.21	6.95
2998.0	6.52	----	0.105	102.43	7.38
3110.0	7.18	----	0.132	103.67	7.89
3226.0	7.93	----	0.180	104.96	8.48

Table 9. Continued.

f	d	d _{pc}	Δ	t	d _a
<u>H7-10</u>					
16.5	3.01	0.04	0.089	1.03	4.87
38.5	3.56	0.04	0.089	2.41	5.28
61.5	4.08	0.05	0.089	3.84	5.68
82.5	4.65	0.05	0.09	5.16	6.12
105.5	5.22	0.04	0.094	6.59	6.56
128.5	5.87	0.04	0.106	8.03	7.06
151.5	6.44	0.06	0.122	9.47	7.51
175.5	7.17	----	0.152	10.97	8.09
199.5	7.86	----	0.200	12.47	8.65
<u>H7-11</u>					
111.5	1.79	-0.05	0.077	6.97	3.92
133.5	2.33	0.0	0.085	8.34	4.34
155.5	2.91	0.0	0.088	9.72	4.79
177.5	3.42	0.04	0.089	11.09	5.18
199.5	3.97	0.04	0.089	12.47	5.60
221.5	4.51	0.06	0.089	13.84	6.02
244.5	5.15	0.05	0.093	15.28	6.50
265.5	5.74	0.07	0.104	16.59	6.96
282.5	6.22	0.08	0.115	17.66	7.34
300.5	6.80	0.09	0.136	18.78	7.80
320.0	7.41	0.16	0.166	20.00	8.28
340.0	8.16	0.22	0.217	21.25	8.90
<u>H7-12</u>					
306.5	2.17	0.04	0.083	19.16	4.22
323.5	2.62	0.04	0.087	20.22	4.57
340.5	3.07	0.08	0.089	21.28	4.91
357.5	3.55	0.13	0.089	22.34	5.28
374.5	4.03	----	0.089	23.41	5.65
392.5	4.61	0.13	0.089	24.53	6.09
410.5	5.13	0.15	0.093	25.66	6.49
428.5	5.66	0.16	0.102	26.78	6.90
449.5	6.32	0.16	0.118	28.09	7.41
467.5	6.93	0.17	0.141	29.22	7.90
486.5	7.61	0.23	0.178	30.41	8.44

Table 9. Continued.

f	d	d _{pc}	Δ	t	d _a
<u>H7-13</u>					
420.5	2.23	0.10	0.084	26.28	4.27
439.5	2.65	0.15	0.088	27.47	4.59
456.5	3.16	0.16	0.089	28.53	4.98
473.5	3.65	0.18	0.089	29.59	5.35
491.5	4.27	0.16	0.089	30.72	5.83
510.0	4.83	0.13	0.091	31.87	6.26
527.5	5.40	0.13	0.097	32.97	6.70
545.5	6.01	0.09	0.109	34.09	7.17
563.5	6.64	0.10	0.130	35.22	7.67
<u>H7-14</u>					
17.5	3.02	0.0	0.089	1.09	4.87
39.5	3.54	0.03	0.089	2.47	5.27
61.5	4.05	0.04	0.089	3.84	5.66
83.5	4.65	0.04	0.090	5.22	6.12
106.5	5.23	0.00	0.094	6.66	6.56
129.0	5.84	0.04	0.105	8.06	7.04
152.5	6.45	0.05	0.122	9.53	7.52
175.5	7.10	0.11	0.157	10.97	8.04
200.5	7.87	0.09	0.196	12.53	8.66
225.5	8.62	0.12	0.257	14.09	9.28
<u>H7-15</u>					
57.5	3.75	-0.35	0.089	3.59	5.43
79.5	4.26	-0.35	0.089	4.97	5.82
101.5	4.84	-0.28	0.091	6.34	6.26
124.5	5.41	-0.30	0.097	7.78	6.71
147.5	6.08	-0.25	0.112	9.22	7.23
170.5	6.67	-0.20	0.130	10.66	7.69
193.5	7.32	-0.15	0.162	12.09	8.21
218.5	8.09	-0.10	0.212	13.66	8.84
244.5	8.90	-0.00	0.286	15.28	9.51

Table 9. Continued.

f	d	d _{pc}	Δ	t	d _a
<u>H7-16</u>					
86.5	1.30	-0.23	0.064	5.41	3.54
108.5	1.82	-0.25	0.077	6.78	3.95
130.5	2.35	-0.22	0.085	8.16	4.36
152.5	2.89	-0.15	0.089	9.53	4.77
174.5	3.42	-0.16	0.089	10.91	5.18
196.5	4.00	-----	0.089	12.28	5.62
218.5	4.52	-----	0.090	13.66	6.02
241.5	5.16	-----	0.094	15.09	6.51
262.5	5.75	-0.13	0.103	16.41	6.97
279.5	6.24	-0.12	0.116	17.47	7.35
297.5	6.83	-0.08	0.136	18.59	7.82
316.5	7.43	-0.05	0.166	19.78	8.30
336.5	8.18	0.00	0.220	21.03	8.91
375.5	9.02	0.07	0.295	22.34	9.61
<u>H7-17</u>					
293.5	2.42	-0.23	0.086	18.34	4.42
310.5	2.91	-0.25	0.088	19.41	4.79
327.5	3.35	-0.22	0.089	20.47	5.12
344.5	3.86	-0.20	0.089	21.53	5.51
362.0	4.34	-0.17	0.089	22.62	5.88
379.5	4.90	-0.16	0.092	23.72	6.31
397.5	5.50	-0.16	0.098	24.84	6.77
415.5	6.00	-0.12	0.109	25.97	7.16
433.5	6.60	-0.06	0.128	27.09	7.64
452.5	7.31	-0.04	0.160	28.28	8.20
471.5	7.98	0.0	0.205	29.47	8.75
<u>H7-18</u>					
320.5	2.65	0.05	0.088	20.03	4.59
337.5	3.09	0.07	0.089	21.09	4.93
354.5	3.57	0.11	0.089	22.16	5.29
371.5	4.07	0.10	0.089	23.22	5.67
389.5	4.64	0.09	0.090	24.34	6.11
407.5	5.17	0.10	0.094	25.47	6.52
425.5	5.69	0.13	0.102	26.59	6.92
445.5	6.21	0.18	0.115	27.84	7.33
464.5	6.94	0.17	0.142	29.03	7.91
483.5	7.62	0.23	0.179	30.22	8.45

Table 9. Continued.

f	d	d _{pc}	Δ	t	d _a
<u>H7-19</u>					
412.5	3.00	0.34	0.089	25.78	4.86
431.5	3.55	0.33	0.089	26.97	5.28
449.5	4.08	----	0.089	28.09	5.68
467.5	4.54	0.28	0.090	29.22	6.03
484.5	5.14	0.28	0.094	30.28	6.49
502.5	5.75	----	0.104	31.41	6.97
520.5	6.28	0.23	0.117	32.53	7.38
539.5	6.98	0.23	0.144	33.72	7.94
558.5	7.71	0.23	0.185	34.91	8.53
<u>H7-20</u>					
66.0	2.01	0.17	0.080	4.12	4.09
87.5	2.55	0.14	0.087	5.47	4.51
108.5	3.03	0.19	0.089	6.78	4.88
130.5	3.55	0.19	0.089	8.16	5.28
153.5	4.16	0.20	0.089	9.59	5.74
175.0	4.73	0.23	0.090	10.94	6.18
198.0	5.38	0.20	0.096	12.37	6.68
221.0	5.98	0.22	0.108	13.81	7.15
244.0	6.63	0.26	0.128	15.25	7.66
265.5	7.24	0.27	0.157	16.59	8.15
284.5	7.90	0.30	0.198	17.78	8.68
<u>H7-21</u>					
126.5	1.92	-0.25	0.080	7.91	4.03
148.5	2.44	-0.24	0.086	9.28	4.43
170.5	2.98	-0.22	0.089	10.66	4.84
192.5	3.53	-0.18	0.089	12.03	5.26
215.5	4.20	-0.25	0.089	13.47	5.77
237.5	4.73	-0.18	0.090	14.84	6.18
259.5	5.31	-0.18	0.096	16.22	6.63
276.5	5.79	-0.15	0.104	17.28	7.00
294.5	6.35	-0.16	0.119	18.41	7.44
312.5	6.90	-0.08	0.140	19.53	7.87
331.5	7.57	-0.05	0.176	20.72	8.41

Table 9. Continued.

f	d	d _{pc}	Δ	t	d _a
<u>H7-22</u>					
252.5	2.08	-0.08	0.082	15.78	4.15
271.5	2.54	-0.06	0.087	16.97	4.50
286.5	2.92	0.0	0.089	17.90	4.80
303.5	3.37	0.02	0.089	18.97	5.14
320.5	3.81	0.0	0.089	20.03	5.48
338.5	4.40	0.0	0.089	21.16	5.93
356.5	4.97	0.05	0.092	22.28	6.36
373.5	5.45	0.06	0.098	23.34	6.73
391.5	6.02	0.0	0.108	24.47	7.18
410.5	6.64	0.0	0.130	25.66	7.67
430.5	7.31	----	0.160	26.91	8.20
<u>H7-23</u>					
294.5	2.41	-0.20	0.086	18.41	4.40
311.5	2.89	-0.23	0.089	19.47	4.77
328.5	3.30	-0.16	0.089	20.53	5.09
346.0	3.83	-0.17	0.089	21.62	5.49
363.5	4.40	-0.18	0.089	22.72	5.93
381.0	4.99	-0.24	0.090	23.81	6.38
398.5	5.47	-0.15	0.098	24.91	6.75
417.5	6.06	-0.14	0.110	26.09	7.21
438.5	6.66	-0.12	0.130	27.41	7.69
456.5	7.26	-0.05	0.156	28.53	8.16
475.5	7.96	0.00	0.202	29.72	8.73
<u>H7-24</u>					
400.0	1.63	----	0.073	25.00	3.80
417.5	2.14	----	0.082	26.09	4.20
434.5	2.64	----	0.087	27.16	4.58
451.5	3.17	----	0.089	28.22	4.99
468.5	3.63	----	0.089	29.28	5.34
486.5	4.20	----	0.089	30.41	5.77
504.5	4.80	----	0.091	31.53	6.23
522.5	5.39	----	0.095	32.66	6.69
540.5	5.96	----	0.108	33.78	7.13

Table 9. Continued.

f	d	d _{pc}	Δ	t	d _a
<u>H7-25</u>					
1352	2.25	----	0.084	84.14	4.28
1450	2.75	0.20	0.088	85.23	4.67
1552	3.20	0.23	0.089	86.36	5.01
1656	3.76	0.22	0.089	87.52	5.44
1760	4.29	0.23	0.089	88.67	5.84
1865	4.81	0.23	0.090	89.84	6.24
1971	5.36	0.24	0.096	91.02	6.66
2081	5.95	0.28	0.108	92.24	7.12
2192	6.61	0.31	0.127	93.47	7.64
2307	7.30	0.32	0.159	94.75	8.19
<u>H7-26</u>					
2437	1.81	0.06	0.077	96.20	3.94
2540	2.34	0.11	0.085	97.34	4.35
2644	2.83	0.13	0.088	98.50	4.73
2747	3.35	0.15	0.089	99.64	5.12
2849	3.82	0.18	0.089	100.77	5.48
2954	4.35	0.17	0.089	101.94	5.89
3060	4.89	0.18	0.092	103.12	6.30
3165	5.47	0.18	0.098	104.28	6.75
3273	6.04	0.20	0.110	105.48	7.20
3385	6.74	0.17	0.134	106.73	7.75
3499	7.44	0.18	0.168	108.00	8.31
3618	8.19	0.24	0.184	109.32	8.89
<u>H7-27</u>					
626.0	1.53		0.072	39.12	3.72
643.0	1.96		0.080	40.18	4.05
660.0	2.57		0.087	41.25	4.52
676.5	2.93		0.089	42.28	4.80
694.0	3.43		0.089	43.37	5.18
711.0	3.93		0.089	44.43	5.56
728.0	4.42		0.089	45.50	5.94
746.0	5.02		0.092	46.62	6.40
763.0	5.47		0.098	47.68	6.75

Table 9. Continued

f	d	d _{pc}	Δ	t	d _a
<u>H7-28</u>					
836.0	1.6	-	0.072	52.25	3.77
854.0	2.25	-	0.084	53.37	4.28
871.0	2.72	-	0.088	54.43	4.64
888.0	3.30	-	0.089	55.50	5.08
905.0	3.78	-	0.089	56.56	5.45
922.0	4.31	-	0.089	57.62	5.85
939.0	4.89	-	0.092	58.68	6.30
957.0	5.44	-	0.098	59.81	6.72
974.0	6.00	-	0.108	60.87	7.16
<u>H7-29</u>					
1049.0	2.34	-	0.085	65.56	4.35
1066.0	2.90	-	0.088	66.62	4.78
1082.0	3.33	-	0.089	67.62	5.10
1099.0	3.81	-	0.089	68.68	5.47
1116.0	4.35	-	0.089	69.75	5.88
1133.0	4.96	-	0.092	70.81	6.35
1151.0	5.44	-	0.098	71.93	6.72
1168.0	6.00	-	0.108	73.00	7.16

Table 10. Summary of axial distance-time measurements taken from movie G3.

f	d	Δ	t	d _a
<u>G3-01</u>				
283.0	1.27	0.088	3.14	6.25
397.0	1.84	0.120	4.41	6.72
514.0	2.50	0.147	5.71	7.25
632.0	3.16	0.169	7.02	7.78
752.0	3.84	0.184	8.35	8.32
875.0	4.60	0.196	9.72	8.92
982.0	5.37	0.196	10.91	9.51
1090.0	6.17	0.196	12.11	10.13
1204.0	7.03	0.200	13.38	10.80
<u>G3-02</u>				
518.0	1.27	0.088	5.75	6.25
633.0	1.82	0.116	7.03	6.70
749.0	2.42	0.143	8.32	7.19
867.0	3.10	0.167	9.63	7.73
968.0	3.69	0.182	10.75	8.20
1070.0	4.41	0.194	11.89	8.77
1177.0	5.17	0.196	13.08	9.36
1283.0	5.96	0.196	14.25	9.97
<u>G3-03</u>				
552.0	0.60	0.046	6.13	5.70
664.0	1.08	0.078	7.38	6.10
778.0	1.67	0.108	8.64	6.58
889.0	2.25	0.137	9.88	7.05
985.0	2.81	0.158	10.94	7.50
1083.0	3.37	0.174	12.03	7.95
1188.0	4.11	0.195	13.20	8.54
1291.0	4.79	0.196	14.34	9.06
1395.0	5.55	0.196	15.50	9.65
1498.0	6.25	0.196	16.64	10.20
<u>G3-04</u>				
1735.0	3.06	0.166	19.28	7.70
1838.0	3.74	0.183	20.42	8.24
1948.0	4.57	0.196	21.64	8.89
2057.0	5.38	0.196	22.85	9.52
2162.0	6.15	0.196	24.02	10.12
2271.0	7.00	0.200	25.23	10.78

Table 10. Continued.

f	d	Δ	t	d _a
<u>G3-05</u>				
158.0	1.82	0.116	1.75	6.70
274.0	2.42	0.143	3.04	7.19
392.0	3.07	0.167	4.35	7.71
512.0	3.74	0.183	5.69	8.24
636.0	4.47	0.194	7.07	8.81
761.0	5.25	0.196	8.45	9.42
885.0	6.11	0.196	9.83	10.09
<u>G3-06</u>				
955.0	2.23	0.136	10.72	7.03
1054.0	2.89	0.161	11.71	7.56
1158.0	3.54	0.178	12.87	8.08
1262.0	4.24	0.192	14.02	8.64
1367.0	5.04	0.196	15.19	9.26
1467.0	5.66	0.196	16.30	9.74
1575.0	6.43	0.196	17.50	10.34
<u>G3-07</u>				
673.0	1.25	0.088	7.48	6.24
787.0	1.80	0.116	8.74	6.68
898.0	2.42	0.143	9.98	7.19
995.0	2.99	0.164	11.05	7.64
1095.0	3.58	0.180	12.17	8.11
1200.0	4.34	0.193	13.33	8.71
1304.0	5.06	0.196	14.49	9.27
1408.0	5.75	0.196	15.64	9.81

Table 10. Continued.

f	d	Δ	t	d _a
<u>G3-08</u>				
1522.0	0.645	0.046	16.91	5.73
1606.0	0.92	0.067	17.84	5.96
1691.0	1.22	0.085	18.78	6.21
1819.0	2.39	0.142	20.21	7.16
1931.0	3.23	0.172	21.45	7.83
2038.0	3.96	0.187	22.64	8.41
2135.0	4.58	0.196	23.72	8.90
2231.0	5.14	0.196	24.78	9.33
2335.0	5.90	0.196	25.94	9.92
2443.0	6.69	0.198	27.14	10.53
<u>G3-09</u>				
2038.0	1.50	0.100	22.64	6.44
2133.0	2.05	0.128	23.70	6.88
2221.0	2.44	0.144	24.67	7.20
2311.0	2.89	0.161	25.67	7.56
2413.0	3.51	0.178	26.81	8.05
2522.0	4.31	0.193	28.02	8.69
2629.0	5.11	0.196	29.21	9.31
2735.0	5.85	0.196	30.38	9.88
2853.0	6.82	0.198	31.70	10.64
<u>G3-11</u>				
2925.0	3.16	0.169	32.50	7.78
3030.0	3.89	0.186	33.66	8.35
3126.0	4.49	0.193	34.73	8.83
3224.0	5.06	0.196	35.82	9.27
3325.0	5.73	0.196	36.94	9.79
3431.0	6.48	0.196	38.12	10.37
3542.0	7.33	0.202	39.35	11.03

Table 11. Summary of axial distance-time measurements taken from movie H5.

f	d	Δ	t	d _a
<u>H5-01</u>				
71.0	0.80	0.060	4.73	5.87
95.5	1.37	0.094	6.37	6.33
121.5	1.97	0.124	8.10	6.82
148.0	2.62	0.150	9.87	7.35
174.5	3.33	0.174	11.63	7.92
<u>H5-02</u>				
161.0	1.07	0.077	10.73	6.09
186.5	1.71	0.110	12.43	6.61
212.0	2.26	0.136	14.13	7.06
238.0	2.85	0.160	15.87	7.53
265.0	3.59	0.180	17.67	8.12
<u>H5-03</u>				
280.0	0.98	0.072	18.67	6.01
305.0	1.50	0.100	20.33	6.44
330.0	2.07	0.130	22.00	6.90
355.0	2.62	0.150	23.67	7.35
382.0	3.34	0.174	25.47	7.92
<u>H5-04</u>				
393.0	0.40	0.032	26.20	5.53
418.0	0.98	0.072	27.87	6.01
443.0	1.56	0.102	29.53	6.49
468.5	2.17	0.133	31.23	6.99
494.0	2.84	0.160	32.93	7.53
515.0	3.50	0.178	34.33	8.05
<u>H5-05</u>				
458.0	1.43	0.097	30.53	6.38
482.0	2.03	0.127	32.13	6.87
504.0	2.56	0.148	33.60	7.30
525.0	3.16	0.168	35.00	7.78
547.0	3.90	0.186	36.47	8.37

Table 11. Continued

f	d	Δ	t	d _a
<u>H5-06</u>				
548.0	0.28	0.023	36.53	5.43
567.0	0.72	0.053	37.80	5.80
588.0	1.28	0.088	39.20	6.26
611.0	2.09	0.130	40.73	6.92
632.0	2.77	0.157	42.13	7.47
654.0	3.49	0.178	43.60	8.05
<u>H5-07</u>				
486.0	1.01	0.073	32.40	6.04
506.0	1.46	0.098	33.73	6.41
525.0	1.91	0.110	35.00	6.77
544.5	2.58	0.150	36.30	7.32
568.0	3.27	0.172	37.87	7.87
<u>H5-08</u>				
512.0	0.76	0.056	34.13	5.83
531.0	1.18	0.084	35.40	6.18
550.0	1.65	0.108	36.67	6.57
572.0	2.41	0.142	38.13	7.18
594.0	3.11	0.168	39.60	7.74
<u>H5-09</u>				
672.0	1.35	0.093	44.80	6.32
693.0	2.01	0.126	46.20	6.86
713.0	2.61	0.15	47.53	7.34
734.0	3.21	0.17	48.93	7.82
755.0	3.86	0.186	50.33	8.34

REFERENCES

1. Adams, R., Plast. Des. Process., June (1971).
2. Bernhardt, E. C., and J. M. McKelvey, Soc. Plastics Engrs. J., 10, 419 (1954).
3. Booy, M. C., Polym Eng. Sci., 7, 5 (1967).
4. Boussinessq, M. S., J. Math. pure et appliquee, 13, 377 (1868).
5. Brodkey, R. S., "Phenomena of Fluid Motion", Addison-Wesley, Princeton, Mass. (1967).
6. Carley, J. F., R. S. Mallouk, and J. M. McKelvey, Ind. Eng. Chem., 45, 974 (1953).
7. Chung, C. I., Mod. Plast., 45, 178 (1968).
8. Chung, C. I., Soc. Plastics Engrs. J., 26, 32, May (1970).
9. Danckwerts, P. V., Appl. Sci. Res., A3, 279 (1952).
10. Darnell, W. H., and E.A.J. Mol, Soc. Plastics Eng. J., 12, 20 (1956).
11. Decker, H., "Die Spritz Maschine", Hanover, Germany, Paul Troester Maschinenfabrik (1941).
12. DeHaven, E. S., Ind. Eng. Chem., 51, 813 (1959).
13. Denny, D. A., Ph.D. dissertation, The Ohio State Univ., Columbus (1966).
14. Doboczky, Z., Der Plast. Verarbeiter, 16, 57 (1965).
15. Donovan, R. C., Polym. Eng. Sci., 11, 361 (1971).
16. Donovan, R. C., D. E. Thomas, and L. D. Leversen, Polym. Eng. Sci., 11, 553 (1971).
17. Eccher, S., and A. Valentinotti, Ind. Eng. Chem., 50, 829 (1958).
18. Griffith, R. M., Ind. Eng. Chem. Fundamentals, 1, 186 (1962).

19. Griffith, R. M., 23rd Annual Technical Conference, Society of Plastics Engineers, Vol. 13, 843, 1967.
20. Glyde, B. S., and W. A. Holmes-Walker, Intern. Plastics Eng., 2, 338 (1962).
21. Heinrichs, D. R., Master thesis, University of Virginia (1969).
22. Kaiser, H., Ph.D. dissertation, Virginia Polytechnic Inst. (1967).
23. Kirby, R. B., Jr., Soc. Plastics Engrs, J., 18, 1263 (1962).
24. Klein, I., 28th Annual Technical Conference, Society of Plastics Engineers, Vol. 18, 516, 1972.
25. Kobayashi, A., "Machining of Plastics", McGraw-Hill, New York (1964).
26. Kroesser, F. W., and S. Middleman, Polym. Eng. Sci., 5, 231 (1965).
27. Lee, K. H., and R. S. Brodkey, Trans. Soc. Rheol., 15, 627 (1971).
28. McKelvey, J. M., "Polymer Processing", John Wiley, New York (1962).
29. McKelvey, J. M., and N. C. Wheeler, Soc. Plastics Engrs. Trans., 3, 138 (1963).
30. Maddock, B. H., Soc. Plastics Engrs. J., 15, 383 (1959).
31. Maillefer, C. H., Ph.D. thesis, University of Lausanne, Lausanne (1952).
32. Maillefer, C. H., Rev. Gen. Caoutchouc, 31, 563 (1954).
33. Mandelkern, L., "Crystallization of Polymers", McGraw-Hill, New York (1964).
34. Marshall, D. I., I. Klein, and R. H. Uhl, Soc. Plastics Eng. J., 21, 1192 (1965).
35. Marzetti, B., Giorn. Chem. Mat. Appl., 6, 567 (1924).
36. Mohr, W. D., R. L. Saxton, and C. H. Jepson, Ind. Eng. Chem., 49, 1885 (1957).
37. Mohr, W. D., Chapt. 13, "Processing of Thermoplastic Materials", E. C. Bernhardt, ed., Reinhold, New York (1959).
38. Mohr, W. D., P. H. Squires, and F. C. Starr, Soc. Plastics Engrs. J., 16, 1015 (1960).

39. Mohr, W. D., J. B. Clapp, and F. C. Starr, Soc. Plastics Engrs. Trans., 1, 113 (1961).
40. Nylén, P., and E. Sunderland, "Modern Surface Coatings", Interscience, New York (1965).
41. Pawlowski, J., unpublished report, Dormagen, Germany, Farbenfabriken Bayer (1949).
42. Pearson, J.R.A., "Mechanical Principles of Polymer Melt Processing", Pergamon, Oxford (1966).
43. Prause, J. J., Plastics Technology, Vol. 13, No. 12, 41, November, 1967.
44. Prause, J. J., Plastics Technology, Vol. 14, No. 2, 29, February, 1968.
45. Platzner, N.A.J., ed., "Plasticization and the Plasticizer Process", ACS, Advances in Chemistry Series, Vol. 48, Washington, D. C. (1965).
46. Ram, A., and M. Narkis, Polym. Eng. Sci., 7, 161 (1967).
47. Rodriguez, F., "Principles of Polymer Systems", McGraw-Hill, New York (1970).
48. Rousselet, Jean-Paul, Technical Papers, 29th Annual Technical Conference, Society of Plastics Engineers, Vol. 17, 206, 1971.
49. Rowell, H. S., and Finlayson, Engineering, 114, 606 (1922).
50. Rowell, H. S., and Finlayson, Engineering, 128, 249 (1928).
51. Shishido, S., and I. Ito, Nippon Kagaku Zashi, 84, 889 (1963).
52. Simonds, H. R., et al., "Extrusion of Plastics, Rubber and Metals", Reinhold, New York (1952).
53. Spencer, R. S., and R. E. Dillon, J. Colloid Sci., 4, 181 (1949).
54. Spencer, R. S., and R. E. Dillon, J. Colloid Sci., 4, 241 (1949).
55. Spencer, R. S., and R. M. Wiley, J. Colloid Sci., 6, 133 (1951).
56. Street, L. F., Intern. Plastics Eng., 1, 289 (1961).
57. Street, L. F., 28th Annual Technical Conference, Society of Plastics Engineers, Vol. 18, 520, 1972.

58. Szymanski, P. J., Math. pure et appliquee, Series 9, 11, 67 (1932).
59. Tadmor, Z., I. J. Duvdevani, and I. Klein, Polymer Eng. Sci., 7, 198 (1967).
60. Tadmor, Z., and I. Klein, "Engineering Principles of Plasticating Extrusion", Van Nostrand Reinhold, New York (1970), (a) Chapter 3, (b) Chapter 4, (c) Chapter 5, (d) Chapter 6, (e) Chapter 7, and (f) Chapter 9.
61. Tompa, H., "Polymer Solutions", Butterworths, London (1956).
62. Wheeler, J. A., and E. H. Wissler, Trans. Soc. Rheol., 10, 353 (1966).
63. Wheeler, N. C., Annual Convention of the Wire Association, Baltimore, Md., October 22-25, 1962.
64. White, J. L., and A. B. Metzner, J. of Appl. Polymer Sci., 7, 1867, (1963).